

THE ROLE OF THE CTD PHOSPHATASE RTR1 AND POST-TRANSLATIONAL
MODIFICATIONS IN REGULATION OF RNA POLYMERASE II

Mary L. Cox

Submitted to the faculty of the University Graduate School
in partial fulfillment of the requirements
for the degree
Master of Science
in the Department of Biochemistry and Molecular Biology
Indiana University

December 2013

Accepted by the Graduate Faculty, Indiana University, in partial fulfillment of the requirements for the degree of Master of Science.

Mark G. Goebel, PhD. Chair

Amber L. Mosley, PhD.

Master's Thesis
Committee

Ronald C. Wek, PhD.

ACKNOWLEDGEMENTS

I would like to express my heartfelt appreciation to the following people; without whom, this work would not have been possible. You have all been true blessings in my life and I will be forever grateful.

- To Dr. Amber Mosley- Thank you for inspiring me to be a better scientist, your endless patience, and friendship. You have gone above and beyond with your support, encouragement and mentoring. I am honored to have been a member of your lab and wish you success beyond measure.
- To Dr. Mark Goebel- Thank you for your guidance and your efforts as a teacher in the Biotechnology Program and mentorship as the chairman of my thesis committee.
- To Dr. Ron Wek- Thank you for your thoughtful participation as a member of my thesis committee. Your knowledge and advice have been extremely helpful and it has been a privilege to learn from you.
- To Sharry Fears- Thank you for your tireless efforts in the laboratory portion of the Biotechnology courses. Your dependable preparation and knowledge of the material made difficult subject matter easier to understand.
- To my colleagues in the Mosley Lab, past and present-Megan Zimmerly, Jerry Hunter, Melanie Fox, Michael Berna, Jason True, and Whitney Smith-Kinnaman- Thank you all for your knowledge and training with equipment, completion of experiments, encouragement, support and friendship. I have truly enjoyed knowing all of you and will miss our time together.

- To my colleagues in the Biochemistry and Molecular Biology Department- Thank you for all your help with equipment and software loans, guidance, and advice: Dr. X. Charlie Dong and lab members, Dr. Timothy Corson and Kamakshi Shishtla, and Dr. Nuria Morral and lab members.
- To my parents, Jack and Shirley: Thank you for instilling in me a sense of wonder about the world and a determination to explore it through education. Your unconditional love, support and encouragement have sustained me through this undertaking. My accomplishments are truly yours as well.
- To my Awesome, Amazing, Incredible Husband, Yoda: “Thank you” is an insufficient sentiment for what you have sacrificed for this endeavor. Your unending kindness, patience, love and support mean the world to me. With each passing day, you are appreciated and loved beyond measure.
- To my children: William, Catherine, Samantha, Alexander, Victoria, Amanda, and Cynthia- Thank you for giving me a life filled with great adventure and joy every day. Your love and patience through all the missed meals and activities is greatly appreciated. You are each extraordinary in your own way and I hope that this experience proves to you that there is nothing you can’t do if you have faith in yourself and are determined to succeed.

Mary L. Cox

THE ROLE OF THE CTD PHOSPHATASE RTR1 AND POST-TRANSLATIONAL
MODIFICATIONS IN REGULATION OF RNA POLYMERASE II

RNA polymerase II (RNAPII) is regulated by multiple modifications to the C-terminal domain (CTD) of the largest subunit, Rpb1. This study has focused on the relationship between hyperphosphorylation of the CTD and RNAPII turnover and proteolytic degradation as well as post-translational modifications of the globular core of RNAPII.

Following tandem affinity purification, western blot analysis showed that MG132 treated *RTR1 ERG6* deletion yeast cells have accumulation of total RNAPII and in particular, the hyperphosphorylated form of the protein complex. In addition, proteomic studies using MuDPIT have revealed increased interaction between proteins of the ubiquitin-proteasome degradation system in the mutant MG132 treated yeast cells as well as potential ubiquitin and phosphorylation sites in RNAPII subunits, Rpb6 and Rpb1, respectively. A novel Rpb1 phosphorylation site, T1471-P, is located in the linker region between the CTD and globular domain of Rpb1 and will be the focus of future studies to determine biological significance of this post-translational modification.

Mark G. Goebel, PhD. Chair

TABLE OF CONTENTS

LIST OF TABLES	viii
LIST OF FIGURES	ix
LIST OF ABBREVIATIONS	xi
INTRODUCTION	
I. The regulation of RNA Polymerase II transcription elongation.....	1
II. Post-translational modification of RNA Polymerase II	5
III. Overview of current known role of Rtr1 and other CTD Phosphatases	8
IV. Mechanisms for RNAPII degradation and recycling pathways	10
V. Proteasome inhibition and alternative approaches to study protein turnover	13
VI. Transformation of yeast for C-terminal domain tagging via homologous recombination	18
VII. Multidimensional protein identification technology (MuDPIT) to determine protein-protein interaction and potential post-translational modifications	21
MATERIALS AND METHODS	
I. Preparation of whole cell lysates following MG132 treatment	27
II. Western Blot Analysis.....	29
III. Transformation of <i>S. cerevisiae</i> deletion strains for C-terminal tagging for Rpb3	30
IV. Silver Staining Procedure.....	39
V. MG132 treatment of TAP-tagged <i>S. cerevisiae</i> mutant strains	40
VI. MuDPIT Analysis	41
VII. Malachite Green Phosphate Assay.....	44

RESULTS

I.	The effects of MG132 treatment on RNA Polymerase II phosphorylation in <i>RTR1</i> deletion strains	45
II.	Generation of <i>S. cerevisiae</i> strains Rpb3-TAP <i>erg6</i> Δ and Rpb3-TAP <i>erg6</i> Δ <i>rtr1</i> Δ TAP tag through homologous recombination.....	49
III.	Isolation of RNA Polymerase II complexes following MG132 treatment from wild-type, <i>RTR1</i> deletion, <i>ERG6</i> deletion, and <i>RTR1/ERG6</i> double deletion strains	50
IV.	Identification of ubiquitination sites in RNA Polymerase II purifications using a two-step bioinformatics analysis	56
V.	Identification of phosphorylation sites in RNA Polymerase II purifications using a two-step bioinformatics analysis	67
VI.	Can Threonine 1471 be dephosphorylated by Rtr1 <i>in vitro</i> ?	69
	DISCUSSION	71
	CONCLUSIONS	83
	REFERENCES	85
	CURRICULUM VITAE	

LIST OF TABLES

1. Summary of CTD kinases and phosphatases in <i>S. cerevisiae</i> and mammals	9
2. Selection of proteins identified by MuDPIT analysis of <i>S. cerevisiae</i>	15
3. Antibodies used for Western Blot analysis	30
4. Details of PCR reaction mixture.....	32
5. Details of PCR parameters	32
6. Comparison of peptide identifications between Proteome Discover/SEQUEST and Scaffold/X!Tandem.....	57
7. Proteins identified using Scaffold analysis for untreated Rpb3-TAP <i>erg6Δ</i>	60
8. Proteins identified using Scaffold analysis for MG132 treated Rpb3-TAP <i>erg6Δ</i>	61
9. Proteins identified using Scaffold analysis for untreated Rpb3-TAP <i>erg6Δ rtr1Δ</i>	62
10. Proteins identified using Scaffold analysis for MG132 treated Rpb3-TAP <i>erg6Δrtr1Δ</i>	63
11. Summary comparison of detected proteins from MS/MS data	78

LIST OF FIGURES

1. PDB-Viewer/Pov Ray generated model of complete ribbon structure for RNAPII complex.....	2
2. Model of regulation of phosphorylation of the RNA Polymerase II CTD during transcription elongation in <i>S. cerevisiae</i>	8
3. RNAPII naturally pauses during transcription elongation.....	14
4. Current working model for RNAPII recycling and degradation following the loss of CTD phosphatases.....	16
5. Structure and sequence of the TAP tag and Schematic representation of TAP strategy.....	20
6. Schematic of TAP tag disruption cassette used to create Rpb3-TAP <i>S. cerevisiae</i> strains.....	21
7. Comparison of RNAPII Serine 5 phosphorylation using Western blot of four strains of <i>S. cerevisiae</i> both MG132 treated and untreated.....	46
8. Comparison of RNAPII Tyrosine 1 phosphorylation using Western blot analysis of MG132 treated and untreated yeast strains.....	47
9. Comparison of RNAPII CTD Serine 2, 5, and 7 phosphorylation Western blot analysis of MG132 treated and untreated yeast strains.....	48
10. Western blot analysis of Anti-CBP in yeast transformants isolated from YNB URA- agar after treatment with LiOAc and pBS1539.....	50
11. Silver Stain results of TAP-tagged deletion strains of <i>S. cerevisiae</i>	51
12. Growth curve comparison of Rpb3-TAP <i>erg6Δ</i> (aka <i>erg6D</i>) vs Rpb3-TAP <i>erg6Δ rtr1Δ</i> (aka <i>erg6D-rtr1D</i>).....	52
13. Representative silver stains comparing yeast lysis methods prior to TAP procedure.....	53
14. Silver stain results from MG132 treated and untreated TAP tagged deletion strains.....	54
15. Comparison of elutions 1 and 2 from MG132 treated and untreated TAP tagged deletion strains as detected by Silver Stain.....	55
16. Peptide sequence coverage of RNAPIIs second largest subunit Rpb2 obtained from <i>erg6Δ rtr1Δ</i> in the presence of MG132 using Scaffold software.....	66

17. Peptide sequence coverage and ion fragmentation spectra of RNAPIIs subunit Rpb6 obtained from <i>erg6Δrtr1Δ</i> in the presence of MG132 using Scaffold software.....	67
18. Sequence coverage of Rpb1 obtained following <i>erg6Δ rtr1Δ</i> in the presence of MG132 using Scaffold software.....	68
19. Ion fragmentation spectra obtained from LC-MS/MS for <i>erg6Δ rtr1Δ</i> in the presence of MG132 using Scaffold software.....	69
20. Malachite Green Phosphate Assay using recombinant GST-Rtr1 for potential substrate	70

LIST OF ABBREVIATIONS

2D-PAGE	Two dimensional-polyacrylamide gel electrophoresis
BER	Base Excision Repair
CBP	Calmodulin binding peptide
ChIP	Chromatin Immunoprecipitation
CID	Collision induced dissociation
CPF	Cleavage and Polyadenylation Factor
CTD	C-terminal domain of yeast RNA polymerase II subunit Rpb1
CTDK-I	C-terminal domain kinase I
ddH ₂ O	Distilled and de-ionized water
DMSO	Dimethyl sulfoxide
DNA	Deoxyribonucleic Acid
DTT	Dithiothreitol
EDTA	Ethylenediamine tetraacetic acid
EGTA	Ethylene glycol tetraacetic acid
EM	Expectation maximization (algorithm)
ETD	Electron transfer dissociation
Fc	Fragment crystallizable region of IgG
FDR	False discovery rate(s)
GTF	General Transcription Factor
GST	Glutathione S-transferase
IEF	Isoelectric focusing
IGEPAL	Octylphenoxypolyethoxyethanol

LiOAc	Lithium Acetate
Mfr	Manufacturer
MRM	Multiple reaction monitor
mRNA	Messenger RNA
MS	Mass spectrometry/mass spectrometer
MuDPIT	Multidimensional protein identification technology
NER	Nucleotide Excision Repair
ORF(s)	Open reading frame(s)
pA	Polyadenylation site
pI	Isoelectric point
PIC	Pre-initiation Complex
PSM	Peptide spectrum match
P-TEFb	Positive transcription elongation factor b
PTM	Post-translational Modification
RNA	Ribonucleic Acid
RNAPII	Yeast RNA polymerase II complex
S2	Serine 2 of yeast RNA polymerase II C-terminal domain
S2-P	Phosphorylated serine 2 of yeast RNA polymerase II C-terminal domain
S5	Serine 5 of yeast RNA polymerase II C-terminal domain
S5-P	Phosphorylated serine 5 of yeast RNA polymerase II C-terminal domain
S7	Serine 7 of yeast RNA polymerase II C-terminal domain
S7-P	Phosphorylated serine 7 of yeast RNA polymerase II C-terminal domain
<i>S. cerevisiae</i>	Baker's yeast, <i>Saccharomyces cerevisiae</i>

SCX	Strong cation exchange
SDS	Sodium dodecylsulfate
SDS-PAGE	Sodium dodecylsulfate-polyacrylamide gel electrophoresis
siRNA	Small interfering RNA
snRNA	Small nuclear RNA
RP	Reversed phase chromatography
TAP	Tandem affinity purification
TBS	Tris buffered saline
TCR	Transcription Coupled Repair
TE	Tris-EDTA
TEMED	Tetramethylethylenediamine
TSS	Transcription start site
TXN	Transcription related
WT	Wild-type

INTRODUCTION

I. The regulation of RNA Polymerase II transcription elongation

Transcription of DNA into cellular RNAs is accomplished by one of three highly conserved enzymes in higher eukaryotes (Vannini & Cramer, 2012). In eukaryotes, RNA polymerase II (RNAPII) is primarily responsible for transcribing DNA into messenger RNA (mRNA) as well as small nuclear RNA (snRNA) (Corden, Cadena, Ahearn, & Dahmus, 1985; D. W. Zhang et al., 2012). When completely assembled, the RNAPII holoenzyme (Figure 1), is ~550KDa consisting of 12 subunits, designated Rpb1 through Rpb12 (Edwards, Kane, Young, & Kornberg, 1991; Woychik & Young, 1990). A unique feature of the largest subunit, Rpb1, is a hepta-peptide repeat ($Y^1S^2P^3T^4S^5P^6S^7$) hence referred to as the C-terminal domain (CTD) that is important for determining whether the RNAPII will initiate transcription based on the phosphorylation status of the hepta-peptide repeats (Cadena & Dahmus, 1987; Payne, Laybourn, & Dahmus, 1989; Phatnani & Greenleaf, 2006).

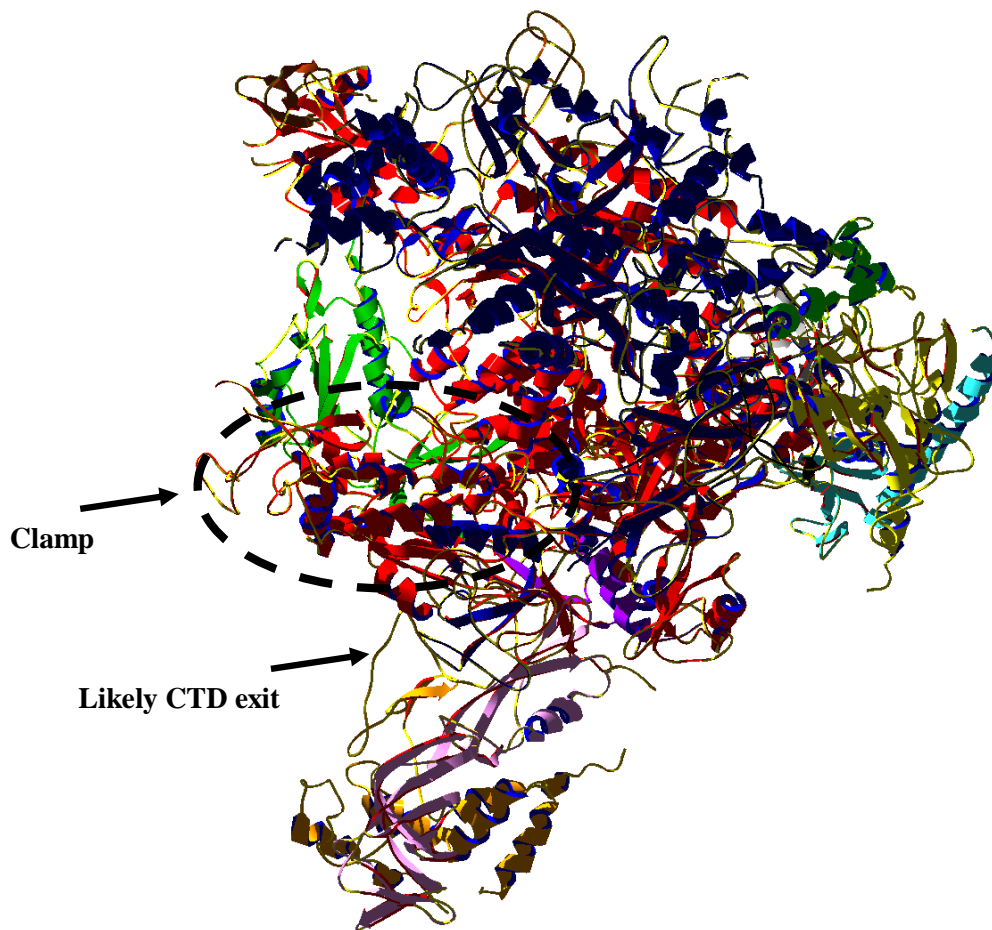


Figure 1. PDB-Viewer/Pov Ray generated model of complete ribbon structure for RNAPII complex. The crystal structure was determined by Armache et al. in 2005 (PDB ID: 1WCM). This model indicates structural features that are critical for major transcription functions.

The transcription cycle is a well-coordinated series of processes which must begin with an initiation competent RNAPII complex associating with the promoter region of the DNA template strand. The CTD has been shown to be a functional scaffold that coordinates transitions between transcription initiation, promoter clearance, elongation, and termination through dynamic changes in post-translational modifications along the CTD repeats (described in detail below and reviewed in Heidemann, Hintermair, Voss, & Eick, 2013). In addition, modifications of interacting protein factors aid in the regulation of the transcription cycle through signals that act to promote or repress

transcription (Bataille et al., 2012; Phatnani & Greenleaf, 2006; Shandilya & Roberts, 2012).

Initiation of transcription begins following hypophosphorylated RNAPII binding to a promoter of a gene (Laybourn & Dahmus, 1989; Lu, Flores, Weinmann, & Reinberg, 1991; Ohkuma & Roeder, 1994). Recruitment of this form of RNAPII is achieved through recognition of the pre-initiation complex (PIC) which includes general transcription factors (GTFs) such as TFIIA, TFIIB, TFIID, TFIIE, TFIIF, and TFIIH. These GTFs facilitate a stable transcription competent complex at the promoter through a number of biochemical activities including: suppression of promoter-proximal stalling of RNAPII, promoter DNA melting, RNA Polymerase II loading onto the template strand, and stimulation of productive transcription (Cramer, 2004; Hirose & Ohkuma, 2007; Hsin & Manley, 2012). Specifically, immediately following RNAPII binding to the promoter, the CTD is phosphorylated at the S5 residue by a TFIIH-associated cyclin-dependent kinase, Kin28 (Komarnitsky, Cho, & Buratowski, 2000) and occupancy of the S5 phosphorylated modified occupancy peaks shortly thereafter in a 5' transition of initiation to elongation (Mayer et al., 2010). Within the last few years, genome-wide analysis of general elongation factors in yeast transcription have been well characterized using chromatin immunoprecipitation (ChIP) followed by microarray, which has shown that elongation factors are often recruited during a short transition just upstream of the transcription start site (TSS) (Mayer et al., 2010). While the initiation and termination factors were found to peak just before and just after the TSS and the polyadenylation sites (pA), respectively, several elongation factors (e.g. Spt4, Spt5, Spt6, Spt16, Spn1, Elf1, Bur1 and Ctk1) were found to have increased gene-averaged occupancy intensities

from ChIP and microarray studies. These intensities did not correlate to either initiation or termination factors and showed three distinct patterns of association based on when they are active in the transcription cycle (Mayer et al., 2010). These results support a coordinated exchange of the initiation complex for an elongation complex at the 5' end of the transcribed region in a uniform transition (Mayer et al., 2010).

The 5' transition from initiation to elongation is marked by the release of RNAPII from the promoter with enhanced levels of serine 5 phosphorylation (S5-P) persisting throughout early and mid-elongation. Meanwhile, simultaneous recruitment of capping and splicing proteins (Fabrega, Shen, Shuman, & Lima, 2003; Mayer et al., 2010; Schroeder, Schwer, Shuman, & Bentley, 2000) occurs which begin to process the lengthening mRNA at the 5' end. As the RNAPII moves along the transcribed region of the gene, the shift of the CTD phosphorylated at serine 5 to serine 2 (S2-P) occurs through the activity of a cyclin-CDK kinase complex known as CTDK-1 (containing the cyclin dependent kinase subunit Ctk1). Consequently, at the 3' end of the transcribed region the CTD is populated predominantly with S2-P CTD at transcription termination of many RNAPII target mRNA genes. As with the 5' end, termination of transcription is marked by dissociation of many of the elongation factors and RNAPII in a coordinated manner to facilitate the completion of the transcription cycle. During the first step of this two-step process, several elongation factors are released (Spt16, Paf1, Bur1 and Ctk1) and the second step of transcription termination involves association of processing and termination factors with RNAPII that facilitate the cleavage and subsequent polyadenylation by the CPF (cleavage and polyadenylation factors) (Licatalosi et al., 2002; Mayer et al., 2010; Y. Zhang, Wen, Washburn, & Florens, 2011). Finally, prior to

re-initiation of transcription by hypophosphorylated RNAPII, S5-P and S2-P residues of the CTD are dephosphorylated by specific phosphatase activity described in more detail in the following sections.

II. Post-translational modification of RNA Polymerase II

Post-translational modifications (PTM) are key biochemical signals that determine regulation of transcription and many other cellular processes. The 26 consecutive repeats of the heptamer $Y^1S^2P^3T^4S^5P^6S^7$ in the yeast CTD (Allison, Moyle, Shales, & Ingles, 1985) has multiple potential sites for post-translational modification such as phosphorylation, glycosylation, and methylation (reviewed in Ponts et al., 2011). Phosphorylation of the CTD is the most widely studied and best characterized among these modifications, as discussed in the previous section, with the majority of previous studies centered on the serine residues at positions 2, 5, and to a lesser extent 7 (S7-P) (Chapman et al., 2007; Egloff, Zaborowska, Laitem, Kiss, & Murphy, 2012). Although these phosphorylation sites are the most widely studied, there is an increasing number of studies exploring phosphorylated tyrosine in the first position (Heidemann & Eick, 2012) and phosphorylated threonine in the fourth position (Heidemann et al., 2013; Sardu & Washburn, 2011b). In addition, isomerization of the proline residues in positions 3 and 5 have been found to add to the complexity of the “CTD code” (reviewed in Buratowski, 2003; Egloff, Dienstbier, & Murphy, 2012).

It is known that RNAPII must be in a hypophosphorylated state in order to become initiation competent *in vitro* (Laybourn & Dahmus, 1989), though the dephosphorylation events that create this RNAPII form are incompletely understood and questions still remain (Egloff, Dienstbier, et al., 2012). The following is a brief summary

of the relevant modifications beginning with RNAPII binding to a DNA promoter. As discussed above, the kinase Kin28 (yeast homolog to CDK7 in higher eukaryotes), a member of the TFIIF initiation complex, phosphorylates the CTD at S5 residues (Komarnitsky et al., 2000; Rodriguez et al., 2000). As the complex clears the promoter of an actively transcribing gene, S5-P peaks near the 5' end of the transcribed region, which also triggers the recruitment of capping and splicing components (Schroeder et al., 2000) to the transcript. S5-P decreases significantly due to the phosphatase activity of Rtr1 (Egloff, Zaborowska, et al., 2012; M. Kim, Suh, Cho, & Buratowski, 2009; Mosley et al., 2009) and Ssu72 (Komarnitsky et al., 2000) during the course of elongation. Dephosphorylation of S5-P coincides with protein kinases Ctk1 (human homolog is CDK9 part of the P-TEFb) and/or Bur1 (human homolog CDK9 and CDK12) phosphorylation of S2 residues on the CTD (K. K. Lee et al., 2011; Qiu, Hu, & Hinnebusch, 2009). S7 phosphorylation also steadily occurs as RNAPII moves along the transcribed region during transcription elongation by the activity of Kin28 (Akhtar et al., 2009; Glover-Cutter et al., 2009; M. Kim et al., 2009). The phosphorylation of the S7 residue has been implicated in snRNA transcription and processing (Chapman et al., 2007; Egloff, Zaborowska, et al., 2012; Sardu & Washburn, 2011a). It has also been hypothesized that S7-P could be used as a mechanism of suppression of cryptic transcription resulting from interrupted transcription and enhanced transcription (Tietjen et al., 2010). In addition, Bataille and colleagues recently (Bataille et al., 2012; D. W. Zhang et al., 2012) attributed dephosphorylation of S7-P to Ssu72 using both *in vivo* and *in vitro* studies.

S2-P peaks at the 3' end of the transcribed region and signals recruitment of termination factors necessary for the cleavage and polyadenylation of the nascent RNA (Ahn, Kim, & Buratowski, 2004; L. Chen et al., 2011; Licatalosi et al., 2002; Ramisetty & Washburn, 2011). At or immediately following termination of transcription the S2-P are removed by the protein phosphatase, Fcp1. In addition to the above modifications, the propyl isomerase, Ess1 (Pin1 in humans), which catalyzes the conversion of cis/trans peptidyl proline bond at S5-P6 of the CTD repeat, has been linked to stimulation of Ssu72 dephosphorylation of S5-P and S7-P at the 3' end of genes (Bataille et al., 2012). This modification is important due to the recent finding that the cis-isomer was the preferred substrate for Ssu72 binding and CTD phosphatase activity (Werner-Allen et al., 2011; Xiang et al., 2010).

Phosphorylation patterns of the actively transcribing RNAPII CTD have been shown to be essential to the successful transcription and processing of mRNA (recently reviewed in Egloff, Dienstbier, et al., 2012; Ponts et al., 2011). As a consequence, the loss of phosphatase activity has been implicated in the loss of RNAPII occupancy and the inability to form competent initiation complexes *in vitro* (Cho et al., 1999; Laybourn & Dahmus, 1989; Mosley et al., 2009). The resulting hyperphosphorylation of the CTD due to inefficient or non-existent dephosphorylation could account for the lack of initiation competent RNAPII and lower gene occupancy in the transcribed region. In order to test this hypothesis, the use of phosphatase deletion or thermosensitive strains of *S. cerevisiae* is proposed to explore whether RNAPII recycling or degradation is affected by the loss of CTD phosphatases and subsequent hyperphosphorylation. In addition, the use of MuDPIT analysis will be used to identify potential post-translational

modifications that occur following deletion of the CTD phosphatase, *RTR1*. Finally, MuDPIT analysis will also be used to determine if additional interactions with specific factors can be identified that may add insight to potential mechanisms for RNA recycling.

III. Overview of current known role of Rtr1 and other CTD Phosphatases

Figure 2 shows our current working model of the role of RNAPII CTD phosphorylation with an emphasis on phosphatase activity. The specific roles of these phosphatases will be investigated further in this present study. In order to test this model it is important to first understand the existing protein kinase and phosphatase activities.

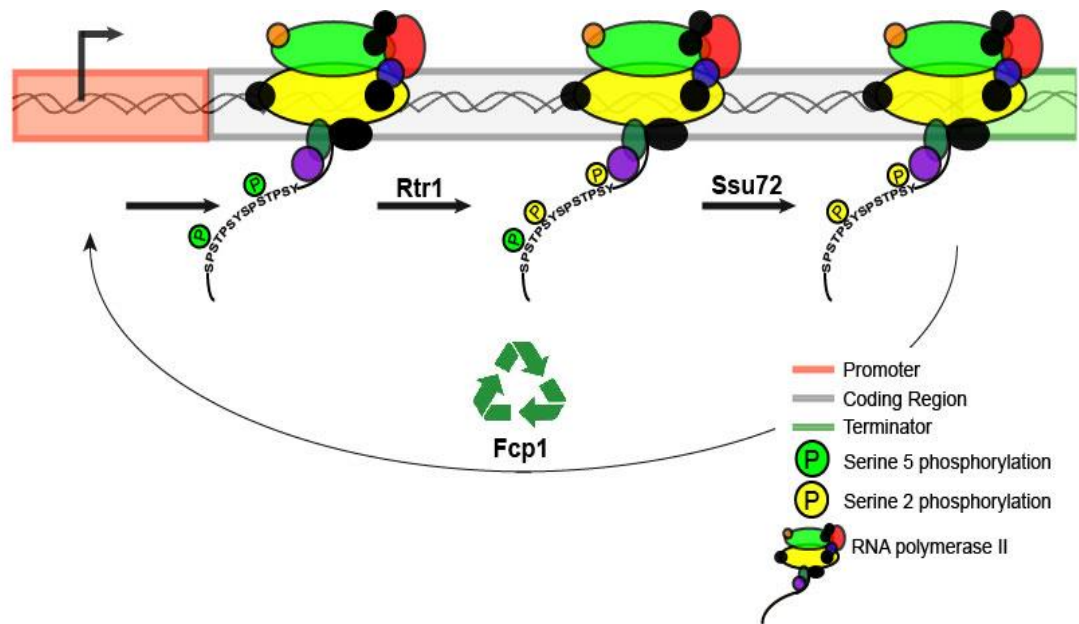


Figure 2. Model of regulation of phosphorylation of the RNA Polymerase II CTD during transcription elongation in *S. cerevisiae*. The roles of the three known protein phosphatases are hypothesized as indicated by serine phosphorylation patterns on the CTD. Dephosphorylation of S5 occurs in early elongation through the activity of Rtr1 (Mosley, et al. 2009), whereas Ssu72 activity has been implicated in removal of S5 from the CTD at the 3' end of the gene and is associated with the cleavage and polyadenylation of the nascent transcripts (Krishnamurthy et al., 2004). Fcp1 catalyzes the removal of phosphates from S2 residues and has been implicated in recycling of RNAPII to a stable initiation complex at the promoter (Cho, Kober et al., 2001).

As presented in Table 1, the paired activity of the protein kinases and phosphorylation occur throughout the transcription cycle. It should be mentioned that the human homologs of the yeast phosphatases have been identified and found to associate with RNAPII (Table 1) (Clemente-Blanco et al., 2011; Egloff, Dienstbier, et al., 2012; Sardu & Washburn, 2010; D. W. Zhang et al., 2012). Given the importance of the activity of dephosphorylation of the RNAPII, it is expected that defects of these regulatory genes have dire consequences. One prominent example is the human homolog of FCP1 (CTDP1) which has been unequivocally linked to a human disease. Congenital cataracts facial dysmorphism neuropathy (CCFDN) is an autosomal recessive, single

Table 1. Summary of CTD kinases and phosphatases in *S. cerevisiae* and mammals

CTD Residue	Function	Mammals	<i>S. cerevisiae</i>	Active Transcription Phase
S2	Kinase	Cdk9, Cdk12 (Cdk13?)	Bur1, Ctk1	Elongation
	Phosphatase	Fcp1, Cdc14	Fcp1	Late Elongation/Termination
S5	Kinase	Cdk7, Cdk8	Kin28, Cdk8 (Srb10)	Early Elongation
	Phosphatase	RPAP2, Scp1, Ssu72?, Cdc14	Rtr1, Ssu72	Early Elongation (yeast Rtr1)/Late Elongation/Termination (yeast)
S7	Kinase	Cdk7, Cdk9	Kin28, Bur1	Early Elongation
	Phosphatase	Ssu72?	Ssu72	Late Elongation/Termination
T4	Kinase	Cdk9?	?	?

? Enzyme has not been identified or suggested enzyme has not been confirmed as having this function. Table adapted from (Egloff et al., 2012)

nucleotide change in intron 6 of the CTDP1 gene which encodes the transcription phosphatase, FCP1 (Varon et al., 2003). This single nucleotide change causes destabilization of the FCP1 mRNA causing a 30% down-regulation in mRNA levels. The characteristics of the disease are abnormalities of the eye including bilateral cataracts,

microcornea and microphthalmia; dysmorphic facial features, and distal peripheral neuropathy (Kalaydjieva, 2006).

As detailed in our current working model (Figure 2), each CTD phosphatase is responsible for the removal of a specific phosphorylation event on the CTD during the transcription cycle, although some overlap exists (i.e. Rtr1 and Ssu72 removal of S5-P). It is not known whether each phosphatase recognizes the modification, catalyzed by a particular kinase or is specific to a particular set of CTD modifications with the exception of Ssu72 recognition of proline isomerization catalyzed by Ess1 (Werner-Allen et al., 2011) or doubly modified heptad repeats (i.e. CTD with S2-P and S5-P). In this thesis we will study the RNAPII modifications on both the CTD and the globular core of the enzyme in the presence and absence of Rtr1.

IV. Mechanisms for RNAPII degradation and recycling pathways

RNAPII recycling is necessary to enable continuous transcription cycles in actively growing eukaryotic cells. Actively transcribing RNAPII must overcome many obstacles that impede elongation and ultimate completion of mRNA production. Obstacles such as nucleosomal blocks, sites of DNA damage, and specific sequences result in natural pausing of the RNAPII independent of the regulatory factors associated with transcription (Svejstrup, 2007; Wilson, Harreman, & Svejstrup, 2013). Many of the key regulatory factors that enhance transcription activity are regulated by the phosphorylation state of the RNAPII CTD. The creation of initiation competent RNAPII following a completed transcription cycle is ultimately dependent upon the activities of the three characterized CTD phosphatases since hyperphosphorylation of the CTD of Rpb1 has been shown to reduce RNAPII occupancy on active genes in the event of CTD

phosphatase defects (Gilmore & Washburn, 2010; Laybourn & Dahmus, 1989; Mosley et al., 2009; Reyes-Reyes & Hampsey, 2007). One specific mechanism that has been hypothesized for efficient recycling of competent RNAPII complexes is gene looping (Sardiu et al., 2009; Singh & Hampsey, 2007). The phenomenon involves the physical interaction between the promoter and termination regions of a transcribed gene. Evidence has been found that links the promoter bound re-initiation scaffold through the GTF TFIIB which is known to associate with the CPF (El Kaderi, Medler, Raghunayakula, & Ansari, 2009). Of particular interest is the finding that Ssu72 was involved in the process (Singh & Hampsey, 2007; Tan-Wong et al., 2012) due to genetic and physical links to TFIIB. A second CTD phosphatase, Fcp1, has also been shown to play a significant role in RNAPII turnover following transcription termination (Fuda et al., 2012; Kobor et al., 1999). As a S2-P phosphatase, Fcp1 activity is essential in the creation of hypophosphorylated RNAPII which can then reinitiate transcription (Gilmore & Washburn, 2010; Kobor et al., 1999). Normal recycling of RNAPII through gene looping is advantageous to transcription in that it allows efficient use of pre-assembled complexes in response to dynamic environmental signals; however, when blocks to transcription are encountered or defects exist in any of the regulatory accessory proteins or complexes (i.e. Mediator, PIC, CPF, or capping, splicing, and/or 3' end processing machinery), transcription may be irrevocably arrested until extraordinary means of rescue are employed.

Natural stalling of transcribing RNAPII complexes occurs frequently in the dynamic process of gene expression (Svejstrup, 2002; Wilson et al., 2013). Causes of this stalling can be dense chromatin structures, nucleosomal blocks, GC rich areas on the

coding DNA strand and DNA damage caused by UV irradiation. One mechanism described for rescue of stalled RNAPII sites of DNA damage or dense chromatin structure utilizes ubiquitination to target stalled RNAPII (Anindya, Aygun, & Svejstrup, 2007; Reid & Svejstrup, 2004; Somesh et al., 2005; Svejstrup, 2007; Woudstra et al., 2002; Y. Zhang, Wen, Washburn, & Florens, 2009). This type of recycling or Transcription Coupled Repair (TCR) associated with DNA damage is accomplished through the mechanisms of Nucleotide Excision Repair (NER) or Base Excision Repair (BER). In both cases, the repair proteins rapidly converge and interact with the stably associated RNAPII/DNA/RNA ternary complex (Somesh et al., 2005; Svejstrup, 2002) when a DNA lesion is encountered during transcription elongation. When recruitment of repair factors is unsuccessful in rescuing the stalled RNAPII elongation complex, the RNAPII is marked for degradation by the ubiquitin/proteasome degradation pathway through addition of polyubiquitin chains (Somesh et al., 2007; Y. Zhang et al., 2009). In fact, two ubiquitin sites have been identified on the largest RNAPII subunit, Rpb1 at positions K330 and K695 by Somesh et al. (2005, 2007). Also of note is studies conducted by the same group, in which a correlation was found between increased turnover of Rpb1 with ubiquitin modification under DNA damaging conditions (Somesh et al., 2005). Although Rpb1 has been a focus of current studies, there is little known about the effects of TCR-coupled ubiquitination and subsequent proteasomal degradation on other RNAPII subunits. Multiple studies have suggested that the cytotoxic effect of proteasome inhibitors on tumor cells is related to suppression of DNA repair pathways (reviewed in Motegi, Murakawa, & Takeda, 2009; Vlachostergios, Patrikidou, Daliani, &

Papandreou, 2009). It is therefore important to understand the mechanisms by which the ubiquitin modification and proteasome degradation of RNAPII are involved in TCR.

V. Proteasome inhibition and alternative approaches to study protein turnover

The proteasomal degradation pathway is an essential mechanism for cellular processes, such as quality control, cell cycle, transcription, protein transport, and DNA repair. When combined, the 19S regulatory subunit and the 20S proteolytic core subunit of the proteasome (Swanson, Florens, & Washburn, 2009) is designated 26S proteasome. Located at the ends of the cylindrical 20S proteolytic core (or CP), the 19S (or RP) is responsible for the recognition and removal of ubiquitin chains from target proteins in an ATP-dependent reaction as it directs that target protein through the narrow channel leading to the center of the protease active site for subsequent degradation of the target protein. As discussed above, RNAPII pauses occur frequently during transcription and these arrests must be resolved in a timely and efficient manner in order to avoid ubiquitin tagging and proteasomal degradation. Figure 3 depicts a model of a stalled RNA and the potential ubiquitin labeling in preparation of proteasomal recognition and degradation.

RNAP II and barriers to transcription

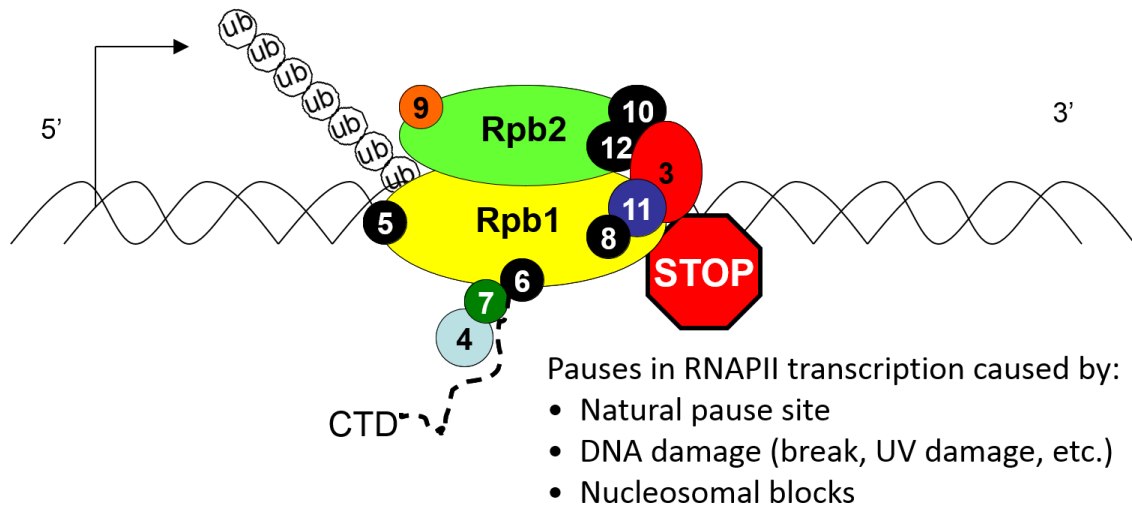


Figure 3. RNAPII naturally pauses during transcription elongation. Fully stalled or arrested RNAPII results in a barrier to mRNA production that the cell must deal with quickly and efficiently. If the stalled RNAPII cannot overcome the obstacle to transcription, the polymerase is targeted for ubiquitination and degraded by the 26S proteasome.

Preliminary data collected by Amber Mosley indicate that the loss of the CTD phosphatase, Rtr1, leads to decreased RNAPII occupancy on active genes (Mosley et al., 2009) as well as an increased association between polymerase and the proteasome as determined by proteomic analysis using mass spectrometry (Table 2). This data, along with previously discussed studies involving hyperphosphorylation in deletion strains with the inability to form initiation competent RNAPII, leads to a modification in our working model (Figure 4) and our hypothesis that the loss of RNAPII recycling is observed *in vivo* in CTD phosphatase mutant strains for *rtr1Δ*, *fcp1Δ*, and *ssu72Δ*. With a loss of the ability to reinitiate transcription and the potential for increased RNAPII stalling, it is possible that hyperphosphorylated RNAPII complexes are marked for degradation and removal from transcription sites. This hypothesis makes an assumption that the dephosphorylation targets in RNAPII for Rtr1, Ssu72, and Fcp1 are different and

therefore loss of any one phosphatase cannot be compensated for. This question is of broad interest and is being addressed by a number of different experiments carried out by other members of the laboratory.

Table 2. Selection of proteins identified by MudPIT analysis of Rpb3-TAP strains

Rpb3-TAP Purification from Wild-type cells				Rpb3-TAP Purification from <i>rtr1Δ</i> cells		
Protein Acronym	Total Number of Peptides	NSAF	Sequence Coverage	Total Number of Peptides	NSAF	Sequence Coverage
Rpb1	3906	0.085831	64.50%	3264	0.059932	63.30%
Rpb2	4025	0.125225	75.10%	3583	0.93148	63.70%
Rpb3	970	0.116159	76.20%	1245	0.124581	71.70%
Rpb4	495	0.085294	81.00%	667	0.096038	71.50%
Rpb5	276	0.048885	55.30%	505	0.074742	48.80%
Rpb6	57	0.014004	58.10%	146	0.029973	45.80%
Rpb7	249	0.055451	87.10%	313	0.58245	84.80%
Rpb8	346	0.090247	50.70%	209	0.045552	50.70%
Rpb9	111	0.034647	66.40%	136	0.035472	66.40%
Rpb10	323	0.175717	54.30%	465	0.211381	62.90%
Rpb11	280	0.88856	59.20%	250	0.066293	62.50%
Rpb12	58	3031553	60.00%	74	0.033639	60%
Spt5	18	0.000645	14.70%	32	0.000958	17%
Ubiquitin	0	0	0	5	0.002093	32.90%
Pre10	0	0	0	2	0.000221	4.90%
Pre6	0	0	0	1	0.000125	5.50%
Pup2	0	0	0	1	0.000122	5.40%
Rpn1	0	0	0	6	0.000192	5%
Rpn2	0	0	0	1	0.000034	1.20%
Rpt1	0	0	0	9	0.000613	10.90%
Rpt2	0	0	0	1	0.000073	4.80%
Rpt4	0	0	0	6	0.000147	10.50%
Rpt5	0	0	0	5	0.000367	8.50%
Rpt6	0	0	0	2	0.000157	6.40%

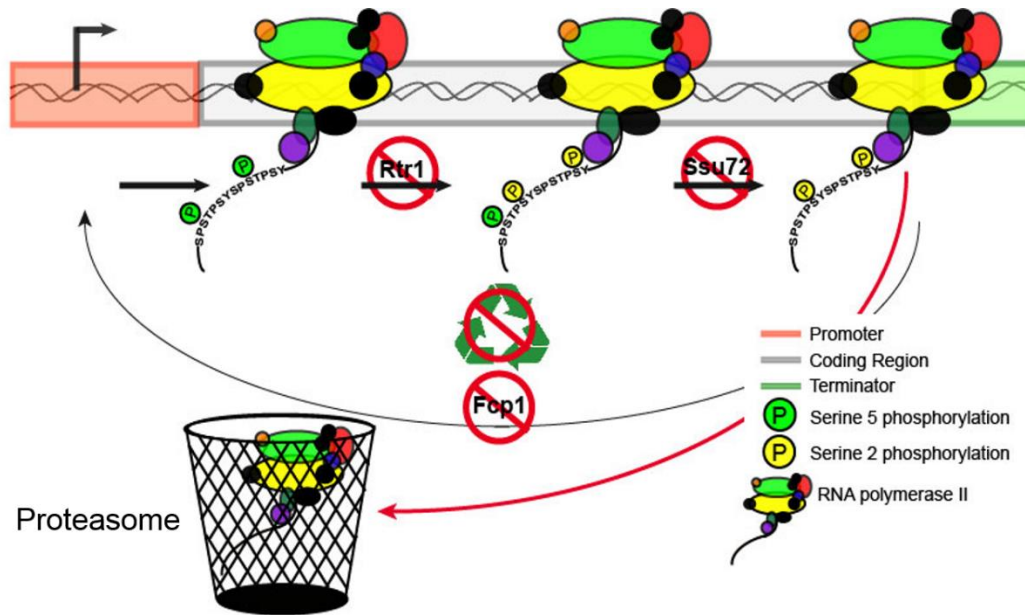


Figure 4. Current working model for RNAPII recycling and degradation following the loss of CTD phosphatases. We hypothesize that hyperphosphorylated RNAPII will be unable to initiate subsequent transcription cycles and are therefore ubiquitinated and targeted for degradation by the proteasome.

The approach we will use to examine the proteasome dependent degradation of RNAPII through chemical induction of proteasomal inhibition. There are several peptide aldehyde inhibitors of proteasomes that have been used reliably in yeast mutated to enhance permeability (D. H. Lee & Goldberg, 1996). These inhibitors function by blocking the active sites of the proteasome (Gaczynska & Osmulski, 2005). One specific reagent that has been used in relevant experiments is Carbobenzoxyl-leuciny-luciny-l-leucinal (MG132) (X. Chen, Ruggiero, & Li, 2007; D. H. Lee & Goldberg, 1996; Liu, Apodaca, Davis, & Rao, 2007; Rock et al., 1994). To test our model, we will inhibit proteasome function to determine if hyperphosphorylated RNAPII accumulates further with disruption of Rtr1 function and proteasome inhibition.

Normally, wild type (WT) yeast cells are impermeable to MG132; however, this can be overcome using an *erg6Δ* deletion in our strain of study (D. H. Lee & Goldberg,

1996). *ERG6* is a methyltransferase enzyme involved in biosynthesis of ergosterol and normal cell membrane function and defects create leakage of the membrane (Gaber, Copple, Kennedy, Vidal, & Bard, 1989; Jensen-Pergakes et al., 1998). The use of mutant yeast strains with enhanced permeability as background to CTD phosphatase deletions will allow the cells to take up the drug resulting in the inhibition of proteasome function. In addition, each strain will be modified with the addition of a TAP tag to the C-terminus of Rpb3 polymerase subunit at its endogenous locus (Washburn, 2008). Purification using Tandem Affinity Purification (TAP) of both *erg6Δ* and *erg6Δrtr1Δ* could reveal novel interactions involved in signaling for proteasome degradation.

There are several alternatives to using proteasome inhibition to study the role of CTD phosphatases in regulation of RNA Polymerase II recycling. For example, the use of temperature-sensitive alleles of some of the predominant 26S subunits (ie *PRN5* and *PRN6* from the 19S RP and *PUP2*, *PRE8*, and *PRE1* from the 20S CP) along with CTD phosphatase mutants would allow proteomic studies to be conducted without risking lethal deletions. The altered function of these proteins can be investigated using tagged constructs to aid in co-purification schemes through TAP. Another approach would use strains with a ubiquitin tag incorporated into the genome, similar to the TAP tag. This approach has been successful recently by Starita et al. (Starita, Lo, Eng, von Haller, & Fields, 2012) in studies which expressed only 8XHis tagged ubiquitin. The His-tagged proteins were isolated, purified and subjected to liquid chromatography tandem mass spectrometry (LC-MS/MS). Alternative studies could express this tagged-ubiquitin in a phosphatase deletion background (ie. *rtr1Δ*, *fcp1Δ*, and *ssu72Δ*) and subject isolated proteins to affinity enrichment and LC-MS/MS.

VI. Transformation of yeast for C-terminal domain tagging via homologous recombination

Transformation of yeast strains for the purpose of introducing stably expressed fusion tags to investigate gene expression in an efficient and cost effective manner is quickly becoming a standard method of proteomic scientists (Banks, Kong, & Washburn, 2012; Li, 2011). The method development began with the discovery that *E.coli* DNA could be stably integrated into a yeast chromosome in an additive or substitutive manner (Hinnen, Hicks, & Fink, 1978). Adding to this finding, Orr-Weaver et al., (1981) described a new method of integration for circular and linear plasmid DNA into yeast chromosomes using the cellular mechanism of double strand break repair. This improved the efficiency of integration and defined integration points within the yeast genome (Orr-Weaver, Szostak, & Rothstein, 1981).

Methods of improving transformation efficiency were also explored at that time and one in particular is still being used today. Gietz et al. determined an optimized transformation method that increased efficiency to 1.2×10^6 transformants per ug of plasmid DNA (Gietz, St Jean, Woods, & Schiestl, 1992) through the introduction of a single-stranded DNA (ssDNA) carrier to bind to the permeable cell membrane allowing the transforming DNA to work in the nucleus. Another improvement was developed in 1993 by Baudin et al. who used the polymerase chain reaction (PCR) amplification of transforming DNA fragments which include oligonucleotides synthesized with homology to chromosomal targets and a selectable marker (Baudin, Ozier-Kalogeropoulos, Denouel, Lacroute, & Cullin, 1993). The high rate of homologous recombination in yeast allowed researchers to forgo the need to construct plasmids to introduce exogenous

genetic material and instead use PCR to amplify only the region that is needed for transformation (Baudin et al., 1993; Puig et al., 1998). This development of gene disruption cassettes became an attractive system to incorporate a method for native protein purification. Along with their colleagues, Rigaut and Puig exploited the features of transformation with the use of methods described previously (Puig et al., 2001; Rigaut et al., 1999) including a disruption cassette that would allow for tandem affinity purification of tagged protein targets at the C-terminus of the endogenous locus with a TAP tag. The TAP tag includes a *Staphylococcus aureus* calmodulin binding protein sequence (CBP), followed by a Tobacco Etch Virus (TEV) protease cleavage site and the IgG binding domain of Protein A of *S. aureus* linked to a selection marker, such as URA3 (Rigaut et al., 1999; Washburn, 2008).

As shown in Figure 5, the TAP tag structure includes a two step-affinity sequence as well the purification strategy used for tagging native proteins (Puig et al., 2001; Rigaut et al., 1999). The tagged protein in this method acts as bait for immunoprecipitation of any proteins in direct interaction or indirect interaction through other subunits of larger functional protein complexes.

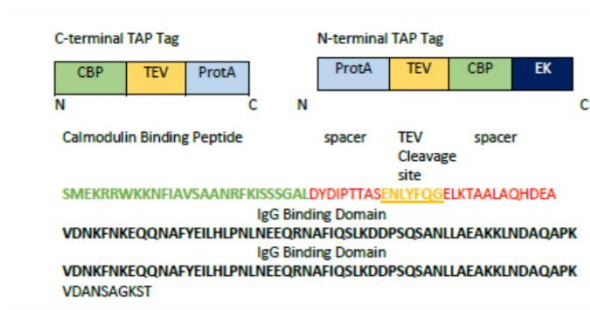
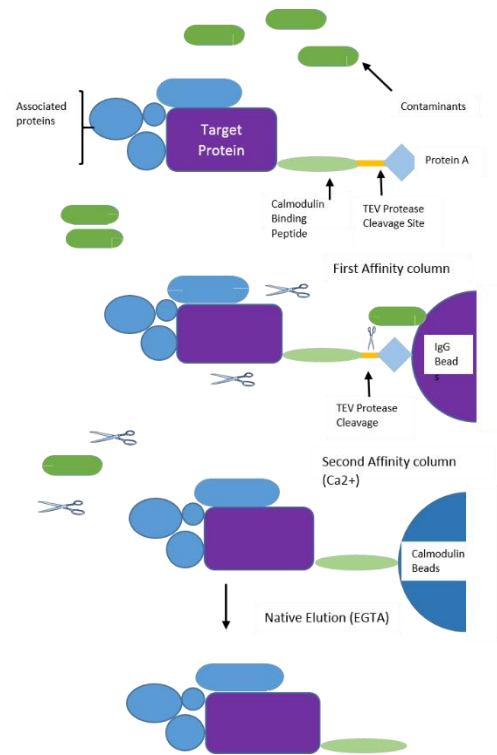
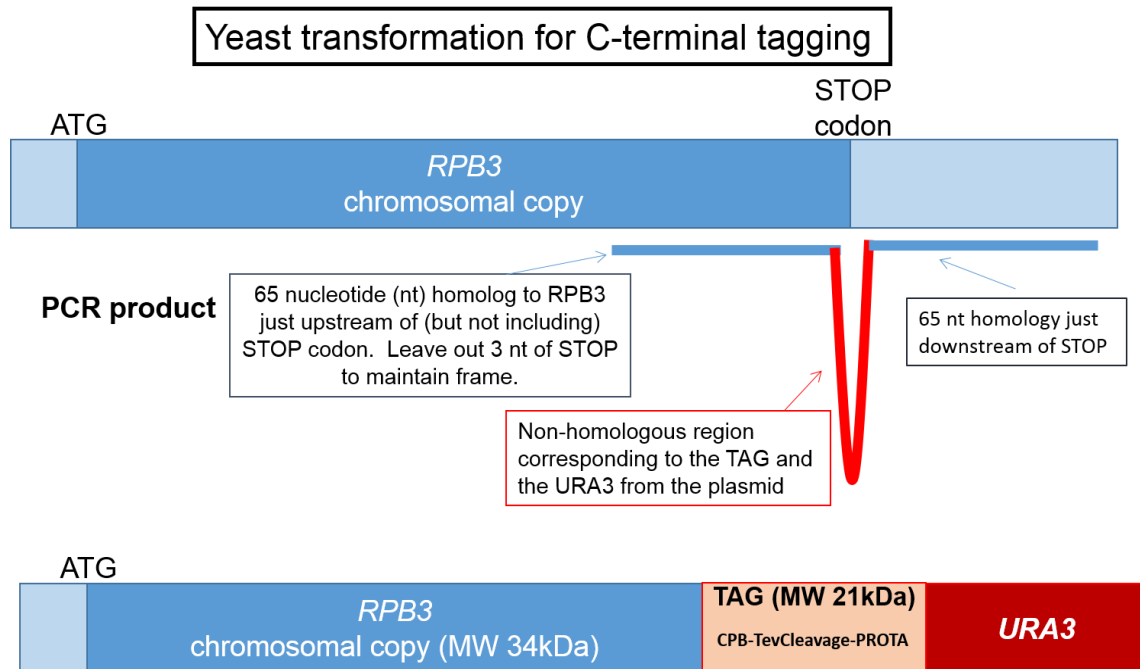


Figure 5. Structure and sequence of the TAP tag (above) and Schematic representation of the TAP strategy (right) adapted from Rigaut et al., 1999 and Puig et al., 2001.



Purification of proteins in physiologically non-denaturing conditions is necessary to maintain native activity related to function and protein interactions. The studies presented here utilized the above TAP method adapted by Mosley et al. (Mosley et al., 2009) to increase the solubility of DNA and chromatin-associated proteins through the addition of heparin sulfate and DNaseI treatment, which was added following extract preparation but prior to centrifugation to tag and isolate the RNAPII subunit, Rpb3 (Mosley et al., 2009). The goal was to identify protein interactions and post-translational modifications through multidimensional protein identification technology. A schematic of the disruption cassette prepared for this experiment can be found in Figure 6.



Rpb3-TAP – expressed protein contains C-terminus with dual-affinity tag for CBP and Protein A separated by a Tev Cleavage sequence and total MW of ~55kDa.

Figure 6. Schematic of TAP tag disruption cassette used to create Rpb3-TAP *S. cerevisiae* strains.

VII. Multidimensional protein identification technology (MuDPIT) to determine protein-protein interaction and potential post-translational modifications

Multidimensional protein identification technology (MuDPIT) was developed in 2001 by Washburn and colleagues and couples two methods commonly employed for protein analysis; liquid chromatography and mass spectrometry (Washburn, Wolters, & Yates, 2001). These analytical methods individually can provide information about specific molecular properties of proteins within a complex, heterogeneous sample; however in combination, they have become a first line technology in protein identification. The evolution of the current technology occurred more than a decade ago when it became clear that there was a real need for more efficient, accurate and comprehensive means of identifying proteins interacting in complex biological systems

(J. S. Lee et al., 2007; Link et al., 1999; Washburn et al., 2001). Development of the method was improved with the addition of pre-separation sample enrichment using TAP technology as described in the previous section (Bauer & Kuster, 2003; Florens et al., 2006; Graumann et al., 2004). Reduction in the complexity of the protein mixture as part of the overall experimental study design is often necessary due to the overwhelming amount of peptide data, which can be generated using the MuDPIT method. Therefore the use of purification techniques, such as TAP, are extremely beneficial when determining specific protein interactions or looking for post-translational modifications (Pavelka et al., 2008).

Determining protein-protein interactions in large protein complexes is key in understanding the function of each constituent, as well as determining the regulatory mechanisms for the complex as a whole. The success of MuDPIT for the identification of protein-protein interactions is often established during preparation when the complex protein samples, such as cell lysates, are subjected to digestion with proteolytic enzymes to produce fragments of the full-length proteins. Meticulous sample preparation to avoid the “junk-in, junk-out” digestion of the protein mixtures for MS analysis is a very important step. Preparation begins with solubilization using 8M urea followed by reduction and alkylation. Since the enzymes used to generate the digested peptide fragments have specific cleavage sites, the fragments created terminate with precise amino acid sequences. One of the most common proteolytic enzymes used is trypsin, which cleaves proteins at the C-terminal side of arginine and lysine residues. The presence of C-terminal basic residues aids in peptide ionization and facilitates shotgun proteomics analysis (Olsen, Ong, & Mann, 2004). In addition to trypsinization, the use

of a second protease such as Endoproteinase Lys-C (Lys-C) has been found to increase the number of peptides identified and improve overall sequence coverage than just using trypsin alone (Florens & Washburn, 2006). This in turn directly impacts the number of unique proteins identified following MS output and data base searching through matching of experimentally and theoretically derived fragments.

Prior to using mass spectrometry, resolution of proteins in complex samples was achieved through a lengthy separation process. SDS-PAGE and liquid chromatography had been used for protein separation traditionally, however each method has limitations for resolution of low abundance proteins, proteins of extreme size or pH, and extremely hydrophobic proteins (Gygi, Corthals, Zhang, Rochon, & Aebersold, 2000). SDS-PAGE, which separates proteins based on their relative size as they migrate through a solid gel while exposed to an electrical charge, achieved the best separations in conjunction with prior separation by isoelectric focusing, which separates proteins according to their individual pIs. This two dimensional electrophoresis (2DE) method also requires staining and removal of proteins isolated in the gel, making this method both time consuming due to the need to excise individual spots of protein from the gel and limiting in the number of low abundance proteins that could be identified since spots of proteins present in low quantities would not be as apparent on the stained gel (Fournier, Gilmore, Martin-Brown, & Washburn, 2007; Gygi et al., 2000).

To improve the separation of the peptides in complex samples of limited quantity, a two dimensional liquid chromatography method using a capillary silico tubing was coupled sequentially to the mass spectrometer (Link et al., 1999; Washburn et al., 2001). The two dimensions involved in separation are a reverse phase (RP) of C18 resin

followed by a strong cation exchange (SCX) resin. This allowed for almost complete separation of the components in the sample using an incrementally increasing salt concentration through the run. The addition of a second RP following the SCX further improved the separation and increased the number of resolved peptide fragments exposed to MS analysis and potential detection in the subsequent database inquiry (Florens & Washburn, 2006).

The final step of protein identification (and the most computationally expensive) in MuDPIT involves the comparison of experimentally obtained peptides to a collection of predicted or theoretically derived peptide sequences in a database (Keller, Nesvizhskii, Kolker, & Aebersold, 2002). There are several important parameters programmed into a database search that can determine whether a peptide match is assigned or not. These include the type of proteolytic enzyme used for sample digest and whether partially or fully digested; intentional and suspected modifications such as acetylation, carbamylation, methylation, phosphorylation, and ubiquitination; limits for acceptable peptide size and cross-correlation (e.g. Xcorr in SEQUEST) or statistical matching score to an *in silico* derived peptide; and high and low limits for false discovery rates (FDR).

One key to obtaining correct protein identifications in MuDPIT data analysis is the calculation of FDRs which is the anticipated proportion of peptide to spectrum matches (PSM) identified incorrectly within a global collection of acquired PSMs (Nesvizhskii, 2010). Importantly, the individual PSMs are subject to a statistical calculation called a posterior probability which is an estimate of the correctly identified PSMs in a collection of peptides with similar database search scores (Nesvizhskii, 2010). Firmly setting the FDR limits helps to define the PSMs, which are considered statistically

valid based on the available parameters and experimental spectra obtained if they fall within the constraints set. This validation of the PSMs contributes to the determination of true versus false peptide identifications and is ultimately how protein identifications in complex MS/MS data analysis are established. Due to the importance of determining accurate protein identifications for a collection of spectra, each individual PSM is first assigned a single spectrum confidence score which ranks them based on the similarity between the experimental spectra acquired by the MS/MS and the theoretical database spectrum (Nesvizhskii, 2010). The ranking is determined by converting each individual score into a *p*-value or *E*-value depending on the database search software used.

These measures can then be used in calculating the FDR using several methods (Nesvizhskii, 2010). Two are discussed here as they relate to data analysis performed in this work. The first method employs the use of Target-Decoy database compare acquired MS/MS spectra to a protein database containing target protein sequences for the experimental dataset, as well as a decoy set of protein sequences generated by using random or reversed sequences of the target proteins of the same size (Elias & Gygi, 2007; Nesvizhskii, 2010).

The calculation for FDR simply is: $\text{False Positive IDs} / \text{total False Positives} + \text{True Positives}$ at a pre-determined score cutoff. This method is commonly used for FDR estimates and is the method contained in our Proteome Discoverer software. One of the drawbacks of this method of calculating FDR is its simplicity. For example, this calculation for FDR does not take into account the lack of complete decoy sequences for post-translational modifications and potential chemical modifications (Nesvizhskii, Keller, Kolker, & Aebersold, 2003).

The second strategy for determining the FDR is a mixed model method, which contains a more advanced FDR calculation by considering additional parameters beyond just the false positive ratio such as the database search scores and other properties of assigned identities to peptides (Nesvizhskii et al., 2003). Briefly, this method estimates the error rate of individual peptide identifications by selecting the most likely peptide or best match from the target database and computing a posterior probability using data from two separate algorithms, the expectation maximization (EM) and the mixture estimation algorithm(Choi & Nesvizhskii, 2008; Keller et al., 2002; Nesvizhskii, 2010). The EM algorithm distinguishes correctly assigned peptides from false positive results using the distribution of search scores and other parameters while the mixture estimation algorithm incorporates the decoy dataset in estimating the false PSMs (Nesvizhskii, 2010). The resulting probabilities are then used to filter the PSMs at a predetermined FDR. This method allows for a more accurate and reliable overall FDR derived from robust posterior probabilities of individual PSMs (Nesvizhskii, 2010). This model is used in many newer analysis software packages including Scaffold™ (aka Scaffold), which was utilized in part for MS/MS data analysis in this current work. Additionally, this type of calculation is now included in the module Percolator in Proteome Discoverer. Unfortunately, we have been unable to employ Percolator since it is implemented within Proteome Discoverer as a 32-bit program and the dataset that we have generated are larger than 2GB, which exceeds the program parameters.

METHODS AND MATERIALS

I. Preparation of whole cell lysates following MG132 treatment

Untagged strains of *Saccharomyces cerevisiae* wild type BY4741, and derived deletion strains containing *rtr1Δ*, *erg6Δ*, or *rtr1Δerg6Δ* were cultured on YPD (10% Yeast Extract, 20% Peptone, 20% Dextrose) medium in liquid or agar plates at 30°C. After 3 days growth, liquid pre-cultures were initiated by inoculating 25ml of YPD broth with a single colony for each strain. Cultures were grown overnight at 25°C with shaking at 150-200rpm. The growth phase of each culture was evaluated by measuring the optical density (OD) at 600nm using a Bio-Rad spectrophotometer by first diluting the sample to approximately OD₆₀₀ ≈ 1 in 200ml of YPD. Yeast cells were allowed to recover for 2 hours before beginning MG132 treatment experiment.

During recovery, 2.4mg of MG132 was resuspended in 1ml DMSO (Sigma Cat. No.D4540) for a stock concentration of 5mM. A working solution of 500μM MG132 (Calbiochem Cat. No. 474790-1MG) was prepared just prior to spiking into cultures by diluting 5μL stock into 45μL DMSO. Following the recovery period, all four cultures were split into two 100ml volumes which were designated for MG132 treatment or untreated. The cultures were then spiked with 10μL MG132 or DMSO control.

Treatment was stopped after 3 hours by harvesting all cultures in the same order in which they were treated. OD₆₀₀ values of the harvested cultures ranged between 4.4 and 5.4. Collected samples were centrifuged (2 x 50ml centrifuge conicals) at 10,000rpm for 5 minutes at 4-6°C. The supernatants from all 8 treatment conditions were discarded and the pellets were frozen at -80°C.

Cell pellets were thawed completely and each treatment was combined into one conical tube and mixed thoroughly. Combined pellets from each treatment were aliquoted into 2 microcentrifuge tubes and one aliquot of each was frozen at -80°C for later studies, whereas the other aliquot was washed with 250ul TAP Lysis Buffer (350mM NaCl, 40mM Hepes, 10% Glycerol, 0.1% tween-20, 0.5mM DTT, and 1X yeast protease inhibitors). After adding the lysis buffer, lysis was performed by vortexing using approximately 250 μl of glass beads (0.5mm, Cat. No. 11079105, Biospec Products, Inc.) in a Disruptor Genie (Thermo-Fisher) at 4°C for 20 minutes. The samples were centrifuged for 10 minutes at 14,000rpm at 4°C in an Eppendorf 5430R centrifuge. The clarified supernatants were then transferred to clean centrifuge tubes. Protein concentrations of each sample were determined using the Bicinchoninic (BCA) Protein Assay (Pierce, Cat. No. 23225). Protein concentrations were calculated by comparing 1:100 dilutions of each sample in duplicate to a standard curve created with known concentrations of bovine serum albumin. Samples (50 μg of total protein) were diluted with 4X SDS-PAGE loading dye and vortexed for 5 seconds. To ensure that no residual sample remained in the tube cap or on the sides of the tube, each sample was centrifuged for 1 minute at 14,000rpm in Eppendorf 5424 microcentrifuge. Samples were boiled for 5 minutes in a dry heat block at $\sim 100^{\circ}\text{C}$, vortexed and centrifuged again and were then loaded onto 10% SDS-PAGE gels (40% polyacrylamide, 1M Tris-HCl, pH 6.8, 10% ammonium persulfate, 10% SDS, and 8 μl TEMED) with molecular weight standards loaded onto adjacent wells of the gels (5 μL of Precision Plus protein dual color standards) Bio-Rad, Cat. No. 161-0374). Electrophoresis of gels was carried out at 175V for 1hr in 1X Tris-Gly-SDS Running Buffer (Bio-Rad Cat. No. 161-0732). The WT

(BY4741) and *rtr1Δ* samples were loaded on one gel and the *erg6Δ* and *erg6Δ rtr1Δ* samples were loaded on a second gel.

II. Western Blot Analysis

Following SDS-PAGE, the stacking gel was removed and the gels were transferred to nitrocellulose membranes (Bio-Rad, Cat. No. 162-0115) overnight in Transfer Buffer (5.8g Tris-HCl, 2.9g Glycine, 100ml Methanol, 3.75μL 10% SDS) at 30V with an ice pack to prevent overheating during transfer. After overnight transfer, the nitrocellulose membranes were removed from the transfer apparatus, marked on the gel-facing side and placed in 5 % milk Blocking Buffer (5 grams dry milk in Tris-buffered Saline (TBS)) for approximately 8 hrs. Prior to incubation of the membrane with primary antibody, each membrane was cut in half horizontally just below the 75 kDa standard mark so two antibody probes could be used on all samples loaded. The top half of the membrane was incubated overnight at 4°C in 1:1000 dilution of anti- serine 5 phosphorylated CTD (Clone H14, Covance, Table 3) in 5% milk blocking buffer. This antibody is specific for the largest protein subunit in RNAPII, Rbp1. The bottom half of the membrane was incubated overnight with 1:1000 anti-Pgk1 (Life Technologies) as a loading control for each experimental sample. Pgk1 stands for phosphoglycerate kinase 1 and was chosen as a loading control because it is a constitutively expressed protein and should be in high concentration for each experimental sample and would confirm similar protein loading for each sample. Primary antibody solutions were removed the following day and membranes were washed 3 x 5 minutes each in TBS. Secondary antibody were prepared as 1:5000 dilutions in TBS. The Rpb1 secondary antibody used was peroxidase conjugated anti-mouse IgM (Sigma) and the secondary antibody used for Pgk1 was

peroxidase conjugated anti-mouse IgG (GE Healthcare). After incubating for 1 hr at room temperature the secondary antibody solutions were removed and the membranes were washed 3 x 5 min in TBS. Visual detection of the reaction products was done using the ECL HRP kit (GE Healthcare Cat. No. RPN2133) according to the manufacturer's instructions and images were taken using the FLA 5000 Scanner (Fuji) at 473nm using a LPB filter.

Antibodies and titers used for additional Western blot analyses are presented in Table 3. Procedures are as described for all Western blots with modifications to incubation times from 4hrs to overnight for primary antibodies as time allowed.

Table 3. Antibodies used for Western Blot analysis				
Antibody Name	Mfr	Secondary Antibody	Titer	Diluent
Anti-Serine 2 RNAPII CTD	Neoclone	Anti-Mouse IgM	1:500	TBS
Anti-Serine 5 RNAPII CTD	Covance	Anti-Mouse IgM	1:500	5% Milk
Anti-Serine 7 RNAPII CTD	Dirk Eick	Anti-Rat IgG	1:250	5% Milk
Anti-Tyrosine 1 RNAPII CTD	Chromotek	Anti-Rat IgG	1:1000	TBS
Anti-Pgk1	Life Technologies	Anti-Mouse IgG	1:1000	5% Milk
Anti-Rpb4	Neoclone	Anti-Mouse IgG	1:1000	TBS
Anti-CBP	Santa Cruz	Anti-Goat IgG	1:1000	5% Milk

III. Transformation of *S. cerevisiae* deletion strains for C-terminal tagging of Rpb3

A frozen sample of bacterial stock (pAM108) containing the pBS1539 plasmid was directly inoculated into LB-Ampicillin (AMP) media (10mL) and incubated overnight at 37°C with shaking. Cell lysis and isolation of the plasmid were performed following the procedure found in QIAprep Miniprep Handbook (12/2006) using a Qiagen Miniprep isolation kit (Qiagen Cat. No. 27106). In brief, the bacterial culture was

centrifuged for 10 minutes at 5400 x g at 4°C after transferring cells to a 15mL conical tube. The supernatant was removed and the cell pellet was drained over a paper towel for 5 minutes. The packed cell pellet was resuspended in 250µL of Buffer P1 until no visible clumps were present and then transferred to a micro centrifuge tube. Buffer P2 (250µL) and Buffer N3 (350µL) were added sequential with mixing by inversion after each addition.

Following centrifugation (17,900xg for 10 minutes at room temperature), the supernatant was decanted into a QIAprep spin column and placed into a clean micro centrifuge tube to collect the flow through. The spin column with collection tube was then centrifuged for 1 minute at 17,000xg at room temperature. The flow through was discarded and the silica gel membrane in the column was washed with 0.75mL of Buffer PE by centrifuging for 1 minute at 17,000xg at room temperature. The column was centrifuged a final time after discarding the flow through and then transferred to a clean micro-centrifuge tube for collection of final isolation product. Buffer EB (50µL) was added to the column and incubated for 1 minute. The column was centrifuged for 1 minute at 17,000xg at room temperature. Spectrophotometric analysis (A260/A280) of the final sample was done to determine the concentration of the isolation product using the dsDNA method on the Eppendorf Biophotometer Plus using a sterile, disposable cuvette after using an aliquot of Buffer EB as a blank. The stock plasmid DNA was then diluted to obtain a 100 pg/µL concentration for the PCR amplification protocol. The isolated plasmid, pBS1539, was used as a template for a standard PCR method set in a total reaction volume of 100 µL. Table 4 shows the reaction components and volumes of each. Table 5 details the thermocycler parameters used for each amplification done.

Three total reactions were necessary to obtain enough purified PCR products containing the TAP construct for the yeast transformations. Ideally, 1 µg of the purified disruption cassette is needed per strain (Baudin, et.al. 1993), however a total of 1.8 µg was recovered and split between the two transformation reactions.

Table 4. Details of PCR reaction mixture

Component	Volume added	Concentration
DNase-free Water	69 µL	N/A
5X GoTAQ Buffer	20 µL	N/A
dNTPs	3 µL	N/A
Rpb3 TAP F primer	3 µL	10 µM
Rpb3 TAP R primer	3 µL	10 µM
DNA pBS1539	1 µL	100 pg/µL
Go Taq	1 µL	N/A
Final Reaction Volume	100 µL	

Table 5. Details of PCR parameters

Cycle	Temperature (°C)	Time
Initial Melting	94	2 min
1-30	94	15 sec
	52	30 sec
	72	2 min
Final Annealing	4	Hold until retrieved

Following amplification, completed reaction mixtures were loaded onto a 1.5% agarose gel (1.5g Agarose, 100mL TBE) with the addition of SYBR green (5µL/100mL) for visual detection. Samples and a 1kB DNA molecular weight markers were electrophoresed for 30 minutes at 140V. Once electrophoresis was completed, the gel was placed in a Chemidoc XRS molecular imager to collect an image of the PCR product bands in the gel using Quantity One software. The bands were cut from the gel and purified using Promega DNA purification kit (Promega Cat. No. A2492).

Excised bands were placed in 1.5mL micro centrifuge tubes and gels were dissolved at 65°C after the addition of 10µL Membrane Binding Solution. Membrane Binding Solution (200µL) was added to the dissolved gel and then transferred to a mini-column and subjected to vacuum filtration to bind amplified PCR products. Following filtration, the membrane was washed twice with 700µL and 500µL of Membrane Wash Solution, respectively. The mini-column with bound DNA was then transferred to a collection tube and centrifuged for 5 minutes at 16,000xg. The mini-column was eluted with 50µL of nuclease-free water by centrifuging for 1 minute at 16,000xg. Spectrophotometric analysis to determine the purity and concentration of the final eluted DNA was determined as described above section and stored at -20°C for later use.

Incorporation of epitope or fusion tags is an efficient way of facilitating the purification of target proteins or protein complexes (Baudin et al., 1993; Puig et al., 2001; Puig et al., 1998). Transformation of yeast strains stimulates uptake of a specific disruption cassette and integration into the yeast chromosome of interest by homologous recombination. C-terminal tagging by homologous recombination allows for the purification of protein complexes under native conditions (Puig et al., 2001). In order to produce TAP tagged cultures for this study, pre-cultures (5mL) of yeast strains deleted for the *ERG6* gene (yAM153) and *RTR1* and *ERG6* (yAM154) genes were grown in YPD media overnight with rocking at 30°C. Yeast cultures (25ml) were inoculated at OD600 ≈0.25 and grown for 6 hours before transferring each a portion of each culture to 15mL conicals (2 x 10mL aliquots for each genotype). The remainder of the initial cultures was discarded.

The transformation was performed by first collecting the cells by centrifugation at 3000 rpm for 5 minutes at 4°C. A separate transformation mixture was prepared to create both *erg6Δ* and *rtr1Δ erg6Δ* transformation competent cells. The supernatants were poured off and the packed cell pellets were resuspended in 100μl fresh TE-LiOAc (100μL of 10X 0.1M Tris-HCl, 0.01M EDTA, pH 7.5 and 100μL of 1M LiOAc, pH 7.5 diluted with 800μL sterile water). The cells were allowed to equilibrate while the remaining reaction components were prepared. Approximately 0.9μg (in 45μL) of amplified PCR product containing the TAP tag construct was added to each cell suspension and vortexed. Salmon sperm DNA (ssDNA) at a concentration of 10 mg/ml was boiled for 10 minutes and kept in ice until ready for use. Following addition of the disruption cassette to each cell suspension, 5 μL of ssDNA was added and vortexed. One aliquot of *erg6Δ* competent cells was set up as a negative control with addition of only ssDNA. To complete the mixture, 600μL of fresh PEG-LiOAc (For 10mL: 8ml 50% PEG 3350, 1mL 10x stock of TE, and 1mL 1M LiAOc) was added and vortexed thoroughly and mixed by inverting each tube several times. The mixtures were then heat shocked at 42°C for 20 minutes. Following overnight incubation at 4°C, transformed cells were collected by centrifugation for 1 minute at 4000xg and supernatants were discarded. Each cell pellet was resuspended in 200 μL sterile water and spread onto pre-warmed YNB URA- agar plates using glass beads. The yeast agar plates were incubated at 30°C until visible colonies began to appear in ~3-4 days.

To ensure that the TAP tag was incorporated by homologous recombination (i.e. integrated) into the *erg6Δ* and *erg6Δ rtr1Δ* strains, Western blots were done to confirm the expression of the Rpb3-TAP fusion protein. Each colony that grew on the YNB

URA- plates was considered a potential transformant and was restreaked for isolation onto a fresh YNB URA- plate. After incubating for 2 days at 30°C, 25ml of YPD media was inoculated with a single colony from the restreak of each of the original colonies and incubated overnight at 30°C. Each sample was centrifuged for 10 minutes at 4000xg at room temperature and whole cell lysates were prepared as described previously for the MG132 small scale study. Samples were run on 10% SDS-PAGE with 2x loading dye (15uL lysate + 15uL 4x loading dye) for 1hr at 200V. The separated protein mixtures were then transferred to nitrocellulose membranes for 3 hrs at 50vV by western blotting in transfer buffer. The nitrocellulose membrane was removed and marked on the gel facing side and blocked in 5% milk blocking buffer for 30 minutes. The blocked membrane was probed using Anti-CBP (Thermo Fisher Cat. No. CAB1001), which is specific to the calmodulin binding peptide portion of the TAP tag that would be present as part of the TAP tag at the C-terminus of Rpb3 if the tag was truly incorporated into the Rpb3 locus in the yeast genome. The primary antibody was diluted at 1:1000 in 5% milk blocking buffer and incubated with the membrane overnight. The primary antibody solution was removed the next day and the membrane was washed 3 x 5 minutes with 1x TBS. Peroxidase conjugated anti-rabbit IgG (GE Healthcare Cat. No. NA934A) was used as the secondary antibody. The secondary antibody was diluted 1:1000 in TBS and incubated with the membrane for 1 hr. After incubation, the membrane was washed in TBS 3 x 5 minutes. As with the previous blot, the ECL HRP (GE Healthcare Cat. No. RPN2133) detection was used and the membrane was imaged using the FLA 5000 scanner.

TAP Method 1: Liquid Nitrogen Freezing Lysis

Before a large scale proteosomal inhibition study was begun, a pilot large scale purification using the new TAP-tagged *S. cerevisiae* mutant strains Rpb3-TAP *erg6* Δ and Rpb3-TAP *erg6* Δ *rtr1* Δ was performed to confirm that the cells would be suitable for the large scale MG132 treatment study. Pre-cultures (25 mL) of the newly created strains were inoculated and grown in YPD media overnight at 30°C. The OD600 of each culture was used to determine the amount to add a 3L YPD batch size to reach an OD600 between 4-6 during an overnight growth. The following day, OD600 determinations were obtained and the Rpb3-TAP *erg6* Δ strain was slightly at 6.2 and the TAP procedure was begun. The Rpb3-TAP *erg6* Δ *rtr1* Δ growth was still less than optimal after allowing an additional 2 hrs growth with OD600 3.0. Both cultures were harvested, centrifuged at 4000rpm for 10 minutes at 4°C and then washed with MilliQ Water. Following centrifugation and removal of the supernatant, the packed cell pellets were frozen until the lysis procedure was performed the following day.

At this point, after observing that the Rpb3-TAP *erg6* Δ *rtr1* Δ strain had a significantly lower growth rate than the Rpb3-TAP *erg6* Δ , a growth curve study was done to get a better estimate of lag time needed for recovery following inoculation and between the two cultures. Small 25 mL cultures of each strain were inoculated at OD600~ 0.5. Cultures were incubated at 30°C for the duration of the study except when samples were removed. Samples (1 mL) of each were removed once every hour for 8 hrs and the OD600 result was recorded.

The TAP procedure for method 1 was performed by resuspending thawed packed cell pellets in TAP Lysis Buffer at ratio of approximately 10:1 of buffer to cell pellet

(vol/vol). The cell mixture was added to a liquid nitrogen bath using an 18-gauge needle and syringe and ground into a fine powder by hand using a mortar. Crushed cells were subsequently transferred to a stainless steel Waring blender to be ground with dry ice pellets. When the frozen cell slurry was completely crushed into a fine powdery mixture, it was transferred to another stainless steel canister and placed in a water bath to facilitate thawing. DNaseI (100 IU, Sigma Cat. No. D4623) and heparin (~300µg, Sigma Cat. No. H3393) were added to the cell lysate, followed by incubation for 10 minutes to solubilize the DNA/chromatin-associated RNAPII complexes before beginning the immunoprecipitation steps of the procedure. The extracts were collected by centrifugation at 14,000xg for 30 minutes at 4°C.

Following clarification, the lysate was transferred to a beaker for immunoprecipitation steps and treated with 200 µL of washed IgG Sepharose resin (GE Healthcare Cat. No. 17-0969-01). The purpose of the IgG resin is to purify the RNAPII associated proteins through interaction of the Protein A section of Rpb3-TAP tag with the resin. The mixture was incubated overnight on a stir plate at 4°C and transferred to a 30 mL Bio-Rad Econoprep column for separation by gravity flow. The retained resin was washed with 30 mL TAP Lysis Buffer and again with 3 mL of TEV Cleavage Buffer (10 mM Tris, pH 8, 150 mM NaCl, 0.1% IGEPAL, 0.5 mM EDTA, 10% Glycerol) and the flow through was saved until the purification was completed. The resin was resuspended with 1 ml of TEV Cleavage Buffer and transferred to a clean micro centrifuge tube. The resuspended resin was then treated with 10µL AcTEV protease (Invitrogen Cat. No. 12575-023) and incubated overnight at 4°C. The suspension was returned to the same Econoprep column the next day and the TEV cleavage products were collected in a 15

mL conical tube by gravity flow. The tube used for TEV cleavage reaction and the column were washed with Calmodulin Binding Buffer (10 mM Tris, pH 8, 1 mM magnesium acetate, 1 mM imidazole, 2 mM calcium chloride, 10% glycerol) and combined with the TEV cleavage product elution. The eluate was then treated with 500 μ L of washed Calmodulin Sepharose (Stratagene Cat. No. 214303) and incubated for 3 hrs at 4 $^{\circ}$ C on a rotating wheel. This step utilizes the affinity of calmodulin located on inserted TAP tag to bind to immobilized Calmodulin to further purify the tagged protein and any associated proteins. Following incubation, the suspension was transferred to a clean Bio-Rad Econoprep column for separation by gravity flow. The retained resin was washed with 30 mL of Calmodulin Binding Buffer. The final products were eluted by the addition of 1 mL volumes of Calmodulin Elution Buffer (10 mM Tris, pH 8, 300 mM NaCl, 1 mM magnesium acetate, 1 mM imidazole, 1 mM EGTA, 10% glycerol) x 5. Elutions were labeled E1-E5 and stored at -80 $^{\circ}$ C until SDS-PAGE analysis was done. Protein samples were separated on 10% SDS-PAGE for 1hr at 150V and visually detected using silver stain procedure.

TAP Method 2: Bead Beating Lysis

Due to incomplete lysis of the cells using the liquid nitrogen TAP method and low protein yields in the extract, a comparison to a different lysis method using glass beads in an aluminum bead beater canister. Rpb3-TAP *erg6* Δ and Rpb3-TAP *erg6* Δ *rtr1* Δ strains were grown overnight at 30 $^{\circ}$ C in 3L of YPD media to an OD₆₀₀ >8. Half of each culture was lysed using both methods. The liquid nitrogen TAP method was performed as described above and the cells used for the Bead Beating method were resuspended in 200-250mL TAP Lysis Buffer and added to the bead beating canister. Glass beads were

added to the canister until the liquid portion of the mixture just reached the top of the opening when blender cover was inserted in place. The apparatus was assembled with water bath attachment in place and closed tightly and inverted onto the blender base. Ice and water were added to the bath attachment and the beater was pulsed 10 times for 20 seconds with a 1 minute rest between pulses. The bead slurry/lysate mixture was transferred to a clean beaker and the lysate was removed from the beads using a serological pipette. The lysate was clarified by centrifugation at 14,000xg for 30 minutes at 4°C and processed using the TAP procedure as described above. Purified protein products were separated on 10% SDS-PAGE for 1 hr at 150V and visualized using silver staining procedure described below.

III. Silver Staining Procedure

In order to confirm successful purification of RNAPII and associated proteins, silver staining was performed on completed SDS-PAGE gels. Following electrophoresis, the SDS gel was placed in stain resistant container after removing stacking gel. All steps in the procedure were performed at room temperature. The gel was initially treated with 100 mL Fixing Solution (30% ethanol (reagent grade), 10% acetic acid, 60% water) with shaking for at least 30 minutes. After discarding the fixing solution, the gel was washed with 100 mL of 30% ethanol (30% ethanol, 70% water) for 10 minutes with shaking. The ethanol was then discarded and replaced with 100 mL water for 10 minutes with shaking. Following the wash, 100mL of Sensitizer Solution (0.2% sodium thiosulfate in water) was added and incubated for 10 minutes in the dark. The Sensitizer Solution was then discarded, the gel was washed as above and 100mL of Silver Nitrate Solution (0.1% silver nitrate, 0.02% formaldehyde, 99.9% water) was added. Following a 10 minute

incubation in the dark the Silver Nitrate Solution was discarded appropriately and the gel was washed quickly (no more than 5 minutes) with water. The stained gel was then developed with 100mL Developing Solution (2.5% sodium carbonate, 0.05% formaldehyde, 0.005% sodium thiosulfate) for 2-10 minutes with shaking. Once protein bands were visible on the gel, the developing solution was removed and the reaction was quenched with 100mL of Stop Solution (0.5% glycine in water) for 10 minutes with shaking. Finally, the Stop Solution was removed and the gels were placed in water until imaged using a digital scanner.

IV. MG132 treatment of TAP-tagged *S. cerevisiae* mutant strains

A small scale comparison of MG132 treatment to untreated controls was performed using newly created Rpb3-TAP strains to see if a treatment effect was evident before proceeding to the large scale study. Pre-cultures of both Rpb3-TAP *erg6Δ* and Rpb3-TAP *erg6Δ rtr1Δ* strains as well as the untagged parent strains of each were inoculated and grown overnight at 30°C in 100mL of YPD media. The OD600 was assessed the following day and the amount of cells needed to inoculate 200mL of media at an OD600 equal to ~1 was determined. Following a 2 hr recovery time, each culture was split into 2 flasks, with 100ml in each. One culture was treated with 50μM MG132 and the other with DMSO control, harvested after 2 hr treatment period, and then lysed as described above (See Section I of Methods for details). Protein concentrations were determined by BCA using known concentrations of bovine serum albumin to make a standard curve. Samples were separated on a 10% SDS-PAGE and subjected to western transfer as described to compare the status of the RNAPII CTD phosphate modifications between experimental groups.

Rpb3-TAP tagged yeast strains were inoculated into large 3L flasks containing YPD media and grown overnight. OD600 was determined and the amount of cells needed to inoculate the study cultures at OD600 ~ 4. Two 1.5L of YPD media were inoculated for each strain and labeled MG132 Treated and Untreated. The cells were placed at 30°C for 2 hrs to allow recovery growth. OD600 was checked again just prior to treatment with 50µM MG132 or DMSO control (i.e. untreated). Each culture was then spiked with MG132 or DMSO as previously described and incubated for 2 hrs at 30°C. The TAP procedure was performed after harvesting of the treated and untreated cultures. Confirmation of purification success was accomplished using silver stains and sample elutions from each purification (E1 and E2) were prepared as previously described for MS evaluation.

V. MuDPIT Analysis

Following the TAP processing, benzonase (1U/ml) was added to final elution products to remove any contaminating nucleic acid residues. Elutions 1 and 2 were combined from each TAP procedure (100µL of each) and prepared for LC/MS analysis by first precipitating with cold trichloroacetic acid (TCA). Prior to addition of TCA, 200µL of 100 mM Tris-HCl was added to each sample in a microcentrifuge tube. One-hundred microliters of TCA (Sigma Cat. No. T6399) was then added and mixed by vortexing. Following overnight incubation at 4°C, samples were centrifuged at 14,000 rpm for 30 minutes at 4°C. The supernatant was carefully removed and 500 µL of cold acetone was added to protein pellets in each tube and mixed by vortexing. Next, the samples were centrifuged at 14,000 rpm for 10 minutes at 4°C and the acetone wash was

repeated a second time as described. The visible protein pellet was then left to dry uncapped at room temperature 1-24 hrs.

Air-dried precipitated protein samples were resuspended in denaturing conditions (8M urea in 100 mM Tris-HCl, pH 8.5). Reconstituted samples were treated for 30 minutes at room temperature with 1.5 μ L Tris (2-Carboxylethyl)-Phosphine Hydrochloride (TCEP, Pierce Cat. No. 77720) to a final concentration of 5 mM TCEP. Samples were then alkylated for 30 minutes in the dark with 0.6 μ L of carboxyamidomethylate (CAM, Sigma Cat. No. 22790) to a final concentration of 10 mM and digested overnight at 37°C with 0.3 μ L of Endoproteinase Lys-C (\geq 150U/mL; Promega, Cat. No. V1071). The next day, the samples were diluted to 2M urea using 90 μ L of 100 mM Tris-HCl and 0.6 μ L of 1M CaCl₂ and digested with addition of 0.5 μ L Trypsin overnight at 37°C with shaking. Prior to loading the sample into a microcapillary tube and analysis by LC/MS, the approximately 100 μ L reaction was quenched using 1% formic acid (7 μ L) (Sigma Cat. No. F0507) and centrifuged at 14,000 rpm for 20-30 minutes to clarify the sample.

Samples were loaded as previously described (Florens & Washburn, 2006). Specifically, prepared samples were pressure-loaded into silica microcapillary columns (100 μ m inner diameter) containing triphasic layers of packing material (8 cm C18 reverse phase/2 cm 5 μ m strong cation exchange/2 cm C18 reverse phase) using a steel pressurization device (Florens & Washburn, 2006). Following sample loading, the column was equilibrated with Buffer A (5% Acetonitrile, 0.1% formic acid).

Each loaded column was placed on a Proxeon nano-liquid chromatograph (LC) in line with a ThermoFisher LTQ Velos linear ion trap mass spectrometer (MS) equipped

with a nano-LC electrospray ionization source. The application used to resolve the peptides in the sample mixture was a 10-step fully automated chromatographic separation, elution, and peptide fragmentation via collision induced dissociation (CID) programmed using the Thermo Xcalibur software. Chromatographic separation of the peptides was accomplished using elution Buffers A, B, and C sequentially, where a gradient shift from Buffer A to Buffer B (80% Acetonitrile, 0.1% formic acid) along with increasing salt concentrations in Buffer C (5-300 mM Ammonium Acetate, 5% Acetonitrile, 0.1% formic acid) was set up. The ten most intense/abundant spectral peaks recorded over a range of 400-1600 m/z were subjected to tandem MS (MS/MS) analysis in a data dependent acquisition. A dynamic exclusion time of 150 seconds was set to allow for sampling and subsequent MS/MS analysis (fragmentation) of lower abundant ions.

The collected mass spectra were subjected to FASTA database searching using the SEQUEST search algorithm in the Proteome Discover software (Thermo). A custom database was used for protein identification that included 5819 *Saccharomyces cerevisiae* protein sequences that were downloaded from National Center for Biotechnology Information genome build (downloaded file on 04-26-2011). The NCBI database also included other common contaminants (i.e. keratin and proteinases) whose protein sequences were obtained from the common repository of adventitious proteins (cRAP) from the Global Proteome Machine (GPM). To estimate the FDR of each unique peptide identified, the reverse sequences were used in the database for decoy protein identification. The FDR is calculated using the following calculation: $\text{False Positive IDs} / (\text{Total False Positives} + \text{Total Positives})$ at the cutoff of 2%. The peptides which have the

highest confidence have a 2% FDR threshold and the peptides with medium confidence were set with a 5% FDR. All spectra searches were done using the following parameters: Trypsin used for digestion; FDR threshold of 2%; Static modifications: +57 Da to cysteine for reduction and CAM addition to peptide mixtures; Dynamic modifications: +16 Da for oxidized methionine. In addition to the above, searches for ubiquitin and phosphorylation post-translational modification events were done with dynamic modifications of +114.1 and +80 Daltons respectively. Further parameters for additional ubiquitination site searches using X!Tandem through Scaffold software were Pyro Glutamic Acid (-18 Da), Pyro Cmc (-17 Da), N-terminal acetylation (+42 Da) and Methionine cleavage (-131 Da).

VI. Malachite Green Phosphate Assay

A phosphatase assay was performed to determine if a recombinant Rtr1 enzyme was active on a synthetic peptide substrate with the sequence “MPEQKITEIEDGQDGGVT*PYS” where T* is phospho-threonine. The assay is a colorimetric method which uses the complex formation between malachite green, molybdate and free orthophosphate and is read at a wavelength of 620 nm. The amount of colorimetric change in the sample is directly proportional to the amount of phosphate released during the phosphatase reaction. Multiple concentrations of the GST-Rtr1 were used to test a fixed amount of substrate.

RESULTS

I. The effects of MG132 treatment on RNA Polymerase II phosphorylation in *RTR1* deletion strains

As discussed previously, the use of proteasome inhibition has been used by several investigators to study protein degradation by the proteasome (W. Kim et al., 2011; D. H. Lee & Goldberg, 1996). The use of untagged strains to investigate the effect of proteasome inhibition on RNAPII recycling was done prior to proceeding to a large scale MG132 treatment experiment. The Western blot analysis seen in Figure 7 shows a high molecular weight product collecting in the top of several wells (4, 6 and 8). This is consistent with other findings (W. Kim et al., 2011; D. H. Lee & Goldberg, 1996; Liu et al., 2007) suggesting that treatment of the mutant strains with the proteasome inhibitor, MG132, results in the accumulation of the RNAPII with S5-P CTD in the whole cell extract. This accumulation is exacerbated upon deletion of *RTR1* (see Figure 7, lane 8, marked with red asterisk).

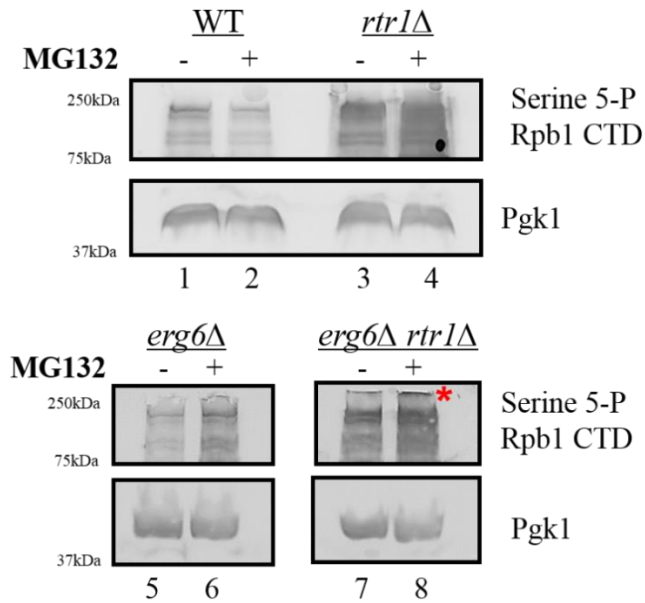


Figure 7. Comparison of RNAPII Serine 5 phosphorylation using Western blot of four strains of *S. cerevisiae* both MG132 treated and untreated. Whole cell extracts were probed with anti-phosphorylated Serine 5 CTD and Anti-Pgk1 antibodies. Accumulation of phosphorylated S5 CTD is seen in MG132 treated cultures of both mutant strains (lanes 6 and 8) when compared to the untreated (5 and 7). The high molecular weight products containing phosphorylated S5, denoted by the red asterisk, can be seen collecting at the interface between the stacking and resolving gel in lane 8.

A small scale MG132 treatment experiment was performed prior to the large scale study using the newly transformed mutant *S. cerevisiae* strains. In addition to providing a preview to the large scale results, purification products were subjected to immunoblot analysis for several CTD modification states. Following treatment as previously described, MG132 treated and untreated cells were lysed in TAP Lysis Buffer using glass beads and disruptor genie. Protein concentrations were measured using BCA and calculated against a bovine serum albumin standard. Four 12% SDS-PAGE gels were prepared and 50 μ g of each sample was denatured in 2X SDS loading dye for 10 minutes at 100°C. Following electrophoresis (1.5hrs at 150V in Tris/Gly/SDS running buffer), western transfer to nitrocellulose membranes was performed overnight as described. The following day, each membrane was cut horizontally at the 100 kDa mark and each half

probed with a different primary antibody.

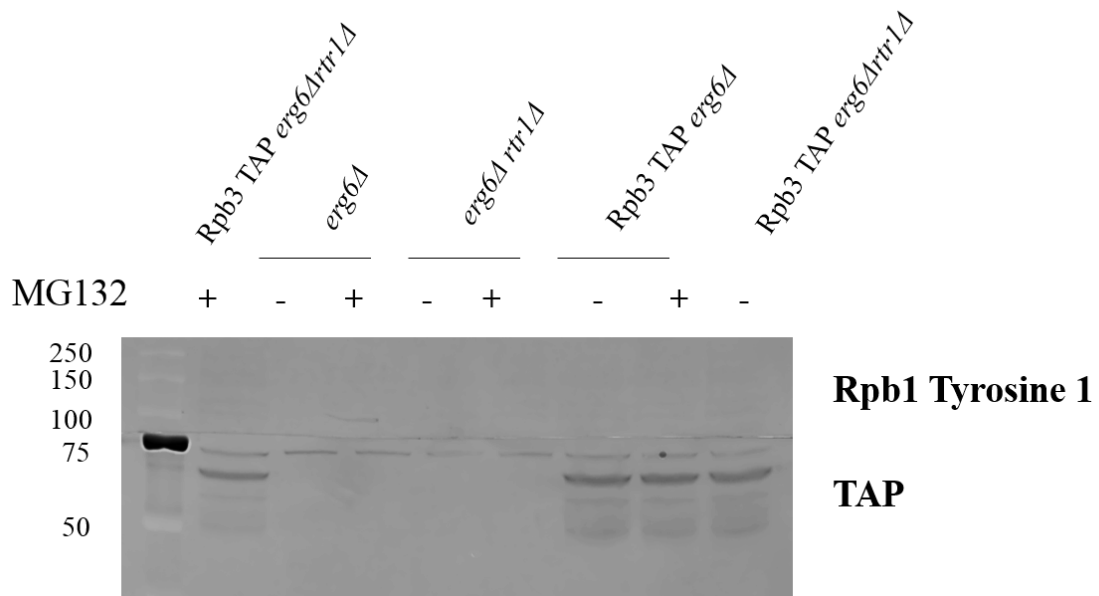


Figure 8. Comparison of RNAPII Tyrosine 1 phosphorylation using Western blot analysis of MG132 treated and untreated yeast strains. Whole cell extracts were then treated with Anti-Tyrosine 1 phosphorylated CTD of Rpb1 and Anti-TAP antibody. There was no apparent detection of Tyrosine 1 phosphorylation in any of the samples tested. Tap tagged strains as expected showed reaction to TAP antibody while the untagged strains did not react to the fusion tag specific antibody.

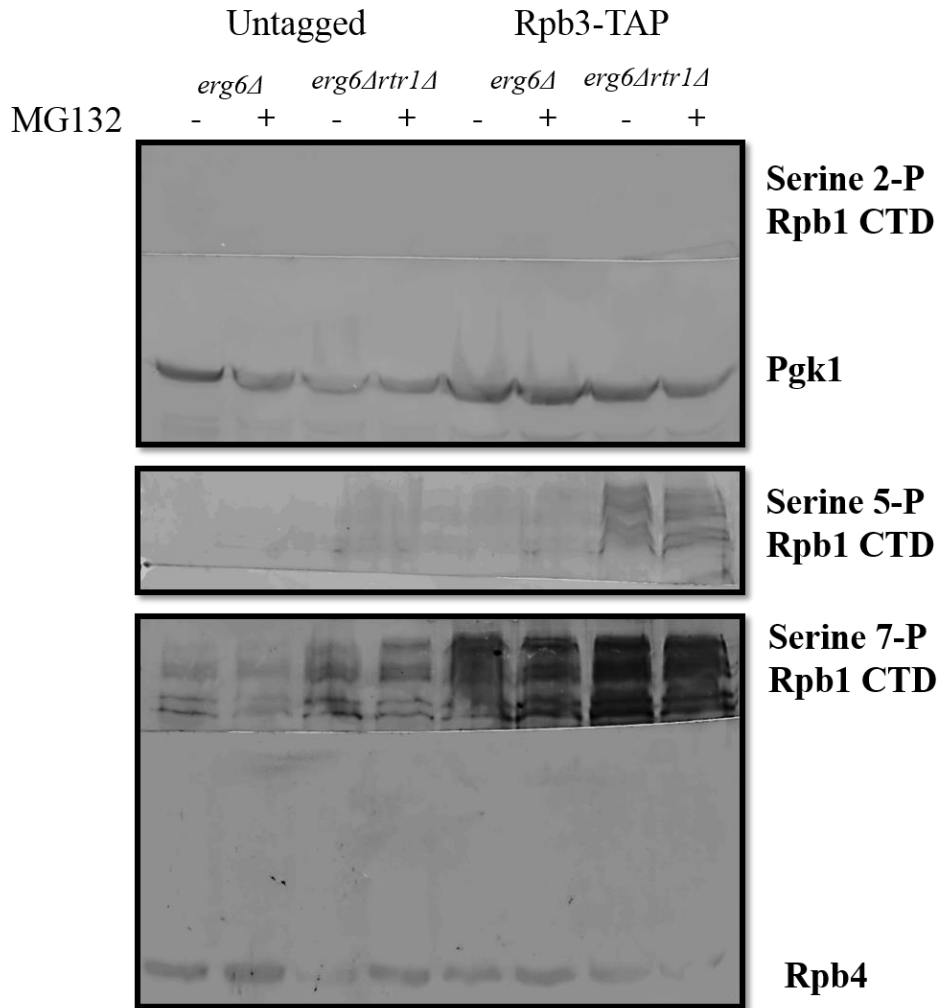


Figure 9. Comparison of RNAPII CTD Serine 2, 5, and 7 phosphorylation Western blot analysis of MG132 treated and untreated yeast strains. Whole cell extracts (50ug from each condition) were incubated with antibodies towards different CTD phosphorylation states of the Rpb1 CTD and protein loading controls. Shown from top to bottom are Anti-Serine 2 phosphorylated CTD, Anti-Pgk1, Anti-Serine 5 phosphorylated CTD of Rpb1, Anti-Serine 7 phosphorylated CTD of Rpb1 and Rpb4. There was no reaction to the Serine 2 phosphorylated CTD in any of the treated and untreated samples, whereas the loading control showed similar levels of the Rpb4 in all samples. Tap tagged mutants showed a greater amount of accumulation of the Serine 5 phosphorylated CTD and Serine 7 phosphorylated CTD than the untagged strains. The difference in the abundance of Rpb4 does not appear to be a consequence of the proteins being tagged and untagged or treated vs untreated.

II. Generation of *S. cerevisiae* strains Rpb3-TAP *erg6*Δ and Rpb3-TAP *erg6*Δ *rtr1*Δ TAP tag through homologous recombination

The use of rapid purification methods has been shown to be invaluable to study protein interactions involving large multiple subunit complexes such as RNAPII (Washburn, 2008). In order to study the interaction between the RNAPII complex and proteasomal activity, the use of TAP-tagged mutant *S. cerevisiae* yeast strains with the single deletion of *ERG6* and a double deletion of *ERG6* and *RTR1* was required to ensure the strains are sensitive to proteasomal inhibition. The first step in transformation involved the amplification of a specific PCR product that contained the disruption cassette. The 5' and 3' ends of this PCR DNA fragment each included 65bp of sequence identifying with the sequences flanking Rpb3 gene and a selectable marker (URA3) amplified from the plasmid (pBS1539).

The *erg6*Δ and *erg6*Δ *rtr1*Δ strains were successfully transformed with the insertion of the C-terminal TAP tag at the endogenous locus of the Rpb3 gene. The single mutant strain, Rpb3-TAP *erg6*Δ, developed two single colony transformants that were each grown up and subjected to western blot analysis to confirm insertion; whereas five transformants were isolated in the double mutant, Rpb3-TAP *erg6*Δ *rtr1*Δ. Figure 10 confirms incorporation of the TAP tag using an Anti-Calmodulin Binding Protein (αCBP) antibody following western transfer.

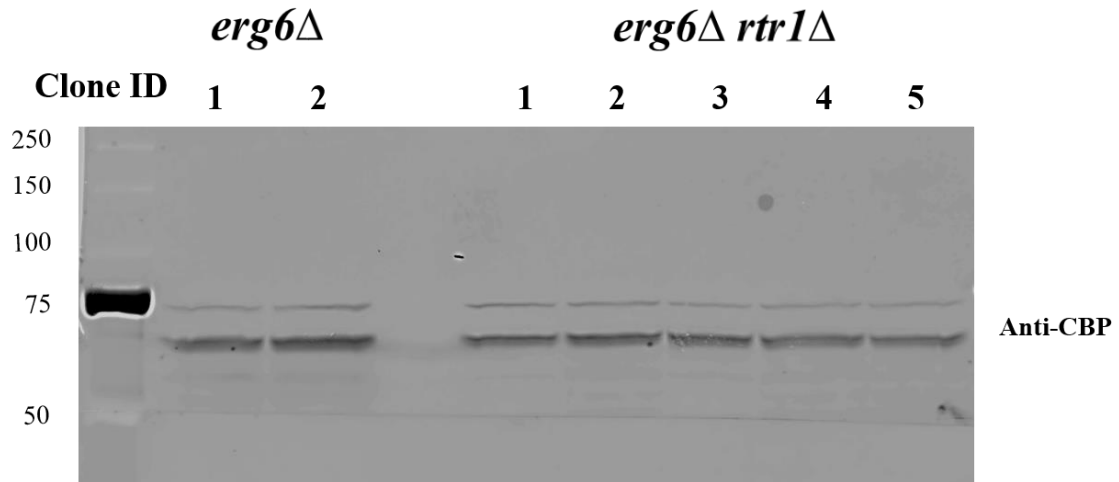


Figure 10: Western blot analysis of Anti-CBP in yeast transformants isolated from YNB URA- agar after treatment with LiOAc and pBS1539. Two transformants were isolated from the *erg6*Δ plate and five transformants were isolated from the *erg6*Δ*rtr1*Δ plate.

III. Isolation of RNA Polymerase II complexes following MG132 treatment from wild-type, *RTR1* deletion, *ERG6* deletion, and *RTR1/ERG6* double deletion strains

A test purification of one colony from both the single deletion (Rpb3-TAP *erg6*Δ) and double deletion (Rpb3-TAP *erg6*Δ *rtr1*Δ) strains was performed to ensure that the strains would be suitable for large scale MG132 treatments. Figure 11 shows representative silver stains of the elution products for TAP procedures from both strains. Elutions 1 and 2 from each procedure illustrate the abundance of RNAPII products with most of the twelve subunits visible. Elutions 1 and 2 from each colony contained the highest levels of purified RNAPII. These results suggest that the TAP tagged strains are appropriate for further studies (Figure 11).

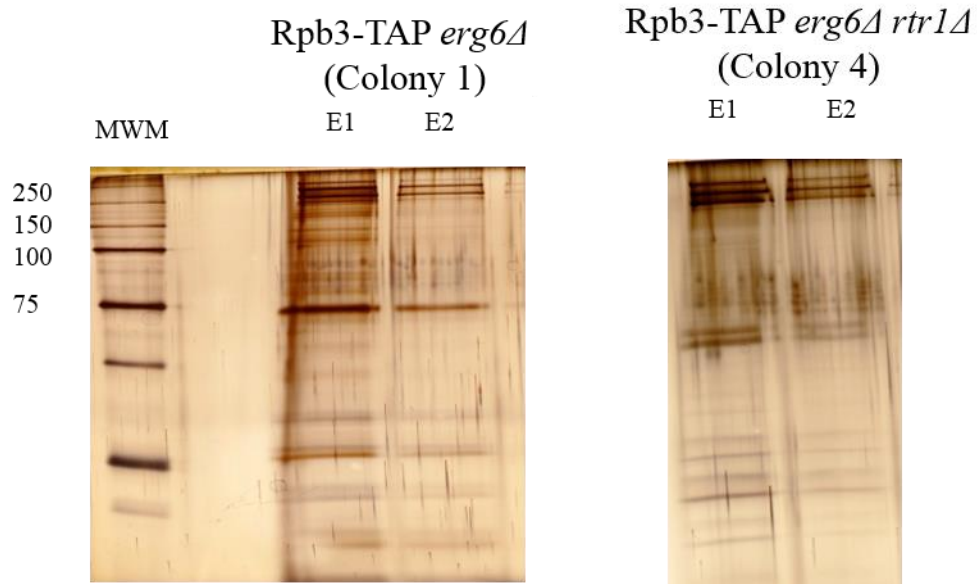


Figure 11. Silver stain results of TAP-tagged strains of *S. cerevisiae*. Final elutions (E1 and E2) in both *erg6Δ* and *erg6Δrtr1Δ* resulted in purification of multiple protein subunits of RNAPII.

It was noted during the cell culture to test TAP isolations that the double mutant strain Rpb3-TAP *erg6Δ rtr1Δ* had a pronounced slow growth phenotype that caused yields of purified RNAPII to be low. In order to perform the next experiments, calculating growth rate was important to allow for direct comparisons to ensure equal cell numbers in mid-log phase of growth for MG132 treatment. Figure 12 displays the results of a growth curve comparison between the single deletion strain Rpb3-TAP *erg6Δ* and the double deletion strain Rpb3-TAP *erg6Δ rtr1Δ*. The growth curve for the double mutant indicates a longer lag phase before exponential growth resumes. For example, at time point 5, the OD600 for Rpb3-TAP *erg6Δ* is twice that of the Rpb3-TAP *erg6Δrtr1Δ*. As a consequence, comparing the two strains requires a greater inoculation volume for the double mutant. The doubling time following lag phase is also slowed relative to Rpb3-TAP *erg6Δ* (90 minute doubling time vs. 180 minute doubling time).

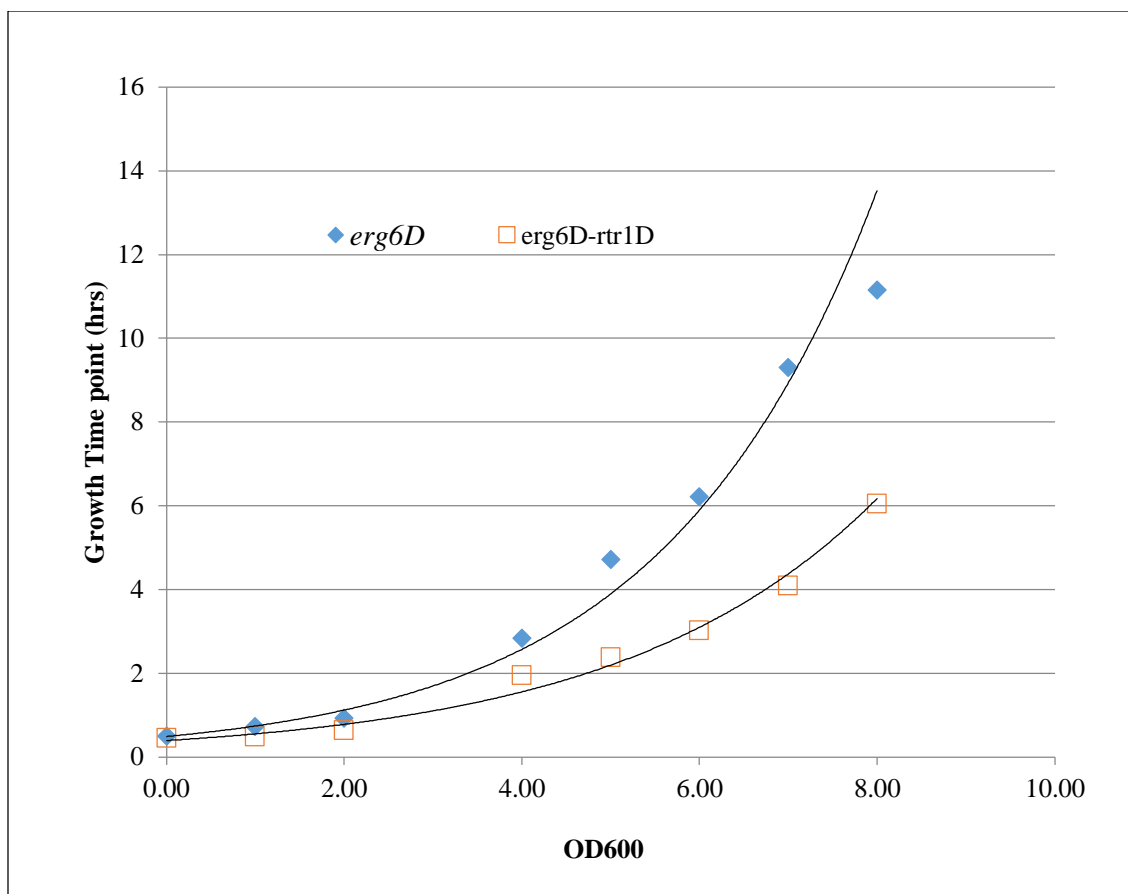


Figure 12. Growth curve comparison of Rpb3-TAP *erg6Δ* (aka *erg6D*) vs Rpb3-TAP *erg6Δ rtr1Δ* (aka *erg6D-rtr1D*). Both deletion strains were grown in YPD media with inoculating OD600 of 0.5. After a 2 hr recovery time, the OD600 measurements for each strain were collected at various time points over approximately 8 hrs. The time point (hrs) was plotted against OD600.

Due to inadequate cell lysis that was monitored through the volume of the cell pellet prior to and following cell lysis, we performed two different lysis procedures for TAP purification as described in the methods section. The TAP lysis method comparison results are presented in Figure 13. Purification products from the bead beating method showed marked improvement in both yield and quality of final purification elutions. Based on these initial purification results, the bead beating lysis was the chosen method for use in the proteasomal inhibition study.

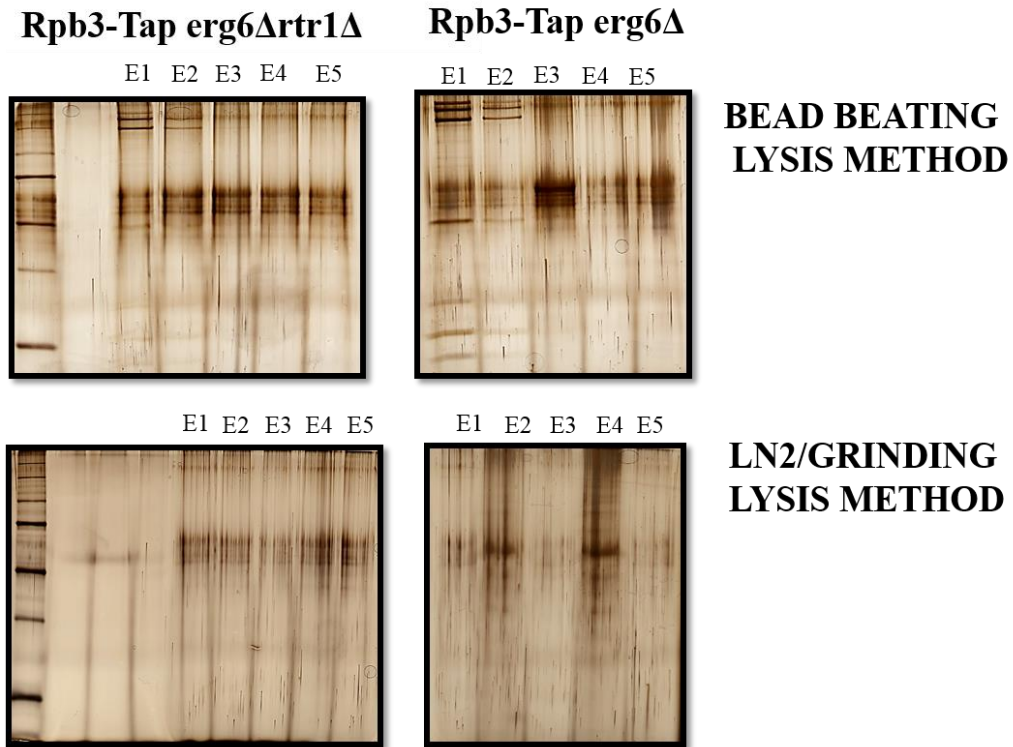


Figure 13. Representative silver stains comparing yeast lysis methods prior to TAP procedure. Both TAP tagged deletion strains were lysed using bead beating and LN2 freeze followed by grinding. Samples derived from bead beating lysis show significantly more purification products with marginally “cleaner” preps, i.e. less contaminating keratin using the same amount of starting material.

Following treatment of the strains with the proteasomal inhibitor MG132, purifications were performed on lysates produced using the bead beating apparatus. The initial silver stain gels from the calmodulin elutions of both MG132 treated and untreated cells from both deletion strains are presented in Figure 14.

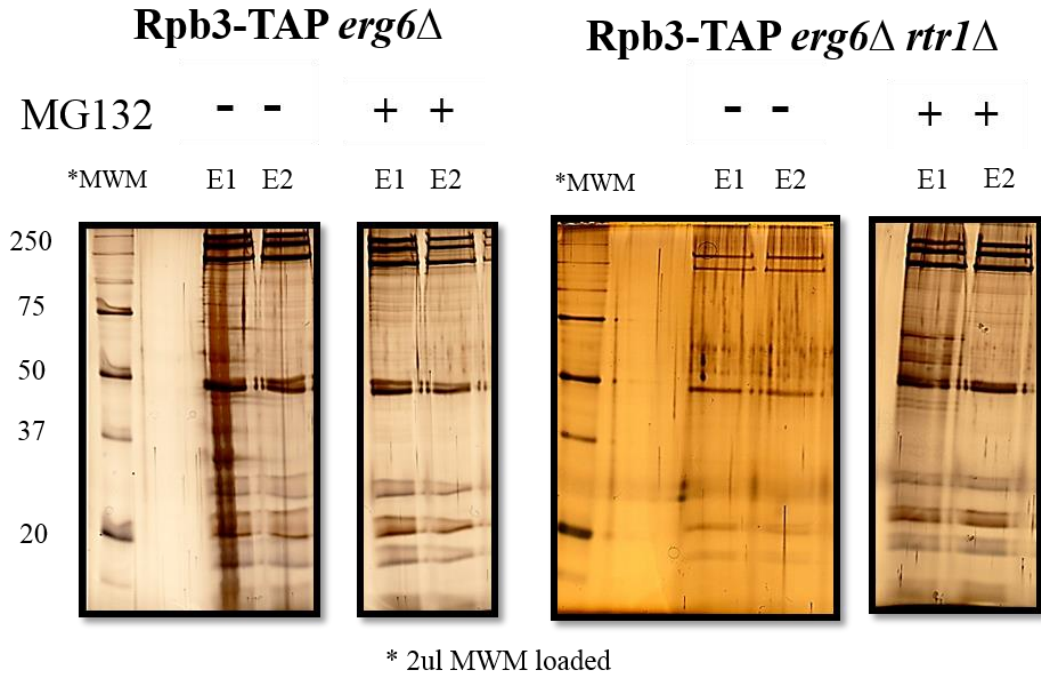


Figure 14. Silver stain results from large scale MG132 treated and untreated TAP tagged deletion strains. Comparing Rpb3-TAP *erg6*Δ MG132 treated and untreated does not show apparent difference in RNAPII abundance, however the MG132 treated Rpb3-TAP *erg6*Δ *rtr1*Δ elutions appear to have more abundant products following separation on 10% SDS-PAGE compared to the untreated samples.

The resulting silver stains suggest that *erg6*Δ*rtr1*Δ cells treated with MG132 have an apparent increased yield of RNA Polymerase II complexes following Rpb3-TAP when compared to the untreated *erg6*Δ *rtr1*Δ. However, it is difficult to determine if the same is the case for the *erg6*Δ comparison since the samples were run on separate gels. In order to confirm these differences in RNAPII abundance calmodulin elutions 1 and 2 from each MG132 treated and untreated samples were run on the same gel and visually detected by silver staining (Figure 15).

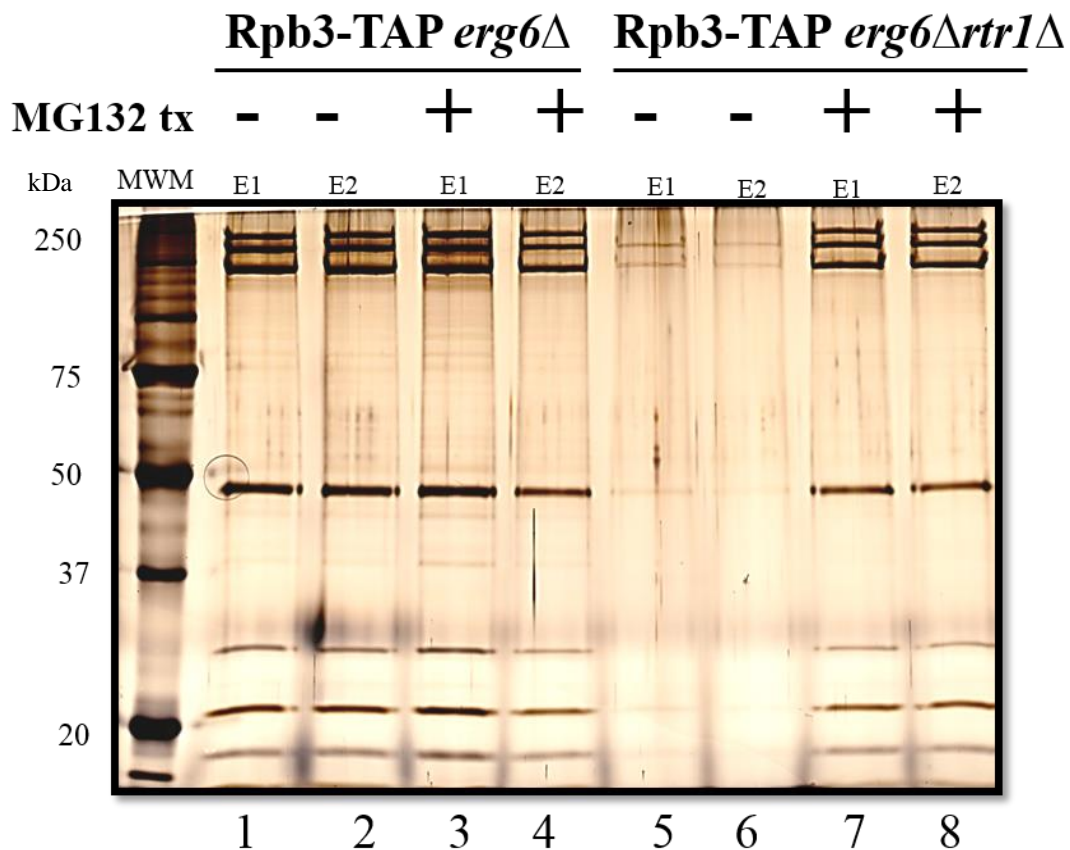


Figure 15. Comparison of elutions 1 and 2 from MG132 treated and untreated TAP tagged deletion strains as detected by silver stain. Relative abundance of RNAPII is greater in MG132 treated wells for *erg6*Δ when comparing lanes 1 + 2 (Untreated) to lanes 3 + 4 (MG132 treated). When comparing *erg6*Δ *rtr1*Δ MG132 treated samples (lanes 7 + 8) to untreated samples (lanes 5 + 6), the effect is the same as for the *erg6*Δ cells with a more pronounced difference.

The results in Figure 15 clearly show an increase in the amount of RNAPII isolated from *erg6*Δ *rtr1*Δ cells following MG132 treatment. However, the treatment effect is not seen in *erg6*Δ cells alone. The data indicates that the total level of RNAPII is decreased in *rtr1*Δ cells that would support our hypothesis that RNAPII turnover rates are increased through proteosomal degradation following the loss of Rtr1 function.

IV. Identification of ubiquitination sites in RNA Polymerase II purifications using a two-step bioinformatics analysis

Analysis of post-translational modifications by LC-MS/MS has been increasingly used to determine regulatory roles in specific biochemical pathways or protein interactions. Isolating potential sites of modification through database search can be difficult due to the transient and reversible nature of PTMs (Farley & Link, 2009). Consequently, the importance of properly designing an experiment and the follow-up database searching and method for PSM determination cannot be understated. Methods of protein identification vary in the algorithms used to determine true versus false PSMs (See Introduction). In this present work, a direct comparison was done to investigate which analytical method would result in the most accurate and robust data. Proteome Discoverer was used in the initial database search using the SEQUEST algorithm identifying spectral matches. This data was then further analyzed using Scaffold software containing X!Tandem algorithm to both confirm and assign additional peptide identifications. The resulting comparison between the initial Proteome Discoverer/SEQUEST results and the two-step analysis using both Proteome Discoverer/SEQUEST and Scaffold/X!Tandem showed an increase in all RNAPII subunit related peptides using the two-step analysis (Table 6). After obtaining these data, we proceeded to use this two-step proteomics data analysis procedure using Proteome Discoverer followed by Scaffold analysis.

Table 6. Comparison of MS/MS results using Proteome Discoverer/SEQUEST vs Scaffold/X!Tandem

Protein	Total Number of Peptides Identified through Proteome Discovery/SEQUEST	Total Number of Peptides Identified through Scaffold/X!Tandem	Increase
RPB1	1746	4561	2.61
RPB2	1051	3568	3.39
RPB3	299	1022	3.42
RPB4	262	615	2.35
RPB5	212	426	2.01
RPB6	125	242	1.94
RPB7	31	149	4.81
RPB8	295	428	1.45
RPB9	151	420	2.78
RPB10	0	40	INFINITE
RPB11	242	495	2.05
RPB12	179	374	2.09
SPT5	2	12	6.00
UBI4	17	0	0.00

The addition of polyubiquitin to lysine side chains of proteins is a post-translational modification that leads to their degradation by the proteasome (Liu et al., 2007). This degradation pathway is essential for cellular processes such as quality control, cell cycle regulation, transcription, protein transport and DNA repair (reviewed by Sorokin, Kim, & Ovchinnikov, 2009). The proteasome is a large complex consisting of 2 sub-complexes, 19S and 20S, which function together to recognize the polyubiquitin signal and catalyzes proteolytic destruction as well as other regulatory functions. The 19S component consists of 9 protein subunits and the 20S core particle is 14 subunit complex. In this current study, we were interested in determining if RNAPII degradation is proteasome-dependent using quantitative proteomic analysis of post translational modifications.

We used LC-MS/MS technology to evaluate purified Rpb3-TAP isolated complexes from mutant strains of *S. cerevisiae* treated with the proteasome inhibitor, MG132 and compared the resulting peptide listing to untreated samples from the same strains. In total, five *erg6Δ* and four *erg6Δ rtr1Δ* samples were digested and subjected to MuDPIT analysis (see Methods section). For each strain, protein identifications including total PSMs were tabulated following Scaffold database searches (Tables 7-10). The protein identification data obtained after MuDPIT were sorted according to the total spectral counts (PSM) and known annotated contaminants listed in our custom FASTA database were removed from the final datasets. Most proteins identified by a total spectral count of less than 20 were also excluded from each list, however, some proteins with <20 identified spectra were included if they were found to be associated with transcription, ubiquitin or the proteasome.

LC-MS/MS results of the *erg6Δ* untreated sample included a total of 35 proteins identified (Table 7). All 12 subunits of RNAPII were detected as well as an additional 7 transcription associated proteins, including Rtr1, with 3 total spectra identified. In addition, 6 ubiquitin related proteins with a total of 22 spectra and 3 proteasome-associated proteins, with a total of 7 spectra were revealed. A total of 32 proteins were identified in the MG132 treated *erg6Δ* sample and included in Table 8. Along with all 12 subunits of RNAPII, an additional 5 transcription related proteins (Ctr9, Dst1, Spt5, Spt6, and Tfg1) were identified in the analysis. Furthermore, proteins associated with both ubiquitin (5 proteins) and the proteasome (2 proteins) were identified. The MuDPIT results for the untreated *erg6Δ rtr1Δ* sample are presented in Table 9. In all, 23 proteins were identified including 3 of the 12 RNAPII subunits (Rpb1, Rpb2, and Rpb9). The

remaining proteins listed in Table 9 did not meet the inclusion criteria of ≥ 20 spectra, but were included as a comparison to the MG132 treated *erg6Δ rtr1Δ* results (Table 10). The lack of RNAPII proteins pulled-down in the untreated *erg6Δrtr1Δ* sample is in agreement with purification results seen in Figures 14 and 15.

Spectra identified in the double mutant, *erg6Δ rtr1Δ* preparation included 80 proteins with 12 of the 13 most abundant comprising subunits of RNAPII. Also present, were 4 proteasomal proteins (Rpn2, Rpn4, Rpn6, and Rpt3) as well as 9 ubiquitin associated proteins.

Table 7. Proteins identified using Scaffold analysis for untreated Rpb3-TAP *erg6Δ*

Accession #	Identified Proteins	Mol Wt	Total Spectra
gi 6320061	Rpb1; TXN	192 kDa	6892
gi 6324725	Rpb2; TXN	139 kDa	5669
gi 6322168	Rpb3; TXN	35 kDa	2090
gi 6322321	Rpb4; TXN	25 kDa	1281
gi 6319630	Rpb5; TXN	25 kDa	1014
gi 6324569	Rpb11; TXN	14 kDa	703
gi 6321368	Rpb9; TXN	14 kDa	484
gi 6320612	Rpb7; TXN	19 kDa	483
gi 6325445	Rpb6; TXN	18 kDa	465
gi 6324798	Rpb8; TXN	17 kDa	458
gi 6324784	Rpb10; TXN	8 kDa	383
gi 6321937	Rpb12; TXN	8 kDa	323
gi 6323196	Rps31p	17 kDa	63
gi 6323462	Sen1p	253 kDa	34
gi 6323522	Taf8p	58 kDa	26
gi 6322881	Set3p	85 kDa	25
gi 6323115	Smc4p	162 kDa	24
gi 10383754	Mrc1p	124 kDa	21
gi 6322409	Tdh1p	36 kDa	21
gi 6321631	Tdh3p	36 kDa	21
gi 37362706	Asr1; TXN	33 kDa	3
gi 330443717	Ctr9; TXN	125 kDa	2
gi 6323931	Bul1p	109 kDa	5
gi 6323525	Bul2p	105 kDa	3
gi 6321395	Dst1; TXN	35 kDa	11
gi 6325360	Pre2p	32 kDa	3
gi 6320859	Rpn3p	60 kDa	2
gi 6325365	Rpn7p	49 kDa	2
gi 6321193	Rtf1; TXN	66 kDa	2
gi 6320987	Rtr1; TXN	26 kDa	3
gi 6323632	Spt5; TXN	116 kDa	9
gi 6321552	Spt6; TXN	168 kDa	12
gi 6320598	Uba2p	71 kDa	3
gi 6320999	Ubp3p	102 kDa	3
gi 6320945	Ubp9p	86 kDa	5

Table 8. Proteins identified using Scaffold analysis for MG132 treated Rpb3-TAP erg6Δ

Accession #	Identified Proteins	Mol Wt	Total Spectra
gi 6320061	Rpb1; TXN	192 kDa	7568
gi 6324725	Rpb2; TXN	139 kDa	5720
gi 6322168	Rpb3; TXN	35 kDa	1486
gi 6324569	Rpb11; TXN	14 kDa	1074
gi 6319630	Rpb5; TXN	25 kDa	755
gi 6322321	Rpb4; TXN	25 kDa	498
gi 6321937	Rpb12; TXN	8 kDa	439
gi 6324784	Rpb10; TXN	8 kDa	431
gi 6324798	Rpb8; TXN	17 kDa	333
gi 6321368	Rpb9; TXN	14 kDa	228
gi 6325445	Rpb6; TXN	18 kDa	219
gi 6320612	Rpb7; TXN	19 kDa	67
gi 330443717	Ctr9; TXN	125 kDa	5
gi 6321395	Dst1; TXN	35 kDa	6
gi 6323632	Spt5; TXN	116 kDa	5
gi 6321552	Spt6; TXN	168 kDa	4
gi 6321625	Tfg1; TXN	82 kDa	2
gi 6319612	Mec1p	273 kDa	41
gi 6324376	YNR048W	45 kDa	32
gi 6323457	Tus1p	149 kDa	32
gi 6320887	Sap1p	100 kDa	30
gi 6323548	Rpm2p	139 kDa	27
gi 6324132	Whi3p	71 kDa	25
gi 6319977	Whi4p	71 kDa	24
gi 6320433	Sir4p	152 kDa	23
gi 6323547	Pre8p	27 kDa	2
gi 6320184	Rpn4p	60 kDa	5
gi 330443700	Ubp10p	89 kDa	7
gi 6320999	Ubp3p	102 kDa	4
gi 6322035	Ubp7p	123 kDa	3
gi 6321623	Ubr1p	225 kDa	3
gi 6323712	Ubx4p	47 kDa	2

Table 9. Proteins identified using Scaffold analysis for untreated Rpb3-TAP *erg6Δtrr1Δ*

Accession #	Identified Proteins	Mol Wt	Total Spectra
gi 6324725	Rpb2; TXN	139 kDa	314
gi 6320061	Rpb1; TXN	192 kDa	221
gi 6324472	Pkh2p	122 kDa	7
gi 6321368	Rpb9; TXN	14 kDa	13
gi 6320512	YDR306C	54 kDa	9
gi 6323568	Tcb3p	171 kDa	2
gi 6322179	Tir3p	26 kDa	2
gi 6321891	Tra1p	433 kDa	5
gi 6321012	Chd1p	168 kDa	2
gi 6321289	Ino80p	171 kDa	2
gi 6322163	Irr1p	133 kDa	2
gi 6320345	Dop1p	195 kDa	2
gi 6325121	Gip3p	141 kDa	2
gi 6323403	Rom2p	153 kDa	2
gi 6322125	See1p	29 kDa	5
gi 6319318	Nup60p	59 kDa	2
gi 6320792	YEL043W	106 kDa	3
gi 330443395	Pkc1p	131 kDa	2
gi 6323587	Cyb2p	66 kDa	2
gi 157285914	YKR005C	59 kDa	2
gi 6319528	Yro2p	39 kDa	2
gi 6322047	Tid3p	80 kDa	2
gi 6322266	Cdc6p	58 kDa	2

Although there were no specific interactions found in the purified samples with ubiquitin, there were several proteins identified that associate with ubiquitin. In addition, several subunits of the proteasome were identified in all samples albeit in low abundance (see Tables 7-10). Notably, although there is an increase in the total number of protein identified, there is a lack of elongation factors associated with the double deletion mutant, *erg6Δtrr1Δ* treated with MG132. Conversely, the number of ubiquitin proteins was the highest, although at low spectral levels, found to associate with RNAPII (Table 10).

Table 10. Proteins identified using Scaffold analysis for MG132 treated Rpb3-TAP *erg6Δtrt1Δ*

Accession #	Identified Proteins	Mol Wt	Total Spectra
gi 6320061	Rpb1; TXN	192 kDa	11465
gi 6324725	Rpb2; TXN	139 kDa	9265
gi 6322168	Rpb3; TXN	35 kDa	2133
gi 6324569	Rpb11; TXN	14 kDa	1617
gi 6319630	Rpb5; TXN	25 kDa	1056
gi 6322321	Rpb4; TXN	25 kDa	894
gi 6321937	Rpb12; TXN	8 kDa	721
gi 6321368	Rpb9; TXN	14 kDa	708
gi 6324798	Rpb8; TXN	17 kDa	673
gi 6324784	Rpb10; TXN	8 kDa	441
gi 6325445	Rpb6; TXN	18 kDa	403
gi 6323854	Cik1p	69 kDa	155
gi 6320612	Rpb7; TXN	19 kDa	144
gi 6319982	Dtd1p	17 kDa	72
gi 6321631	Tdh3p	36 kDa	54
gi 6322409	Tdh1p	36 kDa	50
gi 6319612	Mec1p	273 kDa	46
gi 6324917	Rpa190p	186 kDa	46
gi 6320913	Arg5,6p	95 kDa	45
gi 6323457	Tus1p	149 kDa	44
gi 6324472	Pkh2p	122 kDa	39
gi 6319295	Lte1p	163 kDa	36
gi 6321978	Ssp1p	66 kDa	36
gi 6320887	Sap1p	100 kDa	35
gi 6324553	Tat2p	65 kDa	34
gi 6323548	Rpm2p	139 kDa	33
gi 6325167	Rps6ap	27 kDa	31
gi 6319975	Gcs1p	39 kDa	30
gi 6320433	Sir4p	152 kDa	29
gi 7276233	Yck3p	60 kDa	29
gi 6319279	Cdc19p	55 kDa	28
gi 6319986	Gdh2p	124 kDa	28
gi 6324452	Rpl18ap	21 kDa	28
gi 6325121	Gip3p	141 kDa	27
gi 6325016	Hsp82p	81 kDa	27
gi 10383781	Pgk1p	45 kDa	27
gi 6324445	Rpl25p	16 kDa	27

Table 10 (continued). Proteins identified using Scaffold analysis for MG132 treated Rpb3-TAP *erg6Δrtr1Δ*

Accession #	Identified Proteins	Mol Wt	Total Spectra
gi 6319977	Whi4p	71 kDa	27
gi 6324132	Whi3p	71 kDa	26
gi 6322079	Hos4p	124 kDa	25
gi 6322668	Rpl17ap	21 kDa	25
gi 154200011	Rpl20bp	20 kDa	25
gi 144228166	Ssa1p	70 kDa	25
gi 6323196	Rps31p	17 kDa	24
gi 6325252	Aep3p	70 kDa	23
gi 6321968	Eno2p	47 kDa	23
gi 6323585	Imd4p	56 kDa	22
gi 6325300	Rpl43ap	10 kDa	22
gi 6321754	Rpl8ap	28 kDa	22
gi 6323844	Sgs1p	164 kDa	22
gi 6321921	Arp1p	43 kDa	21
gi 6324870	YOR296W	147 kDa	21
gi 6321948	Rtt107p	123 kDa	21
gi 10383795	Snt1p	138 kDa	21
gi 6319396	Ssa3p	71 kDa	21
gi 6321012	Chd1p	168 kDa	20
gi 6321243	Gcn1p	297 kDa	20
gi 330443652	Hsl1p	170 kDa	20
gi 6323135	Mdn1p	559 kDa	20
gi 6321812	Myo1p	224 kDa	20
gi 14318555	Rpl2ap	27 kDa	20
gi 6322000	Skn7p	69 kDa	20
gi 6320795	Utr2p	50 kDa	20
gi 6321709	Yta7p	157 kDa	20
gi 6323632	Spt5; TXN	116 kDa	16
gi 6322115	Rpn2p	104 kDa	3
gi 6320184	Rpn4p	60 kDa	7
gi 6320106	Rpn6p	50 kDa	14
gi 6320602	Rpt3p	48 kDa	3
gi 6321193	Rtf1; TXN	66 kDa	4
gi 330443605	Set2; TXN	84 kDa	9
gi 6322264	Ubp12p	143 kDa	5
gi 330443411	Ubp13p	84 kDa	6
gi 6325184	Ubp16p	57 kDa	5
gi 6320999	Ubp3p	102 kDa	6

Table 10 (continued). Proteins identified using Scaffold analysis for MG132 treated Rpb3-TAP *erg6Δrtr1Δ*

Accession #	Identified Proteins	Mol Wt	Total Spectra
gi 14318532	Ubp6p	57 kDa	5
gi 6322035	Ubp7p	123 kDa	6
gi 6323879	Ubp8p	54 kDa	3
gi 6321623	Ubr1p	225 kDa	5
gi 6323052	Ubr2p	217 kDa	8

PTM analysis for ubiquitin addition (ie. Gly-Gly or mass shift of +114 in MS/MS) revealed there were potential ubiquitination sites in the *erg6Δ rtr1Δ* in the presence of MG132 identified in Rpb2 and Rpb6. Figure 16 shows the Rpb2 sequence coverage obtained in MS/MS analysis. The sequence of the potential ubiquitination modification site was located in the amino acid sequence: K.RIQYAKDILQK(+114).E. However, it is unlikely that this peptide would truly be a site of ubiquitin modification due several issues. The peptide is short with only 11 residues and only a [M +2] charge state. In addition, there were only 2 spectra counted, and a greater number of counts would be expected if it were truly a site of modification. Furthermore, although a modified lysine residue was identified, it was not covered in the CID spectrum.

gj|6324725|ref|NP_014794.1| (100%), 138,757.2 Da
 Rpb2; TXN [Saccharomyces cerevisiae S288c]
 91 unique peptides, 99 unique spectra, 3568 total spectra, 641/1224 amino acids (52% coverage)

```

MSDLANSEKY  YDEDPYGFED  ESAPITAEDS  WAVISAFFRE  KGLVSSQQLDS
FNQFVDYTLQ  DIICEDSTLI  LEQLAQHTTE  SDNISRKYEI  SFGKIYVTKP
MVNESDGVTH  ALYPQEARLR  NLTYSSGLFV  DVKKRTYEAI  DVPGRELKYE
LIAEESDDDS  ESGKVFIGRL  PIMLRSKNCY  LSEATESDLY  KLKECPFDMG
GYFIINGSEK  VLIAQERSAG  NIVQVFKKAA  PSPISHVAEI  RSALEKGSRF
ISTLQVKLYG  REGSSARTIK  ATLPYIKQDI  PIVIIFRALG  IIPDGEILEH
ICYDVNDWQM  LEMLKPCVED  GFVIQDRETA  LDFIGRRGTA  LGIKKEKRIQ
YAKDILQKEF  LPHITQLEGF  ESRKAFFLGY  MINRLLLCAL  DRKDQDDRHD
FGKKRLDLAG  PLLAQLFKTL  FKKLTKDIFR  YMQRTVEEAH  DFNMKLAINA
KTITSGLKYA  LATGNWGEQK  KAMSSRAGVS  QVLNRYTYSS  TLSHLRRTNT
PIGRDGKLAKE  PRQLHNTHWG  LVCPAETPEG  QACGLVKNLS  RNSCISVGTD
PMPITFLESE  WGMEPLEDYV  PHQSPDATRV  FVNGVWHGVH  LMPARLMETL
RTLRRKGDIN  PEVSMIRDIR  EKELKIFTDA  GRVYRPLFIV  EDDESLGHKE
LKVRKGHIAK  LMATEYQDIE  GGFEDVEEYT  WSSLNNEGLV  EYIDAESEES
ILIAMQPEDL  EPAEANEEND  LDVDPAKRIR  VSHHATTFTH  CEIHPSMILG
VAASIIFFPD  HNQSPRNTYQ  SAMGKQAMGV  FLTNYNVRMD  TMANILYYPQ
KPLGTTTRAME  YLKFRELPAQ  QNAIVAIAICY  SGYNQEDSMI  MNQSSIDRGL
FRSLFFRSYM  DQEKKYGMSI  TETFEEKPQRT  NTLRMKHGTY  DKLDDDGLIA
PGVRVSGEDV  IIGKTTPISP  DEEELGQRTA  YHSKRDASTP  LRSTENGIVD
QVLVTTNQDG  LKFVKKVRVRT  TKIPQIGDKF  ASRHGQKGTI  GITYRREDMP
FTAEGIVPDL  IINPHAIPSR  MTVAHLIECL  LSKVAALSGN  EGDASPFTDI
TVEGISKLLR  EHGYSQRGFE  VMYNGHTGKK  LMAQIFFGPT  YYQRLRHMVD
DKIHARARGP  MQVLTRQPVE  GRSRDGGLRF  GEMERDCMIA  HGAASFLKER
LMEASDAFRV  HICGICGLMT  VIAKLNHNQF  ECKGCDNKID  IYQIHIPYAA
KLLFQELMAM  NITPRLYTDR  SRDF

```

Figure 16. Peptide sequence coverage of RNAPIIs second largest subunit Rpb2 obtained from *erg6Δtrt1Δ* in the presence of MG132 using Scaffold software. Yellow highlighted areas indicate peptide sequences identified by LC-MS analysis; Green highlighted amino acids are residues of possible modification; Red outlined sequence indicates potential ubiquitination site. The identified spectra containing residues 348-358 with sequence: K.RIQYAKDILQK(+114).E modified at K358.

The representative sequence coverage for Rpb6 obtained from the *erg6Δtrt1Δ* in the presence of MG132 seen in Figure 17 displays a sequence containing a potential ubiquitination site which is more likely than that indicated in the Rpb2 subunit when considering the analysis of the ion fragmentation spectra in addition to the high sequence coverage. The sequence, K.DGETTDANGK*IVTGGNGPEDFQQHEQIR.R, where K* is the potential modification site for ubiquitin addition with mass shift +114, contains 33 amino acids and has one missed cleavage at an interior lysine residue. Further confidence in this potential modification site is seen from the spectra (Figure 17). Notably, the precursor ion has a low parent mass error score and a +3 charge state which strengthens

confidence in the identification of this modified peptide as there are potentially more spectra identified with higher charge states.

gj|6325445|ref|NP_015513.1| (100%), 17,910.4 Da
 Rpb6; TXN [Saccharomyces cerevisiae S288c]
 12 unique peptides, 14 unique spectra, 242 total spectra, 79/155 amino acids (51% coverage)

```

MSDYEEAEND GNENFEDFDV EHFSDDEETYE EKPFQFK DGET TDANGKTIVT
GGNGPEDFQQ HEQIR RKTLK EKALPKDQRA TTPYMTKYER ARTLGLTRALQ
TSMNAPVFDV LEGETDPLRI AMKELAEKKI PLVIRRYLPD GSFEDWSVEE
LIVDL
  
```

Rpb6 Peptide: K.DGETTDANGK(+114)TIVTGGNGPEDFQQHEQIR.R
 2 Spectra; ID'd by X!Tandem only
PUTATIVELY IDENTIFIED

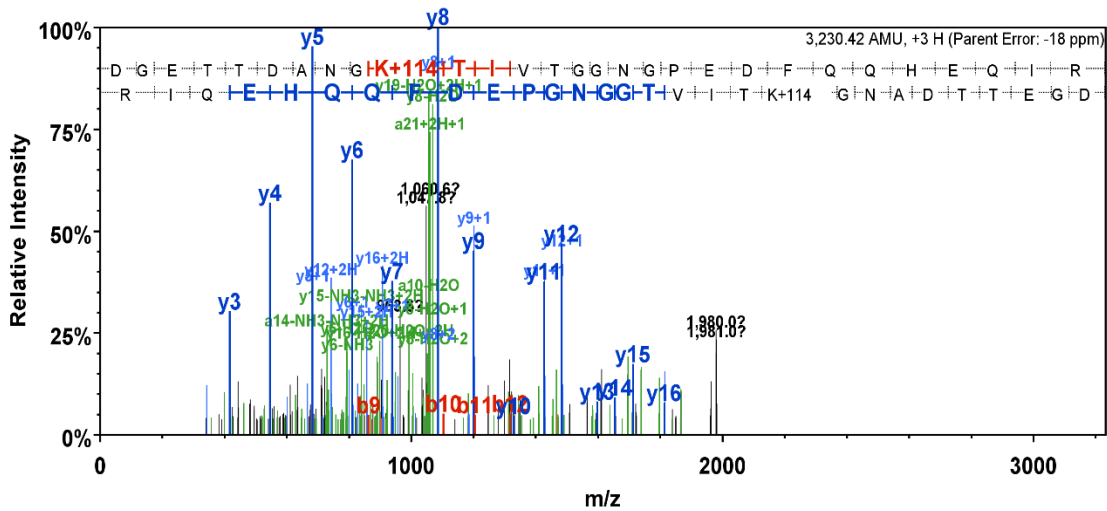


Figure 17. Peptide sequence coverage and ion fragmentation spectra of RNAPIIs subunit Rpb6 obtained from *erg6Δrtr1Δ* in the presence of MG132 using Scaffold software. Yellow highlighted areas indicate peptide sequences identified by LC-MS analysis; Green highlighted amino acids are residues of possible modification; Red outlined sequence indicates potential ubiquitination site. The identified spectra containing residues 37-65 with sequence: K.DGETTDANGK(114+)IVTGGNGPEDFQQHEQIR.R modified at K46.

V. Identification of phosphorylation sites in RNA Polymerase II purifications using a two-step bioinformatics analysis

Since Rtr1 is a protein phosphatase, we also performed a search for changes in the phosphorylation status of RNAPII in the MG132 *erg6Δ rtr1Δ* samples relative to paired controls. One potential site was identified in Rpb1 just before the CTD in the linker region at threonine 1471. The total sequence coverage of Rpb1 provided in Figure 18

indicates the peptide sequence for the potential modification site outlined in red.

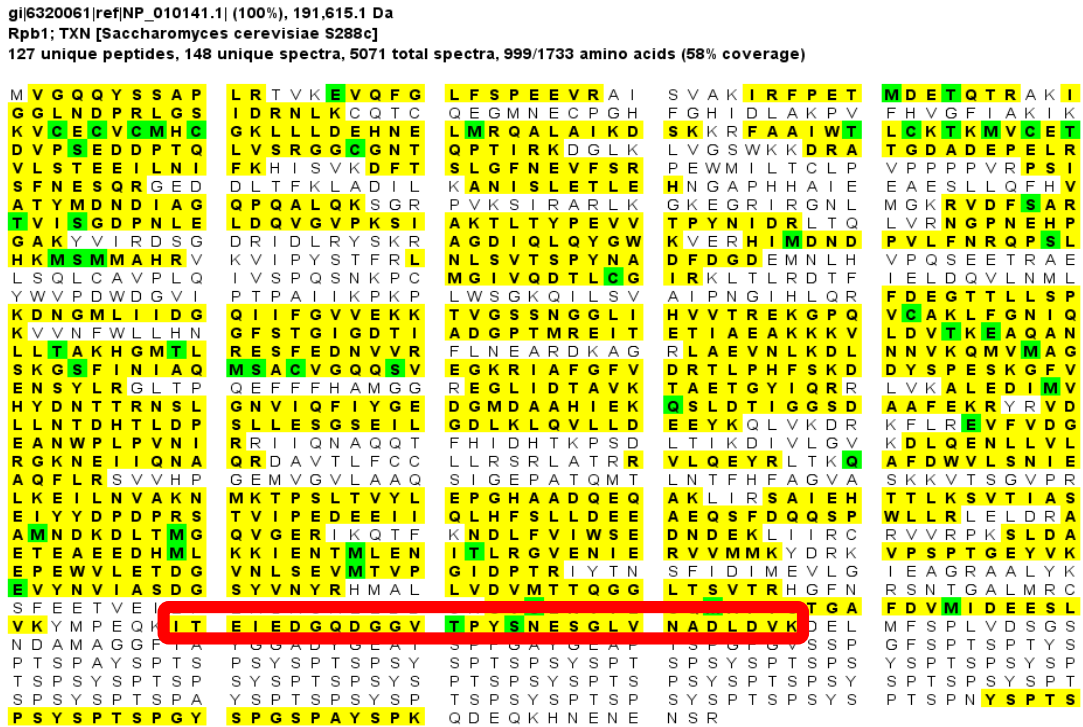


Figure 18. Sequence coverage of Rpb1 obtained following *erg6Δ rtr1Δ* in the presence of MG132 using Scaffold software. Yellow highlighted areas indicate peptide sequences identified by LC-MS analysis; Green highlighted amino acids are residues of possible modification; Red outlined sequence indicates potential phosphorylation site. The identified spectra containing residues 1459-1487 with sequence: K.DGETTDANGK(114+)-IVTGGNGPEDFQQHEQIR.R modified at T1471.

The peptide containing the potential site has 29 amino acids with sequence: ITEIEDGQDGGVT(+80)PYSNESGLVNADLDVK and was observed 33 times in the LC-MS run with an additional 12 unmodified spectra of the same peptide. The fragmentation spectra (Figure 19A and B) shows a +3 precursor ion charge state, low parent error for both spectra and no or limited neutral loss in the modified and unmodified spectra (Figure 19B).

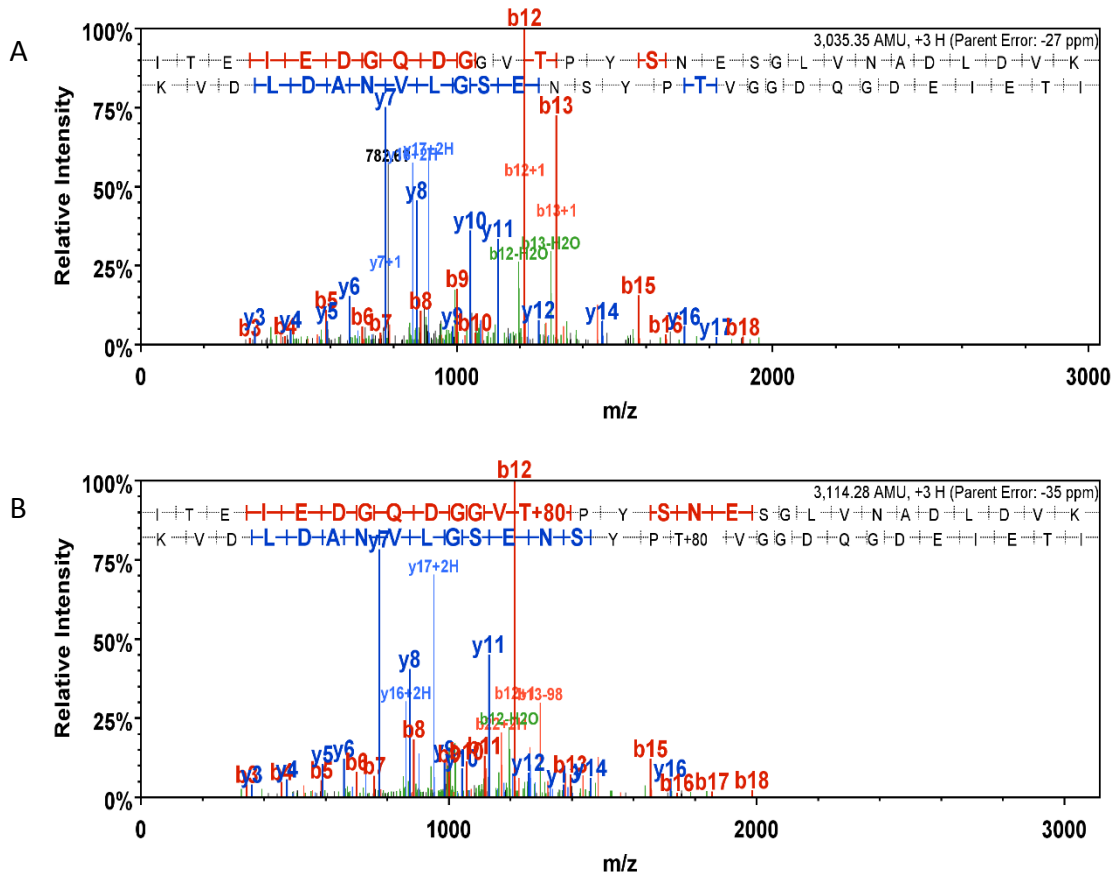


Figure 19. Ion fragmentation spectra obtained from LC-MS/MS for *erg6Δ rtr1Δ* in the presence of MG132 using Scaffold software. A. Unmodified spectra of peptide containing Rpb1 residues 1459-1487 (ITEIEDGQDGGVTPYSNESGLVNADLDVK). B. Spectra of peptide containing Rpb1 residues 1459-1487 (ITEIEDGQDGGVT(+80)PYSNESGLVNADLDVK) with identified phosphorylation site at threonine 1471 (T+80)

VI. Can Threonine 1471 be dephosphorylated by Rtr1 *in vitro*?

In order to determine if the phosphorylated peptide sequence is a substrate of the phosphatase Rtr1, synthetic peptides of both modified and unmodified linker region were generated and used in an *in vitro* phosphatase assay. The assay was performed using a Malachite Green Phosphate Assay using a recombinant GST-Rtr1 added to mixtures containing either modified and unmodified peptides. Figure 20 shows the activity graph for multiple concentrations of Rtr1. The unmodified peptide showed a higher absorbance measurement at 620nm than the phosphorylated peptide indicating that more phosphate

was released in the unmodified reaction wells which is likely background level phosphatase release; therefore, we cannot conclude that the peptide is a substrate of Rtr1 at this time but this part of the project will be continued by other members of the laboratory.

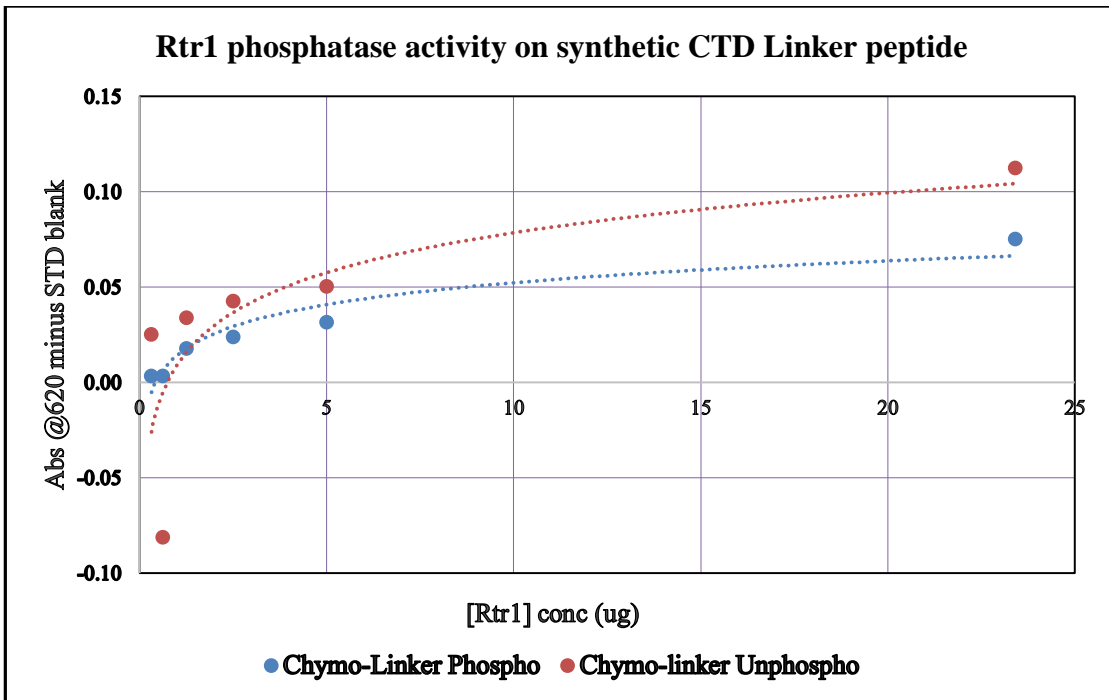


Figure 20. Malachite Green Phosphate Assay using recombinant GST-Rtr1 for potential substrate. Phosphorylated (Blue) and unmodified (Red) synthetic CTD peptides were incubated with various concentrations of Rtr1 and a phosphatase activity curve for each peptide was generated. Data does not conclusively identify the synthetic peptide as a substrate for Rtr1.

DISCUSSION

Through the use of *RTR1* deletion strains, proteomic LC-MS/MS analysis and ChIP experiments, the regulatory role of Rtr1 in dephosphorylation of S5-P during transcription elongation was established (Mosley et al., 2009). In addition to the accumulation of S5-P in the transcribed region in *rtr1Δ*, in an *in vitro* phosphatase assay Rtr1 dephosphorylated RNAPII phosphorylated at S5 residues. Additional studies since have identified an increase in interaction between RNAPII CTD and the proteasome, the cellular protein degradation machinery, in the absence of Rtr1 (see Table 2) which prompted this current investigation into what role Rtr1 plays in the degradation or turnover of the RNAPII during active transcription. Specifically, there were three aims for these studies: 1) Determine if CTD hyperphosphorylation due to loss of the CTD phosphatase, Rtr1, promotes RNAPII turnover and degradation; 2) Determine if CTD hyperphosphorylation due to the loss of the CTD phosphatase, Rtr1, promotes increased interaction with ubiquitin-proteasome associated proteins; and 3) Identify novel post-translational modifications in the RNAPII complex following proteasome inhibition using MuDPIT analysis. To that end, mutant strains of *S. cerevisiae* were subjected to proteasomal inhibition, affinity purification and subsequent proteomic analysis via mass spectrometry to identify any post-translational modifications and potential proteasomal interactions with the RNAPII complex.

The modification state of RNAPII and especially the CTD of its largest subunit, Rpb1, is critical to transcription and gene expression (for recent review see Hsin & Manley, 2012). The results reported from immunoblot analysis (Figure 7 and 9) in this work confirm previous findings of accumulation of S5-P CTD in *rtr1Δ* mutants (Mosley

et al., 2013; Mosley et al., 2009). The importance of this hyperphosphorylation has consequences for transcription in several key ways, as it has been shown to be involved in the recognition or recruitment of elongation factors, chromatin remodeling, histone methylation, capping enzymes, and termination factors (Fabrega et al., 2003; Hampsey & Reinberg, 2003; Phatnani & Greenleaf, 2006; Vasiljeva, Kim, Mutschler, Buratowski, & Meinhart, 2008). The increased accumulation of S5-P in the *RTR1* deletion strains following treatment with the proteasome inhibitor, MG132 (Figure 7 and 9), supports our hypothesis that hyperphosphorylation does in fact promote targeting of RNAPII for degradation. The exact mechanism by which this occurs is not clear from this data, however, the potential link of this modification leading to increased interactions with the ubiquitin and proteasome related proteins are discussed in more detail below.

In contrast to the accumulation of hyperphosphorylated RNAPII, the decreased recovery of RNAPII in the untreated Rpb3-TAP *erg6Δ rtr1Δ* in comparison to the MG132 treated Rpb3-TAP *erg6Δ rtr1Δ* cells was also noted (See Figures 14 and 15 in Results Section). Since the untreated cells were not subjected to proteasomal inhibition by MG132, this result has also been attributed to proteasome-dependent degradation of the RNAPII. Alternatively, it is possible that the ubiquitination of the Rpb3 subunit alone could cause the reduction of overall RNAPII seen in Figures 14 and 15 since all purifications were performed using Rpb3-TAP as the bait. Performing this study with multiple TAP tagged endogenous subunit of RNAPII in replicate studies would possibly confirm that the overall reduction of RNAPII is due to proteasomal degradation and independent of the tagged subunit.

In addition to S5-P accumulation, S7-P was also more abundant in the absence of Rtr1 when compared to the *ERG6* deletion background control pair as indicated in Figure 9. This result is interesting as Rtr1 has not been shown to directly interact with S7-P, so levels throughout the transcribed region of the genes remain steady during transcription, or may even increase slightly toward the end of the reading frame, as previously noted (Chapman et al., 2007; M. Kim et al., 2009); we therefore would not expect to see a dramatic increase in this CTD mark with the loss of Rtr1. However, Egloff and colleagues have reported intriguing results that the S7-P signal is recognized by the human homolog of Rtr1, RNA Polymerase II-associated protein 2 (RPAP2). In fact, they used RPAP2 knockdown in mammalian cells to determine that not only is S7-P on the CTD necessary for interaction with RPAP2, but the mark is involved with RPAP2 recruitment to actively transcribed snRNA genes (Egloff, Zaborowska, et al., 2012). These results highlight the importance of further investigation into what additional roles S7-P may play in gene expression.

In addition to the increase in S7-P observed between *erg6Δ* and *erg6Δ rtr1Δ*, it appears that there is a small increase in S7-P when comparing the untreated to the MG132 treated pairs (Figures 8 and 9). This result may be attributed to the accumulation of transcriptionally active RNAPII that could not be degraded due to the proteasomal inhibition supporting the hypothesis that hyperphosphorylated CTD is more readily targeted for degradation by the proteasome.

In contrast to the increases seen in the S5-P and S7-P modifications, Y1-P and S2-P were not detected in any of the samples by western blot analysis likely due to insufficient levels of these modifications and/or low titer antibodies used for western blot

analysis (Figure 8). The anti-phosphorylated tyrosine antibody used for this study has since been shown to detect Y1-P using purified RNAPII samples instead of whole cell extracts (data not shown) and therefore likely has a low affinity for the modification. Phosphorylation at these CTD sites peaks toward the 3' end of the transcribed region (Mayer et al., 2012; Mayer et al., 2010) and have not been implicated in *rtr1Δ* defects. The lack of phosphorylation at these CTD residues suggests that the RNAPII could have been arrested early in transcriptional activities, possibly before the Y1-P and S2-P could be placed on the CTD, which is consistent with previous results reported by multiple groups (Heidemann & Eick, 2012; Mayer et al., 2012). Importantly, an apparent decrease was seen in overall RNAPII in the MG132 treated and untreated *rtr1Δ* double mutants when compared to the *erg6Δ* background (Figure 15). Our results show that inhibition of proteasomal activity resulted in an increased accumulation of proteins in treated *erg6Δ rtr1Δ* cells in comparison with its untreated counterpart (Figure 7 and 9 and 15). Moreover, when comparing the untreated cells with those exposed to MG132, there is a pronounced increase in the amount of purified RNAPII present in the MG132 treated double mutant cells (Figure 15). These results may indicate that MG132 inhibition decreased the turnover rate of RNAPII in the treated sample, whereas the lower yield of RNAPII seen in the untreated sample could be attributed to normally functioning proteasomal degradation in combination with the defects associated with *rtr1Δ* (Mosley et al., 2009). Notably, the effect is not present in the *erg6Δ* MG132 treated and untreated samples in Figure 15; a result which further increases our confidence in the hypothesis that the loss of Rtr1 is indeed a factor in increased targeting following proteasomal inhibition.

As mentioned previously in the Introduction, there are many recent studies focused on the role of the proteasome and transcriptional regulation as highlighted by recent reviews (Finley, Ulrich, Sommer, & Kaiser, 2012; Wilson et al., 2013). Ubiquitination is the means by which target proteins are marked for degradation by the proteasome through the addition of polyubiquitin chains reviewed in (Pickart & Eddins, 2004). To evaluate the link of proteasomal degradation to RNAPII, proteomic analysis was carried out on all experimental samples. Affinity purification products of the *rtr1Δ* mutants and *erg6Δ* background strains were subjected to a database search in Scaffold software for proteins associated with transcription (TXN) and degradation as well as post-translational modifications for ubiquitin and phosphorylation. Protein identifications will be examined here while results of the post-translational modifications will be discussed below.

The protein identifications obtained following LC-MS/MS analysis for each genotype are presented in Tables 7-10. The MG132 treated and untreated *erg6Δ* background strains had comparable overall total protein identifications with 35 proteins identified in the untreated and 32 proteins identified in the MG132 treated samples within our cutoffs, however, the content of the proteins identified interesting protein interactions (Tables 7 and 9) which appear to be active at different stages of transcription. For example, data presented in Table 7 shows that the untreated *erg6Δ* cells had the most transcription elongation-associated proteins detected of all 4 samples (Ctr9, Dst1, Rtf1, Spt5, Spt6, Asr1, Set3, and Rtr1), but only had one each of proteins associated with transcription initiation (Taf8) and transcription termination (Sen1). There were nine total ubiquitin and proteasomal proteins detected in the MS analysis in this data set. In

contrast, the MG132 treated *erg6Δ* sample recovered only 4 elongation related proteins (Ctr9, Dst1, Spt5, Spt6, see also Table 8), all of which we detected in the untreated sample as well. One transcription initiation protein was detected, Tfg1, which is the largest subunit of the TFIIF complex (*Saccharomyces* genome database at www.yeastgenome.org). There is, however a comparable number of ubiquitin and proteasome-associated proteins identified (Tables 7 and 8) between the untreated and treated *erg6Δ* samples. These results make it difficult to draw any conclusions regarding proteasome degradation since there is not a significant difference between the untreated and MG132 treated conditions. Of note, however, is the lack of elongation factors associated with MG132 treatment. It is possible that the proteasome inhibition caused a reduction of total RNAPII occupancy during elongation, resulting in abrupt dissociation and subsequent reduction in association of the RNAPII with elongation factors. This could be investigated through the use of ChIP following MG132 treatment.

There is a large difference between the total number of proteins identified between the treated and untreated *rtr1Δ* double mutants. As indicated in Tables 9 and 10, there were no proteins associated with the proteasome or ubiquitin in the untreated *erg6Δ rtr1Δ* while the MG132 treated *erg6Δ rtr1Δ* yielded the most proteins and total spectra of the four conditions assessed. The total RNAPII for the untreated *erg6Δ rtr1Δ* was very low (Figures 14 and 15) and this result partially accounts for the overall poor yield of MS/MS data. Poor purification and sample preparation prior to MS analysis could also contribute to poor MS/MS evaluation. The treated *erg6Δ rtr1Δ* sample revealed the most interactions of the 4 assessed conditions with proteins associated with the proteasome (Rpn2, Rpn4, Rpn6, and Rpt3) and ubiquitin related proteins (Ubp12, Ubp13, Ubp16,

Ubp3, Ubp6, Ubp7, Ubp8, Ubr1, and Upr2). The increase in interactions with the proteasome and ubiquitin associated proteins in the MG132 treated *erg6Δ rtr1Δ* cells supports our hypothesis that there is increased interaction of the proteasome with hyperphosphorylated RNAPII.

Presented in Table 11 is a summary comparison of the transcription-related, ubiquitin-related and proteasomal-related proteins detected in the MS/MS results. As noted for the MG132 treated background *erg6Δ* results, there is a distinct lack of elongation factors detected in the MG132 treated *erg6Δ rtr1Δ* cells. Of the four that were identified (Chd1, Spt5, Rtf1, and Set2) only one was common to the MG132 treated *erg6Δ* (Tables 10 and 11). This suggests that the cellular pool of RNAPII was different than that purified from *erg6Δ*, presumably due to the hyperphosphorylation of the CTD, but it is possible the decrease in RNAPII association with elongation factors due to incompetent RNAPII or RNAPII which is not locally available for transcription. An analogous situation has been recently published by Forget and coworkers regarding RPAP2, the human homolog of Rtr1 (Forget et al., 2013). Results of localization studies indicate that the human CTD phosphatase is a bifunctional regulatory enzyme which not

Table 11. Summary Comparison of detected proteins from MS/MS data

		<i>erg6Δ</i>		<i>erg6Δrtr1Δ</i>	
		Untreated	MG132 Treated	Untreated	MG132 Treated
Transcription Phase	Initiation	Taf8	Tfg1	N/A	N/A
	Elongation	Ctr9, Dst1, Rtf1, Spt5, Spt6, Asr1, Set3, Rtr1	Ctr9, Dst1, Spt5, Spt6	Tra1, Chd1	Chd1, Spt5, Rtf1, Set2
	Termination	Sen1	N/A	N/A	N/A
Ubiquitin related		Bur1, Bur2, Uba2, Uba3, Uba9	Ubp10, Ubp3, Ubp7, Ubr1, Ubx4	N/A	Ubp12, Ubp13, Ubp16, Ubp3, Ubp6, Ubp7, Ubp8, Ubr1, Upr2
Proteasome related		Pre2, Rpn3, Rpn7	Pre8, Rpn4	N/A	Rpn2, Rpn4, Rpn6, Rpt3,

only dephosphorylates the CTD in the nucleus, but also regulates the availability of assembled RNAPII complex by co-transporting with it from the cytoplasm into the nucleus (Forget et al., 2013). When RPAP2 was knocked down using siRNA, RNAPII was sequestered in the cytoplasm (Forget et al., 2013). Considering Forget and coworkers found that RNAPII is transported into the nucleus in a fully assembled complex and our findings of the MG132 treatment of *erg6Δ rtr1Δ*, the depleted levels of interaction with elongation factors may be due to RNAPII being exported to the cytoplasm and unavailable for transcription. Additional studies to investigate the localization of RNAPII in MG132 treated *rtr1Δ* will need to be performed to investigate the validity of this mechanism and to determine if the RNAPII is transported out of the nucleus to be targeted for proteasomal degradation.

The most common and best studied PTMs are reversible phosphorylation and ubiquitination for which MS is a uniquely powerful tool suited to their characterization through the peptide fragmentation patterns achieved following collision induced

dissociation. As a goal of these current studies, determination of post translational modifications was important due to a variety of systemic biological functions attributed to the dynamic interactions of these alterations. The first, and most important step in studying PTMs is to determine the type and site of modification (Salzano & Crescenzi, 2005). Consequently, spectra obtained from *erg6Δ* background and *erg6Δrtr1Δ* mutant samples were subjected to a database search using SEQUEST followed by Scaffold analysis. Database searches of obtained MS spectra were conducted for ubiquitination modifications for all experimental conditions. The resulting identification of potential ubiquitination sites not previously reported were found only in the MG132 treated *erg6Δrtr1Δ*. The sites were located in Rpb2 and Rpb6 at locations K358 and K46, respectively (Figures 16 and 17). The confidence in PTM identification is stronger for the Rpb6 modification than that the site of modification identified for Rpb2 based on the collected MS/MS data. This site could be confirmed through the use of an *in vitro* ubiquitination assay and MS analysis to assess whether the synthetic peptide matches the experimentally derived sequence as reported previously (Somesh et al., 2005).

An important point to review here is that only two ubiquitin modification sites related to RNAPII have been reported for Rpb1 using both *in vivo* and *in vitro* methods to elucidate the sites (Peng et al., 2003; Somesh et al., 2005; Somesh et al., 2007), despite evidence of ubiquitin dependent regulation of RNAPII being well documented (Collins & Tansey, 2006; and recently reviewed in Hammond-Martel, Yu, & Affar el, 2012). The lack of ubiquitin site identification can be credited to the discovery that MS sample preparations using iodoacetamide as an alkylating agent caused spectral artifacts that mimicked ubiquitin modifications in MS/MS analysis. The presence of diglycine

modifications on lysines contributed greatly to the high false discovery rates of ubiquitin modifications (Nielsen et al., 2008). As a consequence, the use of chloroacetamide as an alkylating reagent to modify digested samples was recommended. In our study, several factors are thought to have contributed to the low incidence of ubiquitin modification identified. One potential source of low yield is the potential deubiquitinase activity.

Despite the use of chloroacetamide in peptide digest preparations, which alkylated the cysteine(s) in ubiquitin proteases, additional measures should have been taken to inhibit deubiquitinase enzymes during cell lysis to control for ubiquitin degradation during and after purification processing. This would ensure that ubiquitin was not removed by specific proteases and improve the likelihood of ubiquitin modification identification in MuDPIT analysis. In fact, in our data we saw specific association of a number of ubiquitin proteases in the *erg6Δ rtr1Δ* MG132 treated sample (specifically: Ubp12, Ubp13, Ubp16, Ubp3, Ubp6, Ubp7, Ubp8). In addition to the addition of an ubiquitin protease inhibitor during cell lysis, incorporation of an enrichment step into the purification process or even during pre-analytical sample preparations would potentially increase the relative abundance of the modified peptides. In fact, planned follow up studies include the addition of a ubiquitin tag similar to the TAP tag using homologous recombination techniques previously described (See Introduction and Methods). The proposed enrichment involves a two-step affinity purification through immunoprecipitation for RNAPII followed by ubiquitin. The studies will ideally reveal proteome changes associated with ubiquitin.

In the case of phosphorylation a positive mass shift of 80 Da associated with a tyrosine, serine, or threonine residue is seen on the modified spectra. Upon fragmentation

of many of these peptide ions with collision induced dissociation a neutral loss of -98 daltons is often observed. The MS/MS PTM search results obtained for *erg6 Δ rtr1 Δ* revealed a potential phosphorylation site in the linker region between the globular domain and the CTD of the largest RNAPII subunit, Rpb1 (Figures 17 and 18). This T1471 phosphorylation site has not been previously detected in our lab despite exhaustive PTM searches on wild-type *S. cerevisiae* strains. Interestingly, phosphorylation at this site has been independently reported following a phosphorylation analysis using tandem MS in two separate studies although a biological role for this modification is not known (Albuquerque et al., 2008; Mohammed et al., 2008). In the first study, Albuquerque and colleagues performed a global phosphoproteome analysis using various separation strategies to enrich for and then identify low abundance phosphopeptides which yielded an increased amount of phosphorylation. In the second experiment, Mohammed and coworkers were able to achieve almost 100% sequence coverage of the subunits of RNAPII and RNAPIII using multiple proteases (including trypsin, chymotrypsin, and GluC) to digest samples which enriched for phosphoproteins and then subjected them to LC-MS/MS with sequential electron transfer dissociation (ETD) and CID in order to obtain the highest sequence coverage possible. In the process multiple phospho-protein identifications were achieved. Interestingly, the T1471 phosphopeptide was reported by Mohammed et al. although the authors used a high 5% FDR. To our knowledge, no further studies have been reported elucidating the importance of this particular PTM. Future studies in the Mosley laboratory could focus on performed *in vivo* analysis of the role of T1471 phosphorylation in the regulation of RNAPII transcription. Additionally, this dataset indicates that Rtr1 might be involved in the regulation of T1471 levels *in*

vivo. Although our initial attempts at *in vitro* T1471 dephosphorylation failed (Figure 20), future studies could use a more sensitive approach to measure changes in T1471 levels in the presence or absence of Rtr1 such as ELISA and/or multiple reaction monitoring (MRM) experiments.

CONCLUSION

The role that the CTD phosphatase Rtr1 has in the regulation of transcription has been discovered; however, it is still incompletely understood. Preliminary data collected by Mosley and colleagues (Table 2) documented an increased association of RNAPII with members of the ubiquitin-proteasome system in Rtr1 deletion strains of *S. cerevisiae*. As a consequence, the studies presented here aimed to further characterize the role of Rtr1 in RNAPII recycling through the use of proteomic analysis to reveal potential protein interactions with the members of the ubiquitin-proteasome system and potential sites of post-translational modification within the RNAPII complex that may be involved in regulation of transcription.

The original hypothesis that the hyperphosphorylation of the CTD due to a loss of Rtr1 phosphatase activity increased RNAPII complex turnover was supported by the accumulation of S5-P CTD (Figure 7 and 9) following RNAPII purification in the presence of the proteasome inhibitor, MG132. Additionally, hyperphosphorylation was linked to increasing interaction of RNAPII the proteasome through MuDPIT data revealing an increased number of ubiquitin related and proteasomal proteins associated with RNAPII in MG132 treated extracts (Tables 7-10).

The final aim of these studies revealed potential ubiquitin and phosphorylation PTMs in the RNAPII subunits. Rpb2 and Rpb6 had ubiquitin sites identified (Figures 16 and 17), however, there is a low likelihood that the Rpb2 site can be confirmed due to low spectrum quality. The confirmation of the phosphorylation site found on Rpb1, T1471 (Figure 18 and 19), is continuing in our laboratory through the use of a synthetic phosphopeptide matching the sequence obtained from MS data as well as its unmodified

form. Several *in vitro* follow up functional analyses are planned to evaluate the synthetic phosphopeptide with the goal to gain insight into the importance of this modification to transcriptional control. These studies will include additional phosphate assays to investigate whether this site is a substrate of Rtr1 and MS/MS analysis following digestion of the synthetic peptide. Additionally, we propose production of T1471-site specific antibody to be used in assays such as ELISA, Western blot analysis, and ChIP. Finally, the use of site specific mutagenesis could help to determine the biological significance of phosphorylation event and how loss of this modification affects RNAPII function.

REFERENCES

- Ahn, S. H., Kim, M., & Buratowski, S. (2004). Phosphorylation of serine 2 within the RNA polymerase II C-terminal domain couples transcription and 3' end processing. *Mol Cell*, *13*(1), 67-76.
- Akhtar, M. S., Heidemann, M., Tietjen, J. R., Zhang, D. W., Chapman, R. D., Eick, D., & Ansari, A. Z. (2009). TFIIF kinase places bivalent marks on the carboxy-terminal domain of RNA polymerase II. *Mol Cell*, *34*(3), 387-393. doi: 10.1016/j.molcel.2009.04.016
- Albuquerque, C. P., Smolka, M. B., Payne, S. H., Bafna, V., Eng, J., & Zhou, H. (2008). A multidimensional chromatography technology for in-depth phosphoproteome analysis. *Mol Cell Proteomics*, *7*(7), 1389-1396. doi: 10.1074/mcp.M700468-MCP200
- Allison, L. A., Moyle, M., Shales, M., & Ingles, C. J. (1985). Extensive homology among the largest subunits of eukaryotic and prokaryotic RNA polymerases. *Cell*, *42*(2), 599-610.
- Anindya, R., Aygun, O., & Svejstrup, J. Q. (2007). Damage-induced ubiquitylation of human RNA polymerase II by the ubiquitin ligase Nedd4, but not Cockayne syndrome proteins or BRCA1. *Mol Cell*, *28*(3), 386-397. doi: S1097-2765(07)00671-5 [pii]10.1016/j.molcel.2007.10.008
- Banks, C. A., Kong, S. E., & Washburn, M. P. (2012). Affinity purification of protein complexes for analysis by multidimensional protein identification technology. *Protein Expr Purif*, *86*(2), 105-119. doi: 10.1016/j.pep.2012.09.007
- Bataille, A. R., Jeronimo, C., Jacques, P. E., Laramée, L., Fortin, M. E., Forest, A., . . . Robert, F. (2012). A universal RNA polymerase II CTD cycle is orchestrated by complex interplays between kinase, phosphatase, and isomerase enzymes along genes. *Mol Cell*, *45*(2), 158-170. doi: 10.1016/j.molcel.2011.11.024
- Baudin, A., Ozier-Kalogeropoulos, O., Denouel, A., Lacroute, F., & Cullin, C. (1993). A simple and efficient method for direct gene deletion in *Saccharomyces cerevisiae*. *Nucleic Acids Res*, *21*(14), 3329-3330.
- Bauer, A., & Kuster, B. (2003). Affinity purification-mass spectrometry. Powerful tools for the characterization of protein complexes. *Eur J Biochem*, *270*(4), 570-578.
- Buratowski, S. (2003). The CTD code. *Nat Struct Biol*, *10*(9), 679-680. doi: 10.1038/nsb0903-679
- Cadena, D. L., & Dahmus, M. E. (1987). Messenger RNA synthesis in mammalian cells is catalyzed by the phosphorylated form of RNA polymerase II. *J Biol Chem*, *262*(26), 12468-12474.
- Chapman, R. D., Heidemann, M., Albert, T. K., Mailhammer, R., Flatley, A., Meisterernst, M., . . . Eick, D. (2007). Transcribing RNA polymerase II is phosphorylated at CTD residue serine-7. *Science*, *318*(5857), 1780-1782. doi: 10.1126/science.1145977
- Chen, L., Cai, Y., Jin, J., Florens, L., Swanson, S. K., Washburn, M. P., . . . Conaway, R. C. (2011). Subunit organization of the human INO80 chromatin remodeling complex: an evolutionarily conserved core complex catalyzes ATP-dependent nucleosome remodeling. *J Biol Chem*, *286*(13), 11283-11289. doi: 10.1074/jbc.M111.222505

- Chen, X., Ruggiero, C., & Li, S. (2007). Yeast Rpb9 plays an important role in ubiquitylation and degradation of Rpb1 in response to UV-induced DNA damage. *Mol Cell Biol*, *27*(13), 4617-4625. doi: 10.1128/MCB.00404-07
- Cho, H., Kim, T. K., Mancebo, H., Lane, W. S., Flores, O., & Reinberg, D. (1999). A protein phosphatase functions to recycle RNA polymerase II. *Genes Dev*, *13*(12), 1540-1552.
- Choi, H., & Nesvizhskii, A. I. (2008). False discovery rates and related statistical concepts in mass spectrometry-based proteomics. *J Proteome Res*, *7*(1), 47-50. doi: 10.1021/pr700747q
- Clemente-Blanco, A., Sen, N., Mayan-Santos, M., Sacristan, M. P., Graham, B., Jarmuz, A., . . . Aragon, L. (2011). Cdc14 phosphatase promotes segregation of telomeres through repression of RNA polymerase II transcription. *Nat Cell Biol*, *13*(12), 1450-1456. doi: 10.1038/ncb2365
- Collins, G. A., & Tansey, W. P. (2006). The proteasome: a utility tool for transcription? *Curr Opin Genet Dev*, *16*(2), 197-202. doi: 10.1016/j.gde.2006.02.009
- Corden, J. L., Cadena, D. L., Ahearn, J. M., Jr., & Dahmus, M. E. (1985). A unique structure at the carboxyl terminus of the largest subunit of eukaryotic RNA polymerase II. *Proc Natl Acad Sci U S A*, *82*(23), 7934-7938.
- Cramer, P. (2004). RNA polymerase II structure: from core to functional complexes. *Curr Opin Genet Dev*, *14*(2), 218-226. doi: 10.1016/j.gde.2004.01.003
- Edwards, A. M., Kane, C. M., Young, R. A., & Kornberg, R. D. (1991). Two dissociable subunits of yeast RNA polymerase II stimulate the initiation of transcription at a promoter in vitro. *J Biol Chem*, *266*(1), 71-75.
- Egloff, S., Dienstbier, M., & Murphy, S. (2012). Updating the RNA polymerase CTD code: adding gene-specific layers. *Trends Genet*, *28*(7), 333-341. doi: 10.1016/j.tig.2012.03.007
- Egloff, S., Zaborowska, J., Laitem, C., Kiss, T., & Murphy, S. (2012). Ser7 phosphorylation of the CTD recruits the RPAP2 Ser5 phosphatase to snRNA genes. *Mol Cell*, *45*(1), 111-122. doi: 10.1016/j.molcel.2011.11.006
- El Kaderi, B., Medler, S., Raghunayakula, S., & Ansari, A. (2009). Gene looping is conferred by activator-dependent interaction of transcription initiation and termination machineries. *J Biol Chem*, *284*(37), 25015-25025. doi: 10.1074/jbc.M109.007948
- Elias, J. E., & Gygi, S. P. (2007). Target-decoy search strategy for increased confidence in large-scale protein identifications by mass spectrometry. *Nat Methods*, *4*(3), 207-214. doi: 10.1038/nmeth1019
- Fabrega, C., Shen, V., Shuman, S., & Lima, C. D. (2003). Structure of an mRNA capping enzyme bound to the phosphorylated carboxy-terminal domain of RNA polymerase II. *Mol Cell*, *11*(6), 1549-1561.
- Farley, A. R., & Link, A. J. (2009). Identification and quantification of protein posttranslational modifications. *Methods Enzymol*, *463*, 725-763. doi: 10.1016/S0076-6879(09)63040-8
- Finley, D., Ulrich, H. D., Sommer, T., & Kaiser, P. (2012). The ubiquitin-proteasome system of *Saccharomyces cerevisiae*. *Genetics*, *192*(2), 319-360. doi: 10.1534/genetics.112.140467

- Florens, L., Carozza, M. J., Swanson, S. K., Fournier, M., Coleman, M. K., Workman, J. L., & Washburn, M. P. (2006). Analyzing chromatin remodeling complexes using shotgun proteomics and normalized spectral abundance factors. *Methods*, *40*(4), 303-311. doi: 10.1016/j.ymeth.2006.07.028
- Florens, L., & Washburn, M. P. (2006). Proteomic analysis by multidimensional protein identification technology. *Methods Mol Biol*, *328*, 159-175. doi: 10.1385/1-59745-026-X:159
- Forget, D., Lacombe, A. A., Cloutier, P., Lavalley-Adam, M., Blanchette, M., & Coulombe, B. (2013). Nuclear import of RNA polymerase II is coupled with nucleocytoplasmic shuttling of the RNA polymerase II-associated protein 2. *Nucleic Acids Res*, *41*(14), 6881-6891. doi: 10.1093/nar/gkt455
- Fournier, M. L., Gilmore, J. M., Martin-Brown, S. A., & Washburn, M. P. (2007). Multidimensional separations-based shotgun proteomics. *Chem Rev*, *107*(8), 3654-3686. doi: 10.1021/cr068279a
- Fuda, N. J., Buckley, M. S., Wei, W., Core, L. J., Waters, C. T., Reinberg, D., & Lis, J. T. (2012). Fcp1 dephosphorylation of the RNA polymerase II C-terminal domain is required for efficient transcription of heat shock genes. *Mol Cell Biol*, *32*(17), 3428-3437. doi: 10.1128/MCB.00247-12
- Gaber, R. F., Copple, D. M., Kennedy, B. K., Vidal, M., & Bard, M. (1989). The yeast gene ERG6 is required for normal membrane function but is not essential for biosynthesis of the cell-cycle-sparking sterol. *Mol Cell Biol*, *9*(8), 3447-3456.
- Gaczynska, M., & Osmulski, P. A. (2005). Small-molecule inhibitors of proteasome activity. *Methods Mol Biol*, *301*, 3-22. doi: 10.1385/1-59259-895-1:003
- Gietz, D., St Jean, A., Woods, R. A., & Schiestl, R. H. (1992). Improved method for high efficiency transformation of intact yeast cells. *Nucleic Acids Res*, *20*(6), 1425.
- Gilmore, J. M., & Washburn, M. P. (2010). Advances in shotgun proteomics and the analysis of membrane proteomes. *J Proteomics*, *73*(11), 2078-2091. doi: 10.1016/j.jprot.2010.08.005
- Glover-Cutter, K., Larochele, S., Erickson, B., Zhang, C., Shokat, K., Fisher, R. P., & Bentley, D. L. (2009). TFIIF-associated Cdk7 kinase functions in phosphorylation of C-terminal domain Ser7 residues, promoter-proximal pausing, and termination by RNA polymerase II. *Mol Cell Biol*, *29*(20), 5455-5464. doi: 10.1128/MCB.00637-09
- Graumann, J., Dunipace, L. A., Seol, J. H., McDonald, W. H., Yates, J. R., 3rd, Wold, B. J., & Deshaies, R. J. (2004). Applicability of tandem affinity purification MudPIT to pathway proteomics in yeast. *Mol Cell Proteomics*, *3*(3), 226-237. doi: 10.1074/mcp.M300099-MCP200
- Gygi, S. P., Corthals, G. L., Zhang, Y., Rochon, Y., & Aebersold, R. (2000). Evaluation of two-dimensional gel electrophoresis-based proteome analysis technology. *Proc Natl Acad Sci U S A*, *97*(17), 9390-9395. doi: 10.1073/pnas.160270797
- Hammond-Martel, I., Yu, H., & Affar el, B. (2012). Roles of ubiquitin signaling in transcription regulation. *Cell Signal*, *24*(2), 410-421. doi: 10.1016/j.cellsig.2011.10.009
- Hampsey, M., & Reinberg, D. (2003). Tails of intrigue: phosphorylation of RNA polymerase II mediates histone methylation. *Cell*, *113*(4), 429-432.

- Heidemann, M., & Eick, D. (2012). Tyrosine-1 and threonine-4 phosphorylation marks complete the RNA polymerase II CTD phospho-code. *RNA Biol*, 9(9), 1144-1146. doi: 10.4161/rna.21726
- Heidemann, M., Hintermair, C., Voss, K., & Eick, D. (2013). Dynamic phosphorylation patterns of RNA polymerase II CTD during transcription. *Biochim Biophys Acta*, 1829(1), 55-62. doi: 10.1016/j.bbagr.2012.08.013
- Hinnen, A., Hicks, J. B., & Fink, G. R. (1978). Transformation of yeast. *Proc Natl Acad Sci U S A*, 75(4), 1929-1933.
- Hirose, Y., & Ohkuma, Y. (2007). Phosphorylation of the C-terminal domain of RNA polymerase II plays central roles in the integrated events of eucaryotic gene expression. *J Biochem*, 141(5), 601-608. doi: 10.1093/jb/mvm090
- Hsin, J. P., & Manley, J. L. (2012). The RNA polymerase II CTD coordinates transcription and RNA processing. *Genes Dev*, 26(19), 2119-2137. doi: 10.1101/gad.200303.112
- Jensen-Pergakes, K. L., Kennedy, M. A., Lees, N. D., Barbuch, R., Koegel, C., & Bard, M. (1998). Sequencing, disruption, and characterization of the *Candida albicans* sterol methyltransferase (ERG6) gene: drug susceptibility studies in *erg6* mutants. *Antimicrob Agents Chemother*, 42(5), 1160-1167.
- Kalaydjieva, L. (2006). Congenital cataracts-facial dysmorphism-neuropathy. *Orphanet J Rare Dis*, 1, 32. doi: 10.1186/1750-1172-1-32
- Keller, A., Nesvizhskii, A. I., Kolker, E., & Aebersold, R. (2002). Empirical statistical model to estimate the accuracy of peptide identifications made by MS/MS and database search. *Anal Chem*, 74(20), 5383-5392.
- Kim, M., Suh, H., Cho, E. J., & Buratowski, S. (2009). Phosphorylation of the yeast Rpb1 C-terminal domain at serines 2, 5, and 7. *J Biol Chem*, 284(39), 26421-26426. doi: 10.1074/jbc.M109.028993
- Kim, W., Bennett, E. J., Huttlin, E. L., Guo, A., Li, J., Possemato, A., . . . Gygi, S. P. (2011). Systematic and quantitative assessment of the ubiquitin-modified proteome. *Mol Cell*, 44(2), 325-340. doi: 10.1016/j.molcel.2011.08.025
- Kobor, M. S., Archambault, J., Lester, W., Holstege, F. C., Gileadi, O., Jansma, D. B., . . . Greenblatt, J. (1999). An unusual eukaryotic protein phosphatase required for transcription by RNA polymerase II and CTD dephosphorylation in *S. cerevisiae*. *Mol Cell*, 4(1), 55-62.
- Komarnitsky, P., Cho, E. J., & Buratowski, S. (2000). Different phosphorylated forms of RNA polymerase II and associated mRNA processing factors during transcription. *Genes Dev*, 14(19), 2452-2460.
- Laybourn, P. J., & Dahmus, M. E. (1989). Transcription-dependent structural changes in the C-terminal domain of mammalian RNA polymerase subunit IIa/o. *J Biol Chem*, 264(12), 6693-6698.
- Lee, D. H., & Goldberg, A. L. (1996). Selective inhibitors of the proteasome-dependent and vacuolar pathways of protein degradation in *Saccharomyces cerevisiae*. *J Biol Chem*, 271(44), 27280-27284.
- Lee, J. S., Shukla, A., Schneider, J., Swanson, S. K., Washburn, M. P., Florens, L., . . . Shilatifard, A. (2007). Histone crosstalk between H2B monoubiquitination and H3 methylation mediated by COMPASS. *Cell*, 131(6), 1084-1096. doi: 10.1016/j.cell.2007.09.046

- Lee, K. K., Sardi, M. E., Swanson, S. K., Gilmore, J. M., Torok, M., Grant, P. A., . . . Washburn, M. P. (2011). Combinatorial depletion analysis to assemble the network architecture of the SAGA and ADA chromatin remodeling complexes. *Mol Syst Biol*, 7, 503. doi: 10.1038/msb.2011.40
- Li, Y. (2011). The tandem affinity purification technology: an overview. *Biotechnol Lett*, 33(8), 1487-1499. doi: 10.1007/s10529-011-0592-x
- Licatalosi, D. D., Geiger, G., Minet, M., Schroeder, S., Cilli, K., McNeil, J. B., & Bentley, D. L. (2002). Functional interaction of yeast pre-mRNA 3' end processing factors with RNA polymerase II. *Mol Cell*, 9(5), 1101-1111.
- Link, A. J., Eng, J., Schieltz, D. M., Carmack, E., Mize, G. J., Morris, D. R., . . . Yates, J. R., 3rd. (1999). Direct analysis of protein complexes using mass spectrometry. *Nat Biotechnol*, 17(7), 676-682. doi: 10.1038/10890
- Liu, C., Apodaca, J., Davis, L. E., & Rao, H. (2007). Proteasome inhibition in wild-type yeast *Saccharomyces cerevisiae* cells. *Biotechniques*, 42(2), 158, 160, 162.
- Lu, H., Flores, O., Weinmann, R., & Reinberg, D. (1991). The nonphosphorylated form of RNA polymerase II preferentially associates with the preinitiation complex. *Proc Natl Acad Sci U S A*, 88(22), 10004-10008.
- Mayer, A., Heidemann, M., Lidschreiber, M., Schrieck, A., Sun, M., Hintermair, C., . . . Cramer, P. (2012). CTD tyrosine phosphorylation impairs termination factor recruitment to RNA polymerase II. *Science*, 336(6089), 1723-1725. doi: 10.1126/science.1219651
- Mayer, A., Lidschreiber, M., Siebert, M., Leike, K., Soding, J., & Cramer, P. (2010). Uniform transitions of the general RNA polymerase II transcription complex. *Nat Struct Mol Biol*, 17(10), 1272-1278. doi: 10.1038/nsmb.1903
- Mohammed, S., Lorenzen, K., Kerkhoven, R., van Breukelen, B., Vannini, A., Cramer, P., & Heck, A. J. (2008). Multiplexed proteomics mapping of yeast RNA polymerase II and III allows near-complete sequence coverage and reveals several novel phosphorylation sites. *Anal Chem*, 80(10), 3584-3592. doi: 10.1021/ac7024283
- Mosley, A. L., Hunter, G. O., Sardi, M. E., Smolle, M., Workman, J. L., Florens, L., & Washburn, M. P. (2013). Quantitative proteomics demonstrates that the RNA polymerase II subunits Rpb4 and Rpb7 dissociate during transcriptional elongation. *Mol Cell Proteomics*, 12(6), 1530-1538. doi: 10.1074/mcp.M112.024034
- Mosley, A. L., Pattenden, S. G., Carey, M., Venkatesh, S., Gilmore, J. M., Florens, L., . . . Washburn, M. P. (2009). Rtr1 is a CTD phosphatase that regulates RNA polymerase II during the transition from serine 5 to serine 2 phosphorylation. *Mol Cell*, 34(2), 168-178. doi: 10.1016/j.molcel.2009.02.025 S1097-2765(09)00141-5 [pii]
- Motegi, A., Murakawa, Y., & Takeda, S. (2009). The vital link between the ubiquitin-proteasome pathway and DNA repair: impact on cancer therapy. *Cancer Lett*, 283(1), 1-9. doi: 10.1016/j.canlet.2008.12.030
- Nesvizhskii, A. I. (2010). A survey of computational methods and error rate estimation procedures for peptide and protein identification in shotgun proteomics. *J Proteomics*, 73(11), 2092-2123. doi: 10.1016/j.jprot.2010.08.009

- Nesvizhskii, A. I., Keller, A., Kolker, E., & Aebersold, R. (2003). A statistical model for identifying proteins by tandem mass spectrometry. *Anal Chem*, 75(17), 4646-4658.
- Nielsen, M. L., Vermeulen, M., Bonaldi, T., Cox, J., Moroder, L., & Mann, M. (2008). Iodoacetamide-induced artifact mimics ubiquitination in mass spectrometry. *Nat Methods*, 5(6), 459-460. doi: 10.1038/nmeth0608-459
- Ohkuma, Y., & Roeder, R. G. (1994). Regulation of TFIIF ATPase and kinase activities by TFIIE during active initiation complex formation. *Nature*, 368(6467), 160-163. doi: 10.1038/368160a0
- Olsen, J. V., Ong, S. E., & Mann, M. (2004). Trypsin cleaves exclusively C-terminal to arginine and lysine residues. *Mol Cell Proteomics*, 3(6), 608-614. doi: 10.1074/mcp.T400003-MCP200
- Orr-Weaver, T. L., Szostak, J. W., & Rothstein, R. J. (1981). Yeast transformation: a model system for the study of recombination. *Proc Natl Acad Sci U S A*, 78(10), 6354-6358.
- Pavelka, N., Fournier, M. L., Swanson, S. K., Pelizzola, M., Ricciardi-Castagnoli, P., Florens, L., & Washburn, M. P. (2008). Statistical similarities between transcriptomics and quantitative shotgun proteomics data. *Mol Cell Proteomics*, 7(4), 631-644. doi: 10.1074/mcp.M700240-MCP200
- Payne, J. M., Laybourn, P. J., & Dahmus, M. E. (1989). The transition of RNA polymerase II from initiation to elongation is associated with phosphorylation of the carboxyl-terminal domain of subunit IIa. *J Biol Chem*, 264(33), 19621-19629.
- Peng, J., Schwartz, D., Elias, J. E., Thoreen, C. C., Cheng, D., Marsischky, G., . . . Gygi, S. P. (2003). A proteomics approach to understanding protein ubiquitination. *Nat Biotechnol*, 21(8), 921-926. doi: 10.1038/nbt849
- Phatnani, H. P., & Greenleaf, A. L. (2006). Phosphorylation and functions of the RNA polymerase II CTD. *Genes Dev*, 20(21), 2922-2936. doi: 10.1101/gad.1477006
- Pickart, C. M., & Eddins, M. J. (2004). Ubiquitin: structures, functions, mechanisms. *Biochim Biophys Acta*, 1695(1-3), 55-72. doi: 10.1016/j.bbamcr.2004.09.019
- Ponts, N., Saraf, A., Chung, D. W., Harris, A., Prudhomme, J., Washburn, M. P., . . . Le Roch, K. G. (2011). Unraveling the ubiquitome of the human malaria parasite. *J Biol Chem*, 286(46), 40320-40330. doi: 10.1074/jbc.M111.238790
- Puig, O., Caspary, F., Rigaut, G., Rutz, B., Bouveret, E., Bragado-Nilsson, E., . . . Seraphin, B. (2001). The tandem affinity purification (TAP) method: a general procedure of protein complex purification. *Methods*, 24(3), 218-229. doi: 10.1006/meth.2001.1183
- Puig, O., Rutz, B., Luukkonen, B. G., Kandels-Lewis, S., Bragado-Nilsson, E., & Seraphin, B. (1998). New constructs and strategies for efficient PCR-based gene manipulations in yeast. *Yeast*, 14(12), 1139-1146. doi: 10.1002/(SICI)1097-0061(19980915)14:12<1139::AID-YEA306>3.0.CO;2-B
- Qiu, H., Hu, C., & Hinnebusch, A. G. (2009). Phosphorylation of the Pol II CTD by KIN28 enhances BUR1/BUR2 recruitment and Ser2 CTD phosphorylation near promoters. *Mol Cell*, 33(6), 752-762. doi: 10.1016/j.molcel.2009.02.018
- Ramisetty, S. R., & Washburn, M. P. (2011). Unraveling the dynamics of protein interactions with quantitative mass spectrometry. *Crit Rev Biochem Mol Biol*, 46(3), 216-228. doi: 10.3109/10409238.2011.567244

- Reid, J., & Svejstrup, J. Q. (2004). DNA damage-induced Def1-RNA polymerase II interaction and Def1 requirement for polymerase ubiquitylation in vitro. *J Biol Chem*, 279(29), 29875-29878. doi: 10.1074/jbc.C400185200
- Reyes-Reyes, M., & Hampsey, M. (2007). Role for the Ssu72 C-terminal domain phosphatase in RNA polymerase II transcription elongation. *Mol Cell Biol*, 27(3), 926-936. doi: 10.1128/MCB.01361-06
- Rigaut, G., Shevchenko, A., Rutz, B., Wilm, M., Mann, M., & Seraphin, B. (1999). A generic protein purification method for protein complex characterization and proteome exploration. *Nat Biotechnol*, 17(10), 1030-1032. doi: 10.1038/13732
- Rock, K. L., Gramm, C., Rothstein, L., Clark, K., Stein, R., Dick, L., . . . Goldberg, A. L. (1994). Inhibitors of the proteasome block the degradation of most cell proteins and the generation of peptides presented on MHC class I molecules. *Cell*, 78(5), 761-771.
- Rodriguez, C. R., Cho, E. J., Keogh, M. C., Moore, C. L., Greenleaf, A. L., & Buratowski, S. (2000). Kin28, the TFIIF-associated carboxy-terminal domain kinase, facilitates the recruitment of mRNA processing machinery to RNA polymerase II. *Mol Cell Biol*, 20(1), 104-112.
- Salzano, A. M., & Crescenzi, M. (2005). Mass spectrometry for protein identification and the study of post translational modifications. *Ann Ist Super Sanita*, 41(4), 443-450.
- Sardiu, M. E., Gilmore, J. M., Carrozza, M. J., Li, B., Workman, J. L., Florens, L., & Washburn, M. P. (2009). Determining protein complex connectivity using a probabilistic deletion network derived from quantitative proteomics. *PLoS One*, 4(10), e7310. doi: 10.1371/journal.pone.0007310
- Sardiu, M. E., & Washburn, M. P. (2010). Enriching quantitative proteomics with SI(N). *Nat Biotechnol*, 28(1), 40-42. doi: 10.1038/nbt0110-40
- Sardiu, M. E., & Washburn, M. P. (2011a). Building protein-protein interaction networks with proteomics and informatics tools. *J Biol Chem*, 286(27), 23645-23651. doi: 10.1074/jbc.R110.174052
- Sardiu, M. E., & Washburn, M. P. (2011b). Construction of protein interaction networks based on the label-free quantitative proteomics. *Methods Mol Biol*, 781, 71-85. doi: 10.1007/978-1-61779-276-2_5
- Schroeder, S. C., Schwer, B., Shuman, S., & Bentley, D. (2000). Dynamic association of capping enzymes with transcribing RNA polymerase II. *Genes Dev*, 14(19), 2435-2440.
- Shandilya, J., & Roberts, S. G. (2012). The transcription cycle in eukaryotes: From productive initiation to RNA polymerase II recycling. *Biochim Biophys Acta*, 1819(5), 391-400. doi: 10.1016/j.bbagr.2012.01.010
- Singh, B. N., & Hampsey, M. (2007). A transcription-independent role for TFIIB in gene looping. *Mol Cell*, 27(5), 806-816. doi: 10.1016/j.molcel.2007.07.013
- Somesh, B. P., Reid, J., Liu, W. F., Sogaard, T. M., Erdjument-Bromage, H., Tempst, P., & Svejstrup, J. Q. (2005). Multiple mechanisms confining RNA polymerase II ubiquitylation to polymerases undergoing transcriptional arrest. *Cell*, 121(6), 913-923. doi: 10.1016/j.cell.2005.04.010
- Somesh, B. P., Sigurdsson, S., Saeki, H., Erdjument-Bromage, H., Tempst, P., & Svejstrup, J. Q. (2007). Communication between distant sites in RNA polymerase

- II through ubiquitylation factors and the polymerase CTD. *Cell*, 129(1), 57-68. doi: S0092-8674(07)00306-6 [pii]10.1016/j.cell.2007.01.046
- Sorokin, A. V., Kim, E. R., & Ovchinnikov, L. P. (2009). Proteasome system of protein degradation and processing. *Biochemistry (Mosc)*, 74(13), 1411-1442.
- Starita, L. M., Lo, R. S., Eng, J. K., von Haller, P. D., & Fields, S. (2012). Sites of ubiquitin attachment in *Saccharomyces cerevisiae*. *Proteomics*, 12(2), 236-240. doi: 10.1002/pmic.201100166
- Svejstrup, J. Q. (2002). Mechanisms of transcription-coupled DNA repair. *Nat Rev Mol Cell Biol*, 3(1), 21-29. doi: 10.1038/nrm703
- Svejstrup, J. Q. (2007). Contending with transcriptional arrest during RNAPII transcript elongation. *Trends Biochem Sci*, 32(4), 165-171. doi: S0968-0004(07)00053-9 [pii] 10.1016/j.tibs.2007.02.005
- Swanson, S. K., Florens, L., & Washburn, M. P. (2009). Generation and analysis of multidimensional protein identification technology datasets. *Methods Mol Biol*, 492, 1-20. doi: 10.1007/978-1-59745-493-3_1
- Tan-Wong, S. M., Zaugg, J. B., Camblong, J., Xu, Z., Zhang, D. W., Mischo, H. E., . . . Proudfoot, N. J. (2012). Gene loops enhance transcriptional directionality. *Science*, 338(6107), 671-675. doi: 10.1126/science.1224350
- Tietjen, J. R., Zhang, D. W., Rodriguez-Molina, J. B., White, B. E., Akhtar, M. S., Heidemann, M., . . . Ansari, A. Z. (2010). Chemical-genomic dissection of the CTD code. *Nat Struct Mol Biol*, 17(9), 1154-1161. doi: 10.1038/nsmb.1900
- Vannini, A., & Cramer, P. (2012). Conservation between the RNA polymerase I, II, and III transcription initiation machineries. *Mol Cell*, 45(4), 439-446. doi: 10.1016/j.molcel.2012.01.023
- Varon, R., Gooding, R., Steglich, C., Marns, L., Tang, H., Angelicheva, D., . . . Kalaydjieva, L. (2003). Partial deficiency of the C-terminal-domain phosphatase of RNA polymerase II is associated with congenital cataracts facial dysmorphism neuropathy syndrome. *Nat Genet*, 35(2), 185-189. doi: 10.1038/ng1243
- Vasiljeva, L., Kim, M., Mutschler, H., Buratowski, S., & Meinhart, A. (2008). The Nrd1-Nab3-Sen1 termination complex interacts with the Ser5-phosphorylated RNA polymerase II C-terminal domain. *Nat Struct Mol Biol*, 15(8), 795-804. doi: 10.1038/nsmb.1468
- Vlachostergios, P. J., Patrikidou, A., Daliani, D. D., & Papandreou, C. N. (2009). The ubiquitin-proteasome system in cancer, a major player in DNA repair. Part 1: post-translational regulation. *J Cell Mol Med*, 13(9B), 3006-3018. doi: 10.1111/j.1582-4934.2009.00824.x
- Washburn, M. P. (2008). Sample preparation and in-solution protease digestion of proteins for chromatography-based proteomic analysis. *Curr Protoc Protein Sci*, Chapter 23, Unit 23 26 21-23 26 11. doi: 10.1002/0471140864.ps2306s53
- Washburn, M. P., Wolters, D., & Yates, J. R., 3rd. (2001). Large-scale analysis of the yeast proteome by multidimensional protein identification technology. *Nat Biotechnol*, 19(3), 242-247. doi: 10.1038/85686
- Werner-Allen, J. W., Lee, C. J., Liu, P., Nicely, N. I., Wang, S., Greenleaf, A. L., & Zhou, P. (2011). cis-Proline-mediated Ser(P)5 dephosphorylation by the RNA polymerase II C-terminal domain phosphatase Ssu72. *J Biol Chem*, 286(7), 5717-5726. doi: 10.1074/jbc.M110.197129

- Wilson, M. D., Harreman, M., & Svejstrup, J. Q. (2013). Ubiquitylation and degradation of elongating RNA polymerase II: the last resort. *Biochim Biophys Acta*, 1829(1), 151-157. doi: 10.1016/j.bbagr.2012.08.002 S1874-9399(12)00145-9 [pii]
- Woudstra, E. C., Gilbert, C., Fellows, J., Jansen, L., Brouwer, J., Erdjument-Bromage, H., . . . Svejstrup, J. Q. (2002). A Rad26-Def1 complex coordinates repair and RNA pol II proteolysis in response to DNA damage. *Nature*, 415(6874), 929-933. doi: 10.1038/415929a415929a [pii]
- Woychik, N. A., & Young, R. A. (1990). RNA polymerase II: subunit structure and function. *Trends Biochem Sci*, 15(9), 347-351.
- Xiang, K., Nagaike, T., Xiang, S., Kilic, T., Beh, M. M., Manley, J. L., & Tong, L. (2010). Crystal structure of the human symplekin-Ssu72-CTD phosphopeptide complex. *Nature*, 467(7316), 729-733. doi: 10.1038/nature09391
- Zhang, D. W., Mosley, A. L., Ramisetty, S. R., Rodriguez-Molina, J. B., Washburn, M. P., & Ansari, A. Z. (2012). Ssu72 phosphatase-dependent erasure of phospho-Ser7 marks on the RNA polymerase II C-terminal domain is essential for viability and transcription termination. *J Biol Chem*, 287(11), 8541-8551. doi: 10.1074/jbc.M111.335687
- Zhang, Y., Wen, Z., Washburn, M. P., & Florens, L. (2009). Effect of dynamic exclusion duration on spectral count based quantitative proteomics. *Anal Chem*, 81(15), 6317-6326. doi: 10.1021/ac9004887
- Zhang, Y., Wen, Z., Washburn, M. P., & Florens, L. (2011). Improving proteomics mass accuracy by dynamic offline lock mass. *Anal Chem*, 83(24), 9344-9351. doi: 10.1021/ac201867h

CURRICULUM VITAE

Mary L. Cox

EDUCATION

MASTER OF SCIENCE- BIOCHEMISTRY AND MOLECULAR BIOLOGY, DEC 2013

- Indiana University, Indianapolis, IN
- Thesis project: The role of the CTD phosphatase, Rtr1, and post-translational modifications in regulation of RNA Polymerase II.

GRADUATE CERTIFICATE IN BIOTECHNOLOGY, DEC 2010

- Indiana University, Indianapolis, IN

BACHELOR OF SCIENCE, MICROBIOLOGY, MAY 1996

- Ball State University, Muncie, IN
- GPA 3.81/4.0

PROFESSIONAL EXPERIENCE

Indiana Clinical and Translational Sciences Institute, IUPUI, Indianapolis, IN

Key Responsibilities:

- Managed clinical biosample processing, nucleic acid extraction, C14 analysis laboratories and biorepository associated with clinical trials (Phase I-III) support in compliance with defined protocols and guidance from GCP, GLP and ISBER
- Developed, validated and implemented optimized methods for automated DNA/RNA extraction from biospecimens including preparation of protocols and reports of validation studies according to good documentation practices
- Wrote, reviewed, implemented SOPs including training ICSTI and collaborating research clients
- Performed drug management activities for GLP collaborator for GLP and non-GLP pre-clinical studies including protocol review and documentation
Project management with collaborating research clients for timeline optimization, review and approve clinical research protocols for processing support through ICTSI Clinical Research Center and resource allocation

Promotion History: Facility Manager, Specimen Storage Facility (Mar 2010- Dec 2011); Technical Supervisor, Indiana CTSI Processing Lab (July 2011-Dec 2011); Operations Manager, Specimen Storage Facility (SSF) and Clinical and Translational Support Lab (CTSL) (Jan 2011-Mar 2012)

Endgenitor Technologies, Inc. Indianapolis, IN

Key Responsibilities:

- Project leader for cellular therapeutic development products derived from endothelial stem cell, adult peripheral blood mononuclear cells, and venous tissue using proprietary cell culture techniques including isolation of stem cells from umbilical cord blood using immunomagnetic separation, stem cell expansions and functional Colony Forming assays
- Established SOP's and forms for research and manufacturing protocols according to GLP requirements and performed quality control assessments of therapeutic and research products for viability, purity, sterility, and potency/functionality assays and tracked all data through in-house created database
- Prepared cellular products for *in vitro* and *in vivo* functional studies and wrote protocols and reports of pre-clinical studies assessing potential therapeutic products (murine/rodent GLP and non-GLP *in vivo* studies)
- Maintain laboratory through ordering supplies, scheduling/performing equipment maintenance, and cleaning/sterilization of tissue culture equipment

Promotion History: Senior Research Technician (Oct 2006-Jun 2008); Research Associate (Jun 2008-Mar 2010)

Seradyn, Inc. A Thermo-Fisher Scientific Company, Indianapolis, IN

Key Responsibilities:

- Project leader for group developing multiple immunoturbidimetric drug monitoring assay system for therapeutic drugs including designing and managing all aspects of product development, product transfer, verification (510(k) market clearance Nov 2005) and validation, and commercialization
- Prepared and maintained GMP documentation associated with multiple product development including design history file from proof of concept/feasibility to and post market surveillance including all manufacturing, quality control testing and packaging work instructions.
- Prepared and proof-read all technical product documentation including product inserts, labeling and marketing materials
- Provided organizational skills and leadership for professional presentations and multidisciplinary team meetings with consistently increasing knowledge of scientific trends through classroom lectures, readings, conferences and seminars

Promotion History: Product Support Scientist (Oct 2002-Jan 2003); Research Scientist (Jan 2003-Sept 2006)

Infectious Disease Division, Indiana University School of Medicine, Indianapolis, IN

Key Responsibilities:

- Managed biospecimen processing laboratory supporting HIV clinical trials including preparation of samples for College of American Pathologist's accreditation (CAP) for HIV-1 Viral Load (RT-PCR) and CD4/CD8 Determinations (Flow Cytometry)
- Drafted and updated clinical and research protocols ACTG trials and collaborative research studies using flow cytometry in areas such as Apoptosis, isolation of lymphocytic and dendritic cells using FACS (4-color), intracellular cytokine markers, and cell cycle analysis using propidium iodide.

Promotion History: Research Technician, RS07 (Jun 2000-Jul 2001); Research Analyst, PA (Aug 2001-Oct 2002)

Mid America Clinical Laboratories, Indianapolis, IN

Key Responsibilities:

- Maintained QC/QA logs and produced troubleshooting procedure guide for SOPs
- Developed strong attention to detail, troubleshooting and creative problem solving skills while assisting in surgical tissue examinations through set-up, accessioning and preparation of 1/3 of overall case load (approx. 80,000 surgicals/yr)
- Maintained instrumentation including cryo-microtome, balances, tissue processors, automated tissue staining and cover-slipping instruments

Promotion History: Laboratory Assistant, Histology (Sept 1997-Sept 1998); Laboratory Assistant, Pathology (Oct 1998-Jun 2000)

PA Labs, Inc., Muncie, IN

Key Responsibilities:

- Performed testing and reported results for Hematology, Chemistry, Microbiology, Urinalysis, Immunology, and Special Chemistry
- Reviewed QC/QA logs and report any out of specification results to supervisor
- Prepared standards and reagents for calibration and general instrument maintenance

Promotion History: Special Qualified Medical Technologist (1996-1997)